CONTENTS

Optimal Monitoring In Reaction-Diffusion Model Of The Atmospheric Pollution

Xueming Qian[1,2]
1. School of Internet of Things, Wuxi professional college of science and technology, Wuxi 214028, China.
2. School of Internet of Things Engineering, Jiangnan University, Wuxi 214122, China.

***Abstract*—In this paper, an optimal monitoring framework for a class of reaction-diffusion system is proposed. It is assumed that the diffusion process with a moving source. The optimization is performed on the measurements from spatial diffusion process is obtained through a mobile sensor network. A mobile control approach is given by using distributed output feedback control strategy and the Lyapunov functional method ensuring the closed-loop control system to be globally asymptotically stable. Such a framework shown measure form system by static sensor network is just a special case of our results. A numerical example is constructed to illustrate the effectiveness of the theoretical results.**

***Index Terms*—optimal monitoring, mobile sensors, reaction-diffusion equation, atmospheric pollution**

I. INTRODUCTION

With the development of modern industry, the pollution is becoming more and more serious. In particular, composition of the atmosphere has been changing due to significant amounts of pollutants have been released to the air. The air which polluted has been gradually harming the life on earth, including human being, plant and animal. It is found that pollution comes from the following three categories: emissions from factories, vehicles and domestic waste. In recent years, the region of north China, huanghuai, jianghuai and jiangnan have appeared a wide range of smog weather. Smog makes the appearance of outside indistinct, hazy and obscure. Traffic and daily life of city get even worse by smog. And, people's health has been in danger. Therefore, the study for the issue of air pollution has been an important topic for researchers[1-2].

At present, the most critical thing is to establish an efficient monitoring system to prevent and control air pollution. Then, there are two issues must be faced firstly. On the one hand, how to describe the model of air pollution? On the other hand, how to measure the air pollution effectively?

In fact, pollutants transport in the atmosphere is a diffusion process. The reaction-diffusion equation has been used to express the air pollution in [3]. Smog, of course, also can be described as the reaction-diffusion model. The characteristics of the process is the state of system depend on not only time but also spatial. The complexity dynamical behavior has been exhibited in these processes. The method of sliding mode control has been studied for stabilization of parabolic systems in [4]. However, it is difficult to avoid the wobble phenomenon. Also, the semigroup operator theory has been used for distributed parameter system in [5]. A class of semi-linear diffusion equation has studied in [6] using output feedback which measured in static sensors. Recently, H_∞ control for a class of distributed parameter systems has been studied in [7].

Next, the sensor networks are used to monitor the process in many engineering problems. Nowadays, the use of mobile sensors has been receiving attention due to its efficient monitoring[8]. Moreover, power consumption and costs in control system can be improved greatly. Cooperative control of mobile sensors has been studied in a distributed environment[9]. [10] has provided an effective approach for control of distributed parameter system using mobile actuator-sensor networks.

In this paper, an optimal monitoring scheme is proposed in a class of reaction-diffusion system. Also, a moving source will be considered in the diffusion process. By using Lyapunov stability arguments and distributed output feedback control strategy, the stability criterion is presented for closed-loop control system. Obviously, the result obtained by static sensor network is just a special case of our results.

II. PROBLEM FORMULATION

In this paper, we consider the following reaction-diffusion model which described by the air pollution, or smog.

$$\frac{\partial z(t,x)}{\partial t}=\frac{\partial}{\partial x}\left(a(x)\frac{\partial z(t,x)}{\partial x}\right)-b\frac{\partial z(t,x)}{\partial x} \quad (1)$$
$$-cz(t,x)+w(t,x)+u(t,x)$$

where $z(t,x)$ denotes the state of the system at time t and in space x, $x\in[0,l]$ and $t\in\mathbf{R}^+$. The transmission diffusion operator $a(x)\geq a_0>0$ and b,c are known constants. The function $w(t,x)$ denotes the moving disturbance. $u(t,x)$ is the control input.

The initial condition of the system (1) is

$$z(0,x)=z_0(x),$$

and having Dilichlet boundary condition

$$z(t,0)=z(t,l)=0.$$

Simultaneously, N mobile sensors have been used to provide the measurement of the state $z(t,x)$.

$$\begin{aligned} y(t,x;x^s(t)) &= \begin{bmatrix} y_1(t,x;x_1^s(t)) \\ y_2(t,x;x_2^s(t)) \\ \vdots \\ y_N(t,x;x_N^s(t)) \end{bmatrix} \\ &= \begin{bmatrix} \theta(x;x_1^s(t))z(t,x) \\ \theta(x;x_2^s(t))z(t,x) \\ \vdots \\ \theta(x;x_N^s(t))z(t,x) \end{bmatrix} \end{aligned} \tag{2}$$

where the function $\theta(x;x_i^s(t))$, $i=1,2,\cdots,N$ denote the spatial distributions of i th mobile sensor. And, the spatial location $x_i^s(t)\in[0,l]$ denotes the time varying centroid of i th mobile sensor. Such $x_i^s(t)$ is actually the trajectory of i th mobile sensor.

The output of measurement can be rewritten the compact form as follows

$$y(t,x;x^s(t))=\theta(x;x^s(t))z(t,x). \tag{3}$$

The main purpose in this paper is to design mobile monitoring scheme under optimal control of a class of reaction-diffusion system. Without loss of generality, we consider the spatial distribution of i th sensor as follows.

$$\theta(x;x_i^s(t))=\begin{cases} 1 & x_i^s\in[x_i^s-\eta,x_i^s+\eta] \\ 0 & \text{otherwise} \end{cases} \tag{4}$$

Combined with the distributed output feedback, the control strategy can be designed in the following

$$u(t,x;x^s(t))=-\theta^*(x;x^s(t))K\,y(t,x;x^s(t)) \tag{5}$$

III. MAIN RESULTS

To stabilization of control system, the following lemmas are introduced.

Lemma 1(Wirtinger's Inequality[6])

Let $z\in W^{1,2}(a,b)$ be a scalar function, and $z(a)=z(b)=0$. Then the following inequality holds

$$\int_a^b z^2(\xi)d\xi\le\frac{(b-a)^2}{\pi^2}\int_a^b\left(\frac{dz(\xi)}{d\xi}\right)^2 d\xi.$$

Lemma 2 (Young Inequality[6]) Let x,y be any real vectors and let $\varepsilon>0$ be a constant. Then the following inequality holds

$$2xy\le\varepsilon x^2+\frac{1}{\varepsilon}y^2.$$

Together with distributed output feedback, the closed-loop control system is given by

$$\begin{aligned} \frac{\partial z(t,x)}{\partial t} &= \frac{\partial}{\partial x}\left(a(x)\frac{\partial z(t,x)}{\partial x}\right)-b\frac{\partial z(t,x)}{\partial x} \\ &\quad -cz(t,x)+w(t,x) \\ &\quad -\theta^*(x;x^s(t))K\theta(x;x^s(t))z(t,x) \end{aligned} \tag{6}$$

Theorem 1 Under the distributed output feedback control strategy (5), the reaction-diffusion system (1) with a moving source $w(t,x)$ is globally asymptotically stable if N mobile sensors within the spatial domain with specified velocity $x_i^s(t)$, $i=1,2,\cdots,N$.

Proof: Consider a proper Lyapunov functional as

$$V(t)=\frac{1}{2}\int_0^l z^2(t,x)dx. \tag{7}$$

Computing the time-derivative of $V(t)$, along the solution of system (6), we get

$$\begin{aligned} \dot V(t) &= \int_0^l z(t,x)\frac{\partial z(t,x)}{\partial t}dx \\ &= a\int_0^l z(t,x)\frac{\partial}{\partial x}\left(a(x)\frac{\partial z(t,x)}{\partial x}\right)dx \\ &\quad -b\int_0^l z(t,x)\frac{\partial z(t,x)}{\partial x}dx-c\int_0^l z^2(t,x)dx \\ &\quad +\int_0^l z(t,x)w(t,x)dx \\ &\quad -\int_0^l\theta^*(x;x^s(t))K\theta(x;x^s(t))z^2(t,x)dx \end{aligned} \tag{8}$$

By boundary condition and Lemma 1, we have

$$\begin{aligned} &\int_0^l z(t,x)\frac{\partial}{\partial x}\left(a(x)\frac{\partial z(t,x)}{\partial x}\right)dx \\ &-b\int_0^l z(t,x)\frac{\partial z(t,x)}{\partial x}dx-c\int_0^l z^2(t,x)dx \\ &\le -a_0\int_0^l\left(\frac{\partial z(t,x)}{\partial x}\right)^2 dx-c\int_0^l z^2(t,x)dx \\ &\le -(a_0\frac{\pi^2}{l}+c)\int_0^l z^2(t,x)dx \end{aligned} \tag{9}$$

From Lemma 2, we obtain

$$\begin{aligned} &\int_0^l z(t,x)w(t,x)dx\le\left|\int_0^l z(t,x)w(t,x)dx\right| \\ &\le\frac{\varepsilon}{2}\int_0^l z^2(t,x)dx+\frac{1}{2\varepsilon}\int_0^l w^2(t,x)dx \\ &\le\frac{\varepsilon}{2}\int_0^l z^2(t,x)dx+\frac{1}{2\varepsilon}\left|w(t,x)\right|^2_{L_\infty(0,\infty,L_2(0,l))} \end{aligned} \tag{10}$$

Therefore, combining (8)-(10), it follows that

$$\begin{aligned}\dot{V}(t) &= \int_0^l z(t,x)\frac{\partial z(t,x)}{\partial t}dx \\ &\le -(a_0\frac{\pi^2}{l}+c-\frac{\varepsilon}{2})\int_0^l z^2(t,x)dx \\ &\quad +\frac{1}{2\varepsilon}\left|w(t,x)\right|^2_{L_\infty(0,\infty,L_2(0,l))} \\ &\quad -\lambda\int_0^l \theta^*(x;x^s(t))\theta(x;x^s(t))z^2(t,x)dx\end{aligned}$$

where $\lambda = \lambda_{\min}(K)$.

The choice of $\varepsilon = a_0\frac{\pi^2}{l}+c$ provides

$$\begin{aligned}\dot{V}(t) \le & -\frac{\varepsilon}{2}\int_0^l z^2(t,x)dx+\frac{1}{2\varepsilon}\left|w(t,x)\right|^2_{L_\infty(0,\infty,L_2(0,l))} \\ & -\lambda\sum_{i=1}^N\int_0^l\left(\theta(x;x_i^s(t))z(t,x)\right)^2dx\end{aligned} \tag{11}$$

In addition, along the similar line of proof of results in [11], we can derive that the solution of closed-loop control system is globally asymptotically stable.

Accordingly, summarizing the above discussion, an optimal algorithm is proposed in the following.

Algorithm 1 Maximum state deviation for distributed output feedback control strategy of mobile sensors

(1) Place the sensors at initial location and choose the time interval.

(2) Design the distributed output feedback control strategy

$$u(t,x;x^s(t)) = -\theta^*(x;x^s(t))K\,y(t,x;x^s(t)).$$

(3) Pick the dynamics of mobile sensors by utilizing the maximum deviation of the measured state

$$x_i^s(t_{k+1}) = \arg\max_{x_i^s(t_k)-\eta\le x_i\le x_i^s(t_k)+\eta}\left|\theta(x;x_i^s(t_k))z(t,x)\right|.$$

After that, three steps above circular computed.

The system (1) is general. In the following, we consider the case when the system (1) has no moving source and measure form system by a static sensor network. Hence, N static sensors is fixed at x_i^s, namely,

$$\theta(x;x_i^s) = \delta(x-x_i^s). \tag{12}$$

In this case, we can obtain the following corollary.

Corollary 1 Under the distributed output feedback control strategy (5), the reaction-diffusion system (1) is globally asymptotically stable if the distribution of N static sensors satisfied in (12) and the following inequality holds

$$a_0\frac{\pi^2}{l}+c+\lambda>0.$$

Proof: The result of Corollary 1 can be proved along the similar line in Theorem 1. We just need to consider (11),

$$\begin{aligned}\int_0^l\left(\theta(x;x_i^s)z(t,x)\right)^2dx &= \int_0^l\left(\delta(x-x_i^s)z(t,x)\right)^2dx \\ &= z^2(t,x_i^s)\end{aligned}$$

Therefore,

$$\begin{aligned}\dot{V}(t) &\le -(a_0\frac{\pi^2}{l}+c)\int_0^l z^2(t,x)dx-\lambda\sum_{i=1}^N z^2(t,x_i^s) \\ &\le -(a_0\frac{\pi^2}{l}+c+\lambda)\int_0^l z^2(t,x)dx\end{aligned}$$

The choice of $a_0\frac{\pi^2}{l}+c+\lambda>0$, Corollary 1 is obtained.

Ⅳ. A NUMERICAL EXAMPLE

In this section, a simulation is given to show the effectiveness of the main results. Consider the reaction-diffusion model () with two mobile sensors in $[0,1]$. The system with initial condition $z(0,x)=\cos(4\pi x)+4\sin(2\pi x)e^{-5x^2}$ and satisfy Dilichlet boundary condition $z(t,0)=z(t,1)=0$. The coefficients of the elliptic operator are $a_0=0.005$, $b=0.25$ and $c=0.08$. The moving source is given as

$$\begin{aligned}w(t,x) = & 6\times10^{-4}\left(0.4\cos\left(\frac{7\pi t}{t_f}\right)\right) \\ & \times\left(H(x+x_c(t)+\eta)-H(x-x_c(t)-\eta)\right)\end{aligned}$$

where $x_c(t)$ is the centroid of the moving source and $\eta=0.05$. The gains of controller are $k_1=30$, $k_2=45$. The spatial distribution of sensor is given by (4).

The open-loop reaction-diffusion system is simulated in Fig.1 to illustrate the pattern of diffusion process with a moving source intuitively. The closed-loop control system is simulated in $[0,10]$ with two sensors. Here, we consider two static sensors are fixed at $x_1^s=0.15$ and $x_2^s=0.85$ as the standard for comparisons. The location x_1^s, x_2^s also are starting point for two mobile sensors. The trajectories of two mobile sensors are shown in Fig. 2, and the fixed sensors also in it. Finally, the state L_2 norm for closed-loop case, and the case of the mobile sensors are depicted in Fig. 3. It is clear that the performance of mobile case is better than the static case.

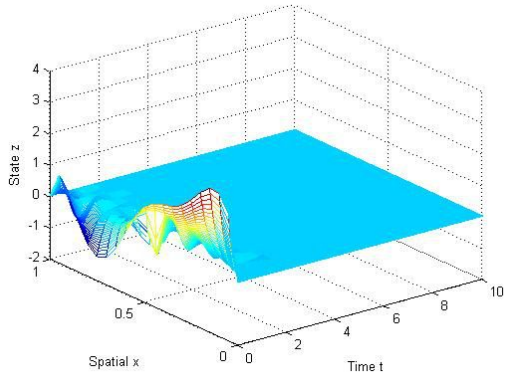

Figure 8. Reaction-diffusion model of air pollution.

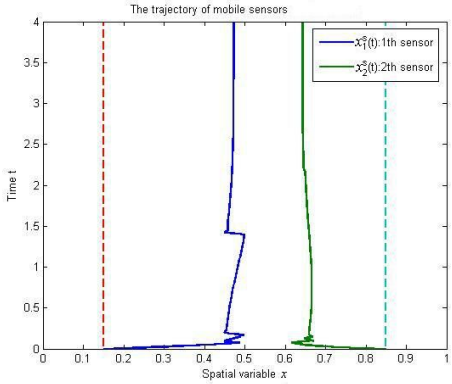

Figure 8. The trajectories of mobile sensors.

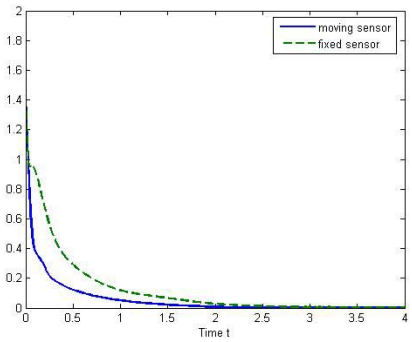

Figure 8. Evolution of spatial L_2 norm.

V. CONCLUSION

In this paper, an optimal monitoring issue for a class of reaction-diffusion system has been studied. Also, a spatial moving source has been considered in the diffusion process. The mobile sensors used a distributed output feedback control strategy as a means to optimize the spatial diffusion process. By using Lyapunov stability arguments, the criterion is presented to ensure the closed-loop control system is globally asymptotically stable. It is clear that measure form system by static sensor network is just a special case of our results. Finally, a numerical example is given to illustrate the effectiveness of the theoretical results.

ACKNOWLEDGMENT

This work was supported by the National Natural Science Foundation of China (No.61174021), the Natural Science Foundation of Jiangsu Province of China (No.BK20131109), Soft Science Research Program of Wuxi of China (No.KX14-B-13).

REFERENCES

[1] S. Vardoulakis, B. E. A. Fisher, K. Pericleous, et al. "Modelling air quality in street canyons: a review," *Atmospheric environment*, vol. 37, no. 2, pp. 155-182, 2003.

[2] J. Harkonen, E. Valkonen, J. Kukkonen, et al. "An operational dispersion model for predicting pollution from a road," *International Journal of Environment and Pollution*, vol. 5, no. 4, pp. 602-610, 1995.

[3] S. R. Hanna. "Applications in air pollution modeling," *Atmospheric turbulence and air pollution modeling*, Springer Netherlands, 1982, pp. 275-310.

[4] B. Cui, W. Wang, F. Deng. "Variable structure control of a class of distributed parameter systems with delays," *Chinese Journal of Engineering Mathematics*, vol. 21, no. 6, pp. 920-924, 2004.

[5] E. M. Hanczyc, A.Palazoglu. "Use of symmetry groups in sliding mode control of nonlinear distributed parameter systems," *International Journal of Control*, vol. 63, no. 6, pp. 1149-1166, 1996.

[6] E. Fridman, A. Blighovsky. "Robust sampled-data control of a class of semilinear parabolic systems," *Automatica*, vol. 48, no. 5, pp. 826-836, 2012.

[7] X. Qian, B. Cui. "H_∞ control for a class of distributed parameter systems with leakage delay and Markovian jumping," Computer Modelling and New Technologies, vol. 18, no. 12, pp. 152-160, 2014.

[8] M. A. Demetriou. "Guidance of mobile actuator-plus-sensor networks for improved control and estimation of distributed parameter systems," *IEEE Trans. on Automatic Control*, vol. 55, no. 7, pp. 1570-1584, 2010.

[9] P. Ogren, E. Fiorelli, N. E. Leonard. "Cooperative control of mobile sensor networks: Adaptive gradient climbing in a distributed environment," *IEEE Trans. on Automatic Control*, vol 49, no. 8, pp. 1292-1302, 2004.

[10] Y. Q. Chen, Z. Wang, J. Liang. "Automatic dynamic flocking in mobile actuator sensor networks by central Voronoi tessellations," *Mechatronics and Automation, 2005 IEEE International Conference*, vol 3, pp. 1630-1635, 2005.

[11] R. F. Curtain, M. A. Demetriou, K. Ito. "Adaptive compensators for perturbed positive real infinite-dimensional systems," *International Journal of Applied Mathematics and Computer Science*, vol. 13, no. 4, pp. 441-452, 2003.

Xueming Qian was born in 1981. He is now pursuing the Ph.D. degree in School of Internet of Things Engineering, Jiangnan University, China, and received the M.S. degree in mathematics from Yangzhou University, China in 2009. His current research interests includes control theory of distributed parameter systems, Modeling and control of mobile sensor networks.

Design And Development Of Intelligent Control Instrument Eps

ZHANG Li-guo[1,2], Dou Man-feng[1]
[1]Northwestern Polytechnical University, Xi'an, China
[2]Northeast Petroleum University, Daqing, China

***Abstract*—In view of the intelligent management of emergency power supply (EPS), this paper put forward the intelligent instrument is adopted to improve the management and control of EPS scheme. This article discusses the function of EPS development module and intelligent instruments. Respectively, this paper introduces the design of each module and function implementation. The overall design scheme of instrument with software and hardware implemented and applied to the EPS control cabinet. Instrument in EPS actual operation condition can meet the design requirements.**

***Index Terms*—EPS, intelligent instruments, intelligent management**

I. INTRODUCTION

Emergency power supply is mainly used in construction, transportation, communications, finance, railways, taxation, schools, military, medical, factory, municipal, fire, and other important areas. Especially the application in the high-rise building is particularly prominent, and become an important part of modern building security facilities. With the development of the society, the construction technology level enhances unceasingly. Social modernization and construction of information makes the building dependence on power supply is becoming more and more closely, emergency power supply for safety play a more and more important role in modern society.

II. EPS DEVELOPMENT SERIES INTELLIGENT INSTRUMENTS

A. Single battery voltage detection of the series storage battery[1][2]

The failure of the battery pack is often from a single block of battery failure begins a vicious cycle. Especially for a long time but not more than the life of the battery pack, rely on the daily maintenance of maintenance personnel is both time-consuming and inconvenient, also do not meet the need of modern management. Therefore, for the operation of the single battery parameters on-line monitoring, timely find problems becomes extremely important.

B. AC current and voltage detection

To the mains supply, or to inverter ac current and voltage detection directly affects the reliable power supply to the load. Therefore, detection of AC current and voltage to provide real-time basis for instrument control.

C. Mains supply emergency conversion module

When normal power supply mains, the mains through each switch device to the critical load power, simultaneous detection of mains and battery charge management, and then to provide DC energy from the battery to the inverter.

D. Charge Management Module

Charging management should not only ensure the battery charged when the feed can be timely but also ensure that the battery can provide sufficient power when emergency mode. Normally, the stand or fall of storage battery can be evaluation by battery internal resistance detection. Capacity detection can learn about the battery power supply capacity.

E.Communication module

Communication module for each module completed sampling data extraction, analysis and storage work and display module provides display data. At the same time, it realizes data remote transmission through hardware.

F. Display instrument

In standby mode， the instrument shows the grid voltage, working current, battery voltage, parameters such as temperature. Under the charging status, the instrument shows the grid voltage, working current, battery capacity, charging current. Under the emergency state, the instrument display inverter current and working current and the residual capacity of the battery. Display instruments should also be able to complete the data query and parameter settings for various operating conditions.

Considering the above aspects, we get the overall structure of intelligent control instruments shown in Figure 1:

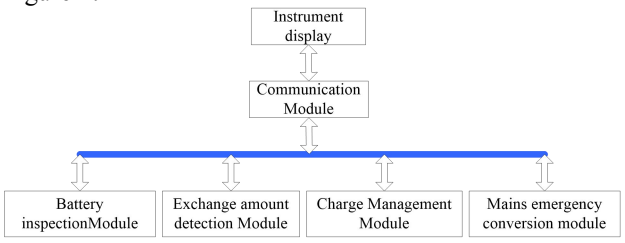

Figure 1 The overall structure of the instrument

III.BATTERY INSPECTION MODULE DESIGN

A. Circuit structure and principle

As shown in figure 2, the first relay closed to A zone, the electrolytic capacitor charging. When measuring the voltage relay closed to area B, the electrolytic capacitor and the battery is isolated, due to the electrolytic capacitor to keep the battery voltage signal, therefore, the test part just measure electrolytic capacitor on the voltage and obtains the corresponding battery voltage. This method possesses the advantages of simple principle and low cost. But because the relay has the mechanical action is slow, low service life of defects, practice has proved that according to the principle of the realization of detection device in speed, service life and reliability of the work of satisfactory. In order to solve the above problem can be changed mechanical relay into optocoupler relay, so no extra electrolytic capacitor can improve the reliability, speed and service life is up to par, but relative cost will greatly improve.

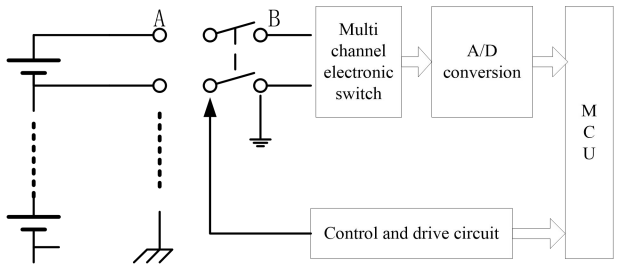

Figure 2 The battery detecting principle diagram

B. Battery checking circuit characteristics

(1) Simple structure, voltage sampling speed is quick

Battery voltage measurement and display of alarm is separated from the hardware, so it is convenient for walk the line, to reduce the complexity of operation. At the same time, the measurement module used in semiconductor relay has good switching performance, fast switching speed, voltage consistency is good.

(2)Intelligent alarm recording function, and provides real-time query alarm point

In the event of abnormal voltage, the instrument can automatically judge and make a report to the police record. Waiting for the alarm status of PC are extracted with the query. The operator can set, inquire abnormal state (including alarm line and emergency alarm current voltage), in order to control display modules.

IV. COMMUNICATION DETECTION MODULE DESIGN

A. Communication principle

The AC value including AC voltage and alternating current flow quantity. The amount of AC voltage through voltage transformer transformation, alternating current flow through the current transformer transformation, they are transferred to the circuit can measure range, precision rectifier for A/D conversion, become the processor can process the data.

B. Design and Implementation

(1)AC voltage acquisition using four independent input mode, there is no public end, not only can measure the phase voltage and line voltage can be measured, connection mode is flexible.

(2)AC voltage transformer using TV1013-1,the maximum measurement range up to AC 1000V.

(3) Since the current transformer input is measured, so using three input methods with a common end, and its range of models based on the transformer varies.

4) 485 communication interface with optical coupling isolation, it can ensure that the sampling and PC board is electrically insulated and ensure the safe and reliable communications.

(5) A/D reference voltage terminations 5 volt reference voltage source, when the grid voltage fluctuations can guarantee the stability of the reference voltage, which can guarantee the accuracy is relatively poor at ambient conditions, the sampling data acquisition board.

V. CHARGE AND DISCHARGE MANAGEMENT AND MAINS SUPPLY EMERGENCY CONVERSION MODULE

A. Charge and discharge management

Charge and discharge management functions including charging current limit alarm, alarm, small current deep discharge float charging temperature compensation, the average floating point of intelligent control (ensure that don't appear overcharge and owe charging).There are two battery maintenance functions in the work process. On the one hand, the module for real-time monitoring of battery pack, at any time make anomalies and battery charging and discharging process of warning. On the other hand, according to the amount of built-in storage battery running records, tips for all maintenance, filling the annual maintenance information such as deep discharge and replace the battery.

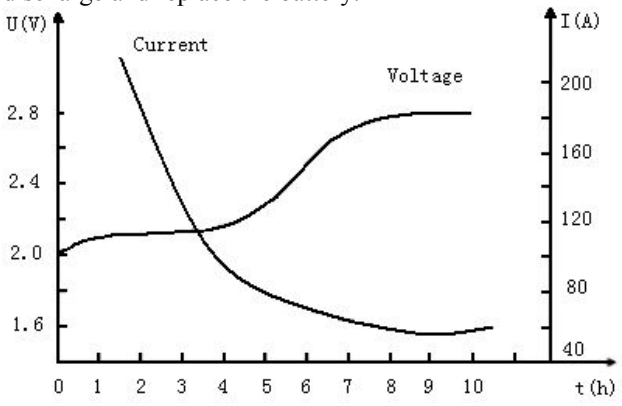

Figure3 charge curves

B. mains supply emergency conversion

To reduce the design cost, conversion module using single chip microcomputer control board instead of PLC. This module adopts the control hardware is designed, reliable operation, which has the function of optical coupling isolation switch input and output control

board, the board input can be an external photoelectric, capacitive and inductive, hall and other sensors.

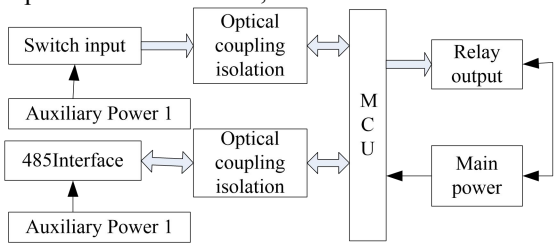

Figure4 Display alarm diagram

VI. DISPLAY ALARM MODULE

A. The main function

First of all, instrument display module can obtain AC, DC acquisition board data acquisition and analysis, but also can analysis the data transfer to PC. Secondly, it analysis the data found abnormal, can sound, light alarm and the use of Chinese characters dot matrix liquid crystal display. Finally, it has the real time clock and EEPROM, can be on the state of alarm record, save parameters, operation time limits, with power off keeping function.

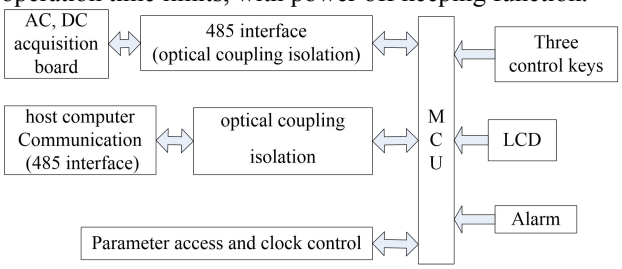

Figure 5 Structure and principle diagram

B. main features

MPU uses a large capacity, a high performance MCU W77E58, dual serial port, can be used to collect board communication, and communication with the host computer. W77E58 encryption function more perfect, the internal program hard to read theft.

Clock control using DS1302 can be year, month, day, week, ten, minutes and seconds, timing. Spare battery can ensure the real-time running clock, thus completing the recording, time limit control alarm of the machine operation.

The parameters of the stored by the chip 24C04, can be repeatedly read and write, data retention time of ten years.

VII. CONCLUSION

Because the EPS intelligent control system complexity, need through the display alarm module to coordinate the work of each module, the more important is the hardware design of reliability of each module is modified and improved after several years, the current EPS intelligent control system has been in the EPS system is greatly make use of put into production. As shown in Figure 6，it is a set of EPS control cabinet.

Figure 6 EPS control cabinet

REFERENCE

[1] HUANG Jun, LING Zhi-bin, CAI Xu, “A passive and isolated battery voltage monitoring method”, Advanced Technology of Electrical Engineering and Energy, China, Vol. 30, No.4, 2011, pp. 13-16,25.

[2] Jiang Yinping, Liu Jiangjiang, Li Jie, “Intelligent battery monitor based on MSP430 microcontroller unit”, Chinese Journal of Scientific Instrument, China, Vol. 29, No.5, 2008, pp. 1040-1043.

[3] Xiang-yang ZHOU;You-lan ZOU, “Cycle life prediction and match detection in retired electric vehicle batteries”, Transactions of Nonferrous Metals Society of China, China, No.10, 2013, pp. 3040-3045.

[4] JIANG Jiu-chun;WANG Zhan-guo, “Design of voltage detection of lithium-ion batteries online and offline”, Chinese Journal of Power Sources, China, Vol. 39, No.1, 2015, pp. 26-29.

[5] Chen Lunqiong, Li bei, “Intellectualized Online Detection System for State of Charge of the Motive Power Battery”, China, Vol. 34, No.12, 2013, pp. 58-61.

Liguo Zhang graduated from Northeast Petroleum University, China, and stayed on to teach today. From teaching period he obtained master degree in Control Theory and Control Engineering from Northeast Petroleum University, China, in 2009. In 2011, he began studying motor and electrical professional doctorate in Northwestern Polytechnical University, China. His main research interests are in permanent magnet synchronous motor and control, smart instrumentation.

Design of Intelligent Water Heater Control System

Sui Zhenyou
Inner Mongolia University for the Nationalities

***Abstract*— This paper introduces intelligent heater control system based on MCU. And C language is used to programme with intelligent heating to achieve the goal of control the water temperature. Software debugging, Keil joint commissioning with Protues and simulation run successfully. By welding components, debugging hardware circuit , the system is proper and can basically achieve intelligent control of the functions. This design of electric water heater is functional and practical and simple, and the MCU can improved system stability and accuracy.**

***Index Terms*— MCU; Intelligence control; Temperature sensor; Control system**

I. INTRODUCTION

In recent years, the development of the water heater is very rapid, with the development of power electronics, more and more types of water heaters. Earlier period is mainly water heaters heat resistance wire, its energy consumption, insecurity, low efficiency, was quickly eliminated. Water heater is the modern family in daily life, can provide bathing and washing and other daily use hot water for the family. As people's living standards improve, more and more people of all ages heater. Water heaters on the market currently features a simple, accurate water temperature can not be controlled. Most electric water heater with mechanical temperature control, reliability is poor, generally only a simple measurement and control. Later, with the gradual development of the application of electronic devices, electric water heater performance is greatly improved. Solar water heaters due to weather and climate and the impact of difficult installation conditions occupy a larger market share, so the rapid rise of the water heater and growing, has very important significance.

Smart water heater uses a digital measurement techniques in line with modern trends, traditional water heater features a single, low accuracy. Intelligent people can not meet the requirements, the results of the use of the latest electronic technology to improve the performance of the water heater is completely possible and necessary. This paper uses microcontroller digital water heater temperature control, to achieve automatic control of the water heater, designed a kind of automated, intelligent, easy to operate, control of high precision, cost-effective control system for electric heaters.

A.Structure of the system

This paper is mainly used as an electric water heater controller AT89S52 with key module, the temperature acquisition module, LCD module, electric heating module, alarm modules and other components. As shown in Figure 1.

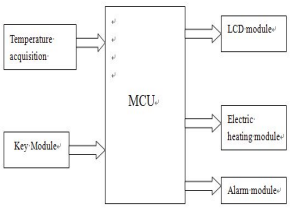

FIGURE1 Structure of system

System uses a digital temperature sensor DS18B20, easy wiring, can be used after the package into a variety of occasions. For example: a variety of general temperature measurement and control system temperature control greenhouse vegetables, hot water heaters, room temperature measurement devices, etc. [3-5]. It is a unique single interface mode, only one line will be able to interface with the microcontroller to achieve two-way communication, high temperature detection accuracy can reach 0.5 degrees. But this article is required accuracy was on it, so you can be able to achieve the target by the software design requirements. It is suitable for a large range of voltage 5V power supply can be used around, he also supports multi-point temperature measurements, can have up to eight connected together to provide precise temperature, simple structure, only three pins: data interface, power connector. The temperature measurement accuracy, can meet the needs of the majority of occasions. It outputs a serial digital signal is transmitted to the microcontroller, anti-interference ability, as well as self-correcting capabilities. Very easy to use, no external other originals, will be able to work properly. Compared with conventional AD converter circuit, has a great advantage, without going through the analog to digital conversion, control of high precision, simple programming, so this is the only use of integrated digital temperature sensor. As shown in Figure 2.

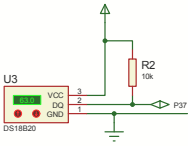

FIGURE2 Circuit of DS18B20

When measuring the water temperature is higher than 65 ℃, the microcontroller will output a signal to the port, after the amplifier capable of driving the buzzer alarm (buzzer does not sound due to the simulation, the result is not easy to see the change, so the buzzer between the device and ground plus a yellow LED lights display). In

this case the electric heating module stops working, the temperature is below the set value of electric heating module starts heating work, (as is the weakness of strong electric control, so this paper is to use LED to replace the resistive heating signal). When set to a temperature between 65 ℃, electric heating does not work. Alarm circuit input terminal is connected with the microcontroller P2.5, P2.4 heating circuit with the microcontroller is connected electrically heated with green LED instead. Note the LED wiring should not be reversed, and it is positive or negative points. Heating lamp module which need to add pull-up resistor drive, otherwise not too bright lights. Alarm circuit and the heating circuit shown in Figure 3.

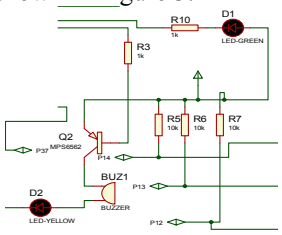

FIGURE3 Alarm and Heating Circuit

II.SOFTWARE DESIGN

A. Temperature acquisition program design

Must be initialized before processing such as display program, there are several common subroutines can be called directly before use.

Initialization process: initializing -ROM command - memory operation command - processing data

① DS18B20 all operations are initialized to the data line. Initialization block diagram is shown in Figure 12.

② ROM command

DS18B20 is detected on the bus, you can send ROM operating instructions [10]. This process is shown below in Table 1.

TABLE1 ROM operation code

INSTRUCTIONS	CODE
Read ROM	[33H]
Skip ROM	[CCH]
Match ROM	[55H]
Search ROM	[F0H]
Alarm search	[ECH]

① memory operation command, as shown in Table

TABLE2 Memory operation command

INSTRUCTIONS	CODE
Write Scratchpad	[4EH]
Read Scratchpad	[BEH]
Copy Scratchpad	[48H]
Convert Temperature	[44H]
Recall EPROM	[B8H]
Read Power supply	[B4H]

MCU starts running, the water temperature is first detected, if no other operations, it will always show the water temperature, the system default setting temperature is 45 ℃, the water temperature will maintain this temperature. If the water temperature is greater than the upper limit, the buzzer has been ringing until the water temperature decreases. And through treatment, the results are displayed on the LCD monitor, if normal, the keyboard detects whether there is pressed, the delay through the program, to confirm whether a button is pressed, if there is discrimination is plus or minus key is pressed key and enter the appropriate handler, when the water temperature drops below the set value, the electric heating wire begins to heat (due to limited conditions, this time using LED lights, lights on behalf of the heating circuit), so that the temperature reaches the set temperature. Buttons to set and display, KEY key first key is to select the function key is pressed again, the alarm temperature, set temperature, is recognized when the third press. Button is used to set query mode, programming easier.

About Digital temperature sensor monitors the initialization procedure called directly, this paper is a modular design, programming simple hardware circuit is more reasonable. As shown in Figure 4.

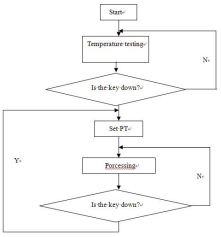

FIGURE4 Program Flow

III. CONCLUSION

In this paper, MCU is as the control center for smart water heater control system to meet the requirements after the design is complete. After the first by a digital temperature sensor DS18B20 collecting temperature, the microcontroller processing, into the LCD1602 LCD display. Wherein the temperature detection accuracy is 1 ºC. Microcontroller based on the current temperature values to control heating, alarm. When the temperature is greater than the current value of the buttons to set the water temperature is detected, the microcontroller to control the heating output, so that the temperature rises, heated to the set value. The current temperature is higher than the set value, not treated, the water heater automatically cool down, if the water temperature is higher than 65 ºC, stop heating, alarm buzzer. Preset temperature is 45ºC, adjustable via button. Design as well as imperfections, such as additional timing, water level monitoring, to be further improved and perfected.

REFERENCE

[1] GAO Lin. design and Application of Synthetic Software Simulation System for Multi-courses
Research and Exploration in Laboratory,2014.33 (6)
[2] ZHANG Jun. Smart Temperature Sensor DS18B20 and Its Application . INSTRUMENTATION TECHNOLOGY,2010(4).
[3] YU Hong-zhen Qin Zong-feng. Design of a Digital Temperature Alarm Based on AT89S52 and DS18B20. Techniques of Automation and Applications,2012.31(12).

The Change of Micropore Defect in Polyacrylonitrile Fibers during the Stabilization

Yurong Yang, Li Liu, Guomin Yan, Min Qiu, Yanmei Pi,
Department of Physics and chemistry, Heihe University, Heihe, China

***Abstract*—The change of micropore defect in polyacrylonitrile (PAN) fibers during the stabilization were studied.Based on the data of scattering intensity of the specimens, the size of micropore and the relative percentage of big micropore were calculated by using Fankuchen gradual tangent method, and the surface fractal dimension of the micropore were analyzed by a small angle X-ray scattering intensity method. The variety of micropore defect in PAN fibers during the stabilization was given. The results demonstrated that micropore size increased continuously in this process, the relative percentage of big micropore decreased. The axis ratio of micropore becomes smaller and smaller, and the surface fractal dimension of fiber increases with the temperature. The mechanical properties of fibers change with increasing heat treatment temperatures, and the variations of mechanical properties can be associated with changes in the structure of micropore. Both tensile strength and modulus decreased with increasing size of micropore.**

***Index Terms*—fibers, micropore, stabilization, mechanical properties, fractal dimension**

I. Introduction

Polyacrylonitrile (PAN)-based carbon fibers offer high strength, high modulus and light-weight. Owing to their excellent properties, PAN-based carbon fibers have gained more and more attraction. It has been widely used as reinforcement materials in many areas, such as aviation, aerospace and many other industrial fields [1].

In the preparation of PAN-based carbon fibers, precursor fibers undergo stabilization, carbonization and graphitization in order to gain high modulus fiber. Stabilization is a vitally important and time-consuming step, which is carried out in air at the temperature range from 180 to 300 °C, sometimes even higher up to 400 ºC [2], makes the fiber thermally stable for the next process. In this process, a series of complex chemical and physical changes can take place. Accompanying with oxygen atoms ingress and the non-carbon atom spill, a number of micropores produce in carbon fiber during this process. Additionally, micropore defect can change with the progress of thermal reaction. The micropore in carbon fibers seriously impair the mechanical properties [3]. Consequently, the micropore evolution during stabilization is essential to improve the quality of PAN-based carbon fibers. Takaku et al. Characterized micropore in PAN-based carbon fibers. Kaburagi et al. investigated the scattering from micropore within the fibers by small angle X-ray scattering during the stabilization and carbonization stages [4]. Thunemann et al. studied micropores in PAN-based fibers. We also discussed micropore in PAN-based carbon fiber and its effects on mechanical properties before. However, previous study was focused on the existence of micropore in carbon fibers and evolution during carbonization or during the tensile deformation. Up to now, the micropore mean size, and internal structure evolution in carbon fibers during the stabilization have not been investigated in detail. Some researchers believed that the best stabilized temperature is 270°C. Consequently, in this study we discussed the micropore evolution of carbon fibers stabilized from 270 °C to 310 °C. Additionally, the relationship between pore and mechanical properties was also measured.

II. Experiment

2.1 Precursor fibers

Acrylonitrile/itaconic acid (99.35/0.65) copolymer fibers fabricated in laboratory were used as precursor fibers in this study. The fibers were wet-spun in dimethylsulfoxide and had 1000 filaments in each single tow, 4.4 GPa tensile strength, 126GPa Young's modulus.

2.2 Stabilization

A continuous stabilization process was conducted in a five-zone tube furnace. The temperatures of the 5 zones were programmed as 270 °C -280 °C -290°C -300°C -310°C. Stretching was applied on PAN fibers by controlling the speed differences between the feed rollers and the take-up rollers, and the duration time in each furnace zone was controlled by the average feeding speed of fibers, the total residence time for 50 minutes.

2.3 Measurements and characterization

The microscopic surface of samples was studied by scanning electron microscopy (S-570, Japan, 20kv). Small angle X-ray scattering (SAXS) measurement was carried out with an 18kW rotating-anode X-ray generator (Rigaku, Cu-Kα, λ=0.15418nm). The X-ray beam scanned parallel to the carbon fiber axis and vertically to the fiber axis, respectively. A tensile test for each fibermultifilament was also carried out using a universal testing machine (AG-1S, Shimadzu, Japan), with a load cell of 1 kN at a crosshead speed of 20mm/min, according to GB/T 3362-1982.

The micropore size and relative percentage were calculated by Fankuchen gradual tangent method with SAXS measurements. The microstructure of PAN-based carbon fiber belongs to the band structure model. When the strip of fibers is not coordinated distribution, micropore forms between each other. The long axis of micropore preferred orientation along the fiber axis, the

short axis is perpendicular to the fiber axis. Therefore, it is assumed that the micropore shape is ellipsoid. The size of micropores in fibers is various and complex comparatively. Consequently, the calculated size of micropores is assembly average.

In this work, fractal surface of the micropore in fibers is analyzed by small angle X-ray scattering intensity method.

III. RESULTS AND DISCUSSION

Fig.1 is the SEM photos of transect of PAN fibers in different stage during the stabilization. It is shown that fibril of PAN fibers is closely combined, while the core organization is loose. Besides, there are many micropore defects in PAN fibers during the stabilization. Along with thermal reaction, the structure of micropore defect varied. The structure of PAN fibers is sheet radiation during the temperature zone of 270~310°C. It appeared large-sized structure defect in anaphase of the stabilization process, such as hollow, which were caused by the skin-core structure of PAN fibers.

Fig. 2 shows SAXS patterns for the five fibers. Based on the patterns, the micropores were characterized by the above mentioned method. The micropore length of long axis and short axis were determined by the formula (1) and (2), respectively.

$$I = I_e N n^2 \exp(-c^2 h^2 / 5) \tag{1}$$

$$I = I_e N n^2 \, exp(-a^2 h^2 / 5) \tag{2}$$

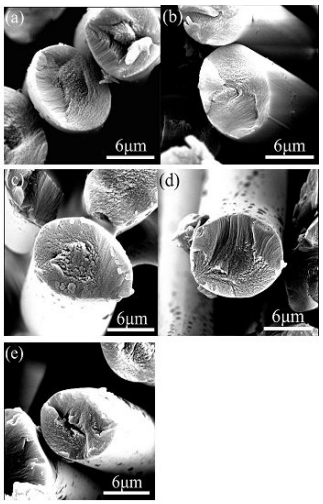

The microscopic surface of transect of PAN fibers(a)270 °C (b) 280 °C (c) 290 °C (d) 300 °C (e) 310 °C

Where I_e is one electron scattering intensity, N is the total amount of particles irradiated by X-ray scattering, n is the total amount of electrons in one particle, h is the diffraction vector, and h can be described as the formula (3).

$$h = |h| = 4\pi \sin\theta / \lambda \tag{3}$$

The micropore relative percentages were analyzed by the formula (4).

$$V_1 : V_2 : V_3 ..... = K_1 / R_1^{\,3} : K_2 / R_2^{\,3} : K_3 / R_3^{\,3} : ..... \tag{4}$$

Normalize formula (4) can obtain formula (5).

$$\sum_i V_i = 1 \tag{5}$$

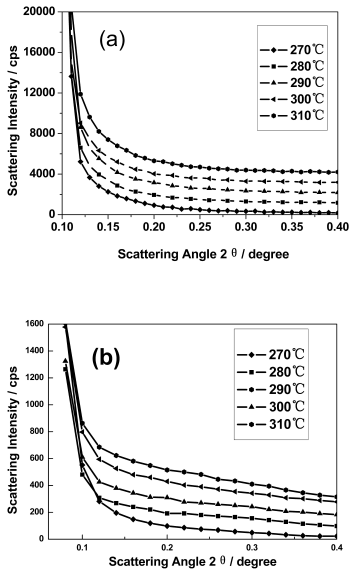

Figure 2. SAXS patterns of fibers (a) parallel to the fiber axis; (b) vertical to the fiber axis

Tab. 1 shows parameters and the surface fractal dimension of micropore in fibers. Generally, the size of micropore increased continuously with thermal stabilization processing. However, the relative percentage of big micropore decreased. It can be attributed to that both crystalline region and amorphous region in fibers participated in cyclization with increasing stabilization temperature [5]. The heat-resisting trapezoidal structure formed after reaction is compact，which lead to relative percentage of big micropore decreased. Moreover, temperature is high in the later thermal stabilization period, local overheating caused by heat release acutely and heat quantity accumulation of single filament lead to cleavage fracture of molecular chain, and big micropore defect formed. In addition, the axis ratio becomes smaller and smaller, indicating that the shape evolution of fiber from ellipse to circle.

From Tab 1, it is also found that the surface fractal dimension of fiber increases with the temperature. It is suggested that the roughness of the surface of micropore in fiber increase continuously during the temperature zone of 270~310°C.In the stabilization process, the structure of fibers became more and more compact [6]. After 270°C, the skin-core structure appeared possibly .Such non-homogeneous structure causes non-uniform thermal stress in fibers within the heating-up process after 270°C, which lead to microcrack appearance. Moreover, cyclization reaction in fibers is acute, molecular chain deformed and broken chain in the

effect of stretch [7], which leads to the surface of micropore became more and more rough.

TABLE I.
PARAMETERS OF MICROPORE IN FIBERS

Specimen	Size of Micropore long axis [nm]	Size of Micropore short axis [nm]	Big Micropore relative percentage[%]	Axis ratio (long axis / Short axis)	Fractal dimension *D*
A	1.76	4.23	52.19	2.40	2.01
B	2.23	4.36	42.53	1.96	2.13
C	2.89	4.52	37.74	1.53	2.29
D	3.14	4.61	33.65	1.42	2.47
E	3.71	4.75	31.86	1.28	2.58

The mechanical properties of fibers change with increasing heat treatment temperatures, and the variations of mechanical properties can be associated with changes in the structure of micropore [8]. The tensile strength and modulus treated at different temperatures are shown in Fig. 3 and Fig. 4. The changes in tensile strength can be divided into three zones. From 270 to 290°C, the tensile strength decreased rapidly with elevated temperature. In this temperature range, the size of micropore was small relatively. According to the Griffith theory, the strength of carbon fibers is influenced by the size of inherent cracks. The sizes of inherent cracks may be related to the sizes of micropore, and it can be seen that larger sizes lead to a weaker tensile strength. From 290 to 300 °C, the tensile strength decreased slowly due to the size of micropore increased slowly. From 300 to 310°C, the tensile strength decreased rapidly again, because of the size of micropore increased rapidly. Furthermore, the elasticity modululus decreased slowly below 280°C, due to the smaller size of micropore. Above 280°C, the elasticity modululus drop in a straight line. The results may be attributed to the formation of more and more defect structure.

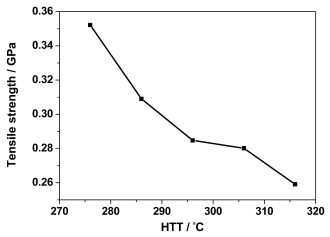

Figure 3 . The tensile strength of fibers treated at different temperatures

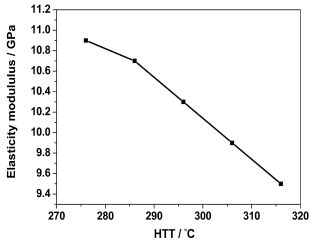

Figure 4. The modulus of fibers treated at different temperatures

IV. CONCLUSIONS

The change of micropore defect in PAN fibers during the stabilization were studied by SEM and SAXS. The results reveal that the size of micropore increased continuously with thermal stabilization processing, the relative percentage of big micropores decreased. The axis ratio become smaller and smaller, indicating that the shape evolution of fiber from ellipse to circle. Moreover, the surface fractal dimension of fiber increases with the temperature. It is suggested that the roughness of the surface of micropore in fiber increase continuously during the temperature zone of 270~310°C. Consequently, the mechanical properties of fibers change with increasing heat treatment temperatures, and the variations of mechanical properties can be associated with changes in the structure of micropore. Both tensile strength and modulus decreased with increasing heat treatment temperatures.

ACKNOWLEDGMENT

Financial support from the youth science fund of Heilongjiang province (QC2013C005) and youth research talents of Heihe University are gratefully acknowledged.

REFERENCES

[1] Y. Bai, C. Wang, N. Lun, Y. Wang, M.Yu, and B. Zhu, “HRTEM microstructures of PAN precursor fibers,” Carbon ,vol.44, pp.1773-1778 , February 2006.

[2] M. Rahaman, A. Ismail, and A. Mustafa, “A review of heat treatment on polyacrylonitrile fiber,” Polym Degrad Stabil, vol.92, pp.1421-1432, April 2007.

[3] C. Zhu, X. Liu, X. Yu, N. Zhao, and J. Liu., “A small-angle X-ray scattering study and molecular dynamics simulation of microvoid evolution during the tensile deformation of carbon fibers,” 2012, vol.50, pp.235-243, August Carbon.

[4] M. Kaburagi, Y. Bin, D. Zhu, C. Xu, and M. Matsuo, “Small angle X-ray scattering from voids within fibers during the stabilization and carbonization stages,” Carbon, vol.41, pp.915-926, November 2003.

[5] M. Yu, C. Wang, Y. Bai, Y. Wang, Q. Wang, and H. Liu, “Combined Effect of Processing Parameters on Thermal Stabilization of PAN Fibers,” Polym Bull, vol.57, pp.525-533, May 2006.

[6] Y. Xue, J. Liu, and J. Liang, “Correlative study of critical reactions in polyacrylonitrile based carbon fiber precursors during thermal-oxidative stabilization,” J. Polym Degrad Stabil, , vol.98, pp.239, November 2013.

[7] D. Edie, “The effect of processing on the structure and properties of carbon fibers,” Carbon, vol.36, pp.345-362, August 1998.

[8] A.Gao, C. Zhao, S. Luo, Y. Tong, and L. Xu, “Densification mechanism of polyacrylonitrile-based carbon fiber during heat treatment,” Mater Lett, vol.65, pp.3444-3446, July 2011.

The Research of Internet Remote Control

Sui Zhenyou
Inner Mongolia University for the Nationalities

***Abstract*— The remote control theory has a very wide range of applications in industrial processing, aerospace navigation, blasting, military and other industries and fields. The remote computer network cybernetics is in new application areas - network research in this particular area of and theoretical development, which has a network, information technology and other features, combined with control theory, system theory and the theory of network protocols, and gradually developed self-contained. The purpose of the computer network control is to improve and regulate the function or development of one or more network objects, it need to acquire and use information by adjusting the system input output controlled part of the state to achieve the desired goal. First, from the perspective of a computer network control system to study the network objects, certain properties of the network object, a process or some kind of problem on the network to study a certain range in order to better describe the network, research networks and control network. In summary, the network cybernetics is the study of a variety of internal communication network systems, control, coordination, organization, balance, stability, calculation and with the external environment of mutual feedback scientific methodology.**

***Index Terms*— internet, remote control,**

I. INTRODUCTION

Remote control system architecture and communication protocol is a major component of the computer network remote control.Computer network architecture network remote control system is a "minute" and "and" the network entities, network system is divided into two: the master network architecture and controlled network architecture, they make up the entire computer network remote control.May also be referred to as the master network server, the network may also be referred managed client, based on the service requirements. And achieve functional detailed classification. Managed network services, while maintaining the client in a relatively stable state; master network request service, to apply for the required services in accordance with the user's permission. Remote control system from a functional point of view can be divided into three parts: the main network systems, data transmission through. Road and controlled network system. Three parts work together to achieve the purpose of remote contro [l].

II. MASTER NETWORK

Network Cybernetics (Network Cybernetics) is a common theory of network system regulation and control process. Network control theory is the study of a variety of internal communication network systems, control, coordination, organization, balance, stability, calculation and with the external environment of mutual feedback scientific methodology. The main contents of cybernetics including network topology, information architecture and state structure and so on. Construction of the theoretical basis of the master network is the network cybernetics. Master network acting on information, network entities, in order to improve and regulate the function of a network or some object, the use of information systems by adjusting the input, the output of the controlled part to achieve the desired goals. Master network system to provide remote controller and the controlled interfacial interaction between devices. Its main features include input control command and its parameters, show that the accused device feedback information, and other necessary operations.[2] Currently, a wide range of applications and networks continue to expand the size of the computer network, the computer is the main operating platform for remote monitoring terminal. Messaging network architecture is shown in Figure 1.

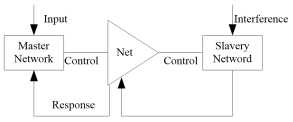

Figure 1 Messaging network architecture

III. SLAVERY NETWORK

Controlled network is a substantial nature, controllability and safety net system, which in the network cybernetics. Based on the use of certain control components, including software and hardware, the implementation of appropriate control mechanisms to provide the necessary control services. Central task is to provide managed network control services. Tightly controlled network connection controlled equipment. It is carried out in accordance with the control commands issued by the remote monitoring terminal transfer analysis, the accused device control, while monitoring the operational status of the controlled device, the necessary analysis, then as feedback data to the host system via the network data transmission channel. Controlled network system is a set of computer-centric site control, management, and data collection for Integrated control systems, computer hardware devices can be controlled, it can be a data resource. Controlled network architecture controlled by the network center, intermediate control node, acquisition node and user interface Structure, shown in Figure 2.

The overall design of the remote control system contents include: the overall structure of a remote control system and the implementation environment. A detailed description of the composition of the overall structure of a remote control system, and as a basis for design and implementation; achieve environmental introduce this system needs to develop software and hardware. Entire

computer network remote control system by the master network server, resource controlling node, a communication network, the firewall, the data service center resources, user control terminal and a controlled network resources and other components. Master network and controlled network system each composition, communications and operations between them is via a local area network or the Internet for delivery and communication. Network server is the master control information processing main site, its classified information, issued and monitor the operation of environmental equipment resources. Staff at the control terminal of the user operation performed after coding, the data format of a fixed transmission network through a communication network to a master server, the master server of the network interprets the received information, and performs a specific operation instruction specified by the network issued commands to the managed network servers. Controlled network server parses the command received and analyzed results to a specific device, and then the device status and operating results of the feedback information to the remote control terminal. Entire computer network remote control system structure shown in Figure 3.

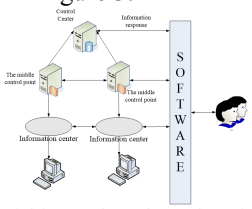

Figure 2 acquisition node and user interface Structure

IV. THE OVERALL DESIGN OF THE REMOTE CONTROL SYSTEM

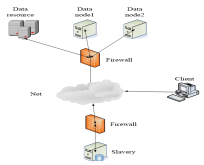

Figure 3. Computer Network Remote Control System Structure

Master network computer network remote control system is the ultimate user requirements and network application protocol based on

Norms, according to the functions, hierarchical to design and implementation. Generally speaking, the main functions of networks including service registration, device management, user settings and controlled end control and management, and thus divided into several main characters; the details of speaking, is in strict accordance with the master network Remote control network requirements and network communication protocols, and through the hierarchical relationship between the various parts of the organization, write code and implement various functions of the system. Web server hosting service resource management entity, is a computer network remote control resources Dynamic Tube.

The realization of one of the core management, so the quality of their relationship to the system to achieve the success of efficient and stable operation.

This section contains a network server computer network remote control master many key businesses, including: service resource registration, service resource management, user management, and other services, the different mechanisms of these services are interrelated, forming a complete service entities, to provide users more efficient resource management service. The main function of the service module is registered under the TCP / IP network protocol, the network communication port can be customized, port size must meet the design requirements.

Firewall, Multi-use firewall stateful inspection technology. State detection technology is from the TCP connection is established to carry out the termination of both tracking and detection technology. Detection process a full stateful inspection firewall is: to judge when to initiate a connection, if they meet the rules, registered in the memory of this connection state information (address, port, options), subsequent packets belonging to the same connection, it is does not require re-testing, and directly through. In addition, the firewall generally low ports (1-1024) packet inspection rarely, usually by default, while the high-port packet inspection and more stringent. In most cases, the firewall always as little as possible to open the port. In general, unique port can be used is 80, which is the port used by Web. Port remote control system developed by the subject using a high port, host and managed client communication, communication data will be subject to inspection firewall, or even be rejected. In the case of a firewall in order to run, the normal data packet communication systems to solve this problem is to transmit the information package. The solution is: channel transmission of information outside of the package the HTTP header, so that the information transmitted macro

The concept consists of two parts:

HTTP header + data reported

For each datagram plus HTTP header information through port 80 low transmission, without affecting

Under normal circumstances a firewall running through inspection firewall, enabling the system to normal operation.

V. CONCLUSION

This system can be applied to distance education, remote maintenance and other fields. In remote maintenance, you can count. Computer network equipment for remote management and maintenance, increase efficiency; in the network teaching, teachers can instruct multiple student teaching, learning to keep abreast of the situation. Therefore, the computer remote control technology of this research have broader application prospect

REFERENCES

[1] Chen Jianer,Wang Guo-Jun,Chen Song qiao. Locally subcube-connected hypercube networks: Theoretical analysis and experimental results.IEEE Transactions on Computers, 2002, (05):530-540.

[2] Zussman G,Segall A. Energy efficient routing in ad hoc disaster recovery networks[A]. San Francisco, CA, USA, 2003.682-691.

Construction Monitoring On Wide Prestressed Concrete Continuous Box Girder Bridge

Shidi
School of civil engineering and architecture , Chongqing Jiaotong University, Chongqing 400074,China

***Abstract*—In large span prestressed concrete continuous girder bridge wide construction process, in order to ensure that the bridge structure stress and deformation is always in a safe range, and after linear comply with the design requirements of girder structure dead load stress state close to design expectations, must carry out strictly the scene monitoring and control calculation.**

***Index Terms*— wide; The continuous beam; Construction monitoring**

I. Summary

As the number of traffic volume and traffic lanes increases, the girder section become wider, this situation make the girder stress calculation is different from other ordinary bridges, combined with many factors such as cantilever construction, it is necessary to monitor the bridge construction, to make sure the safety and reliability at every construction stage, Stability, linear structure, displacement and state
Construction monitoring is the construction monitoring and control.In bridge construction process, the weight of structure and construction load, construction process, concrete creep and shrinkage of the factors such as temperature, in different extent influence to achieve the goals of the bridge, bridge and could lead to the final closure difficulties, as a bridge is not in conformity with the problems such as linear and design requirements.Construction monitoring is based on the construction monitoring was carried out on the structural parameters of the real value of the phase calculation, identify each suspension pouring segment formwork elevation, and in the process of construction according to the monitoring results to the error analysis, forecast and to adjust the next formwork elevation, in order to ensure the bridge deck line after two cantilever, closure segments elevation relative deviation is not greater than the specified value as well as the structural internal force meets the design requirements.

II. The project summary

The construction monitoring of main bridge of prestressed concrete variable cross-section continuous box girder bridge, bridge approach for prestressed concrete section continuous box girder, the total length of 1188 m.Bridge standard section full width 49.5 m, divided into the upper, downward separation of two, single bridge 24.25 m wide, two bridge net distance of 1 m.The whole bridge using C50 concrete, hanging basket cantilever construction.Main monitoring scope includes the first triple (50 + 8 + 50 × 80), first approach (40 + 60 + 40) and the second league (40 + 60 + 40).

III. The main girder section stress monitoring

Construction control is mainly based on the construction process of real-time monitoring, real-time adjustment and correction all affect the factors of goal, ensure the bridge construction process to achieve the goals of safety and design into a state of bridge, make sure to bridge structural stress and linear meet the design requirements.During the continuous girder bridge construction of main girder elevation, stress in the process of implementation of double entry control;Main girder construction stage is given priority to with control level, control stress is complementary.
Through the normal stress of concrete box girder control section of monitoring, to observe whether the normal stress of box girder cross section in the process of concrete construction within the design requirements;Observed in the tension of prestressed steel beam, anchor, dead load and structure system conversion conditions, the change of the normal stress of box girder concrete, etc.

A. stress testing sensor layout

For prestressed concrete types of Bridges, based on my years of experience in the construction monitoring unit, using embedded steel string strain sensor is accurate and effective stress of the test.This bridge the ZX - 215 ct embedded intelligent concrete strain transducer (test range + 1500 mu for epsilon, sensitivity of 0.1 Hz).Sensor layout should not affect the construction of the construction unit, the objective of the number of sensor placement mainly is to ensure that the stress and temperature data collection, prevent the damage of the sensor and the interaction between the sensor data checking.Both satisfy the box girder stress data sampling and does not affect the subsequent construction, the construction units do not affect the safety of construction personnel to walk across the bridge, also can better protect the sensor, ensure the safety of monitoring the team at the time of data collection, the team decided to adopt below sensor embedded mode.Because the blocks 0 #, 1 # bridge adopts stent placement at the same time, the stress testing sensor embedded between 1 # and 2 # block, on the cross section of the concrete arrangement as below.

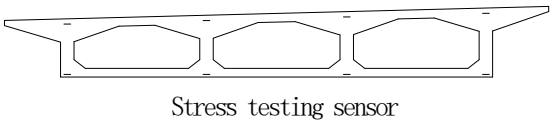

Figure 1 Girder stress of section near 2 # block sensor layout

B. stress monitoring

To prevent damage to the sensor for concrete pouring, sensor embedded in the corresponding position of longitudinal reinforcement side, side under transverse reinforcement or close to 1 # lead block section.For each section suspension pouring of tested the following three stages:

(1)before concrete pouring, monitoring station of the affected each section readings;

(2) after the concrete pouring, monitoring station of the affected each section readings;

(3) after the prestressed tensioning, monitoring station of the affected each section readinas.

Monitor the control process is as follows:

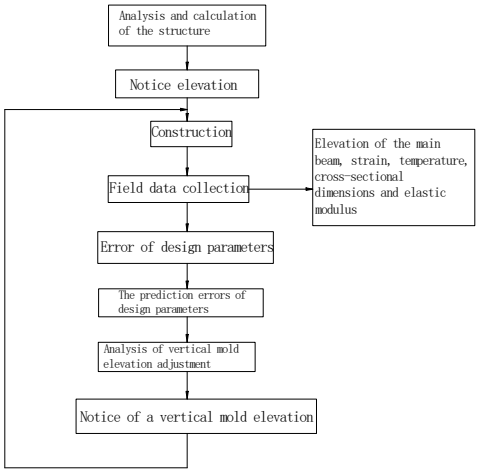

Figure 2 Construction control block diagram

To process the measured stress data for each construction condition, and compared with the theoretical value of Midas Civil modeling to calculate and make detailed analysis on the measured results.To approach the left picture # 3 # pier pile as an example

The main reason for the deviation are:

(1) the bridge is wide, and Midas Civil to truss unit modeling, not considering the influence of shear lag effect, there exist deviations in leading to the actual measured value with the theoretical value.

(2) modeling computation load, not considering the accumulation of actual construction of bridge deck can make under some stress is larger.

(3) used to observe stress strain gauge itself is error.

C. the model elevation control

In the process of cantilever construction of this bridge, elevation of beam section of the model of the reasonable, is related to the main girder of linear whether smooth, whether to comply with the design of a key.If the consideration in determining the model elevation is in line with the actual, and to the right control, eventually into a bridge line generally is relatively good;On the contrary, if you don't conform to consider the factors and the actual situation, control, will eventually into line with the design line bridge have larger deviation.Therefore require surveyors under various operating conditions on the control points of elevation accurately measuring, strictly control the elevation, the model to the school before concrete pouring mold.

IV. THE KNOT LANGUAGE

Judging from the current monitoring data, the stress test results are in conformity with the actual construction situation, and the theory of stress calculation values were similar, local deviation is due to the local stress (bridge pile load has some influence on stress) and the main box beam shear lag effect, and the overall test stress satisfy the requirement of the specification for construction stage of stress, at this stage bridge main body structure overall stress in a safe range.

REFERENCES

[1] LiKai,Fan Liang, Peng Guorong , ZhaoHui, ZhangFan, Si Jinyan, Lu Kaiyan. Suspension pouring construction of main girder deformation monitoring principle and the procedural operation method[J].Highway,2012,32(4):177-181.

[2] Shi Debin, Cheng Langzhou, Zhu Wenqing . Large span cross-section of prestressed concrete continuous girder bridge construction monitoring [J]. Railway standard design, 2006, (2) : 51-53.

[3] Bao Weigang ,Zhou Yongtao .Large prestressed concrete girder bridge design and construction technologyguide[M].Beijing:people'strafficpress,2009.

[4] Zhang Hanwu. Continuous girder bridge construction monitoring analysis [D]. Xi 'an: chang 'an university, 2012.

Empirical Analysis and Evaluation on Chinese Real Estate Regulation Policy -- a Case Study of the Housing Market

Zhang Xuefeng[1,2]
1. Finance Research Centre, Fudan University, Shanghai, China;
2. Business School, Jiaxing University, Jiaxing, China

***Abstract*—Huge economic and social risks exist in the housing prices continuing to rise behind, it also highlights the importance of effective regulation and control policy. This paper constructs a SVAR model of housing price index, area of land acquisition, domestic enterprises loans and housing loan interest rates to carry out the empirical analysis. The results show that, the pushing up effect of domestic loans to housing prices is the most obvious function, and increasing the supply of land and housing loan interest rates policy did little to curb housing prices rose. Cooperation, execution and persistence of macro policy are the key to effective control of the housing price.**

***Index Terms*— housing price, regulation policy, SVAR model, positive feedback**

I. INTRODUCTION

Chinese housing market appears to be "irrational prosperity" in recent years. Housing prices in China also are in the fast rising trend in most of the time. As shown in figure 1, we set the ordinary commercial housing price in the year 2000 as the base 100 and give the price index trend figure in the last fifteen years. From the visual point of view, the average price of ordinary housing in China rise too fast in the past fifteen years and the amount of increase even reached more than doubled.A series of regulatory measures have being promulgated on the rapid rise in housing prices that closely related to the people's livelihood. But the results are not ideal. On the contrary, housing prices began to fall into a vicious circle of "regulation – wait and see -- rebound". This will lead to greater economic and social risk. What are the influence direction and extent of the national regulation and control policies to housing prices? How should we to improve the policies? The investigation of these problems is the research motivation of this study. This paper innovatively constructs a multi factors SVAR model and carries out the empirical analysis. Then we derive the conclusion of the study, and puts forward relevant policy suggestions. The research has important positive significances for the improvement of housing supply structure, alleviating residents purchase burden and improving the housing regulation policy at present.

The remaining sections are as follows: the second part is the literature review; the third part is the empirical research design; the fourth part is the empirical results and analysis; the last part is the conclusion and policy suggestion.

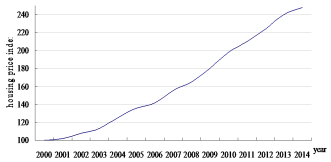

Figure 1. Trend index of Chinese residential price in 2000-2014

II. LITERATURE REVIEW

Overall, most of the relevant literature is qualitative research and quantitative research less. These studies mainly focus on three aspects:

One is the discussion of regulation and control policy based on the analysis of several factors impact on housing price. Karsten Lieser & Alexander Peter Groh (2014) argue that financial regulation and control policy are unable to curb costs increase in the investment funds in housing industry. Instead, they lead to the dilemma burden of other industries and market atrophy. Heinz Rehkugler et al. (2012) and Alireza Bozorgi(2015) argue that location, subway, occupancy, time and direction etc. have significant influence on housing price. Fu-zhou Luo and Yu-ze Wang (2012), Alireza Bozorgi (2015) also did the similar research.

The second is the analysis based on certain policy. Michael Berlemann & Julia Freese (2013) argue that the money supply is more significant than the interest rate policy based on the cointegration analysis on monetary policy. David H. Downs & Lan Shi (2015) argue that the effect of monetary policy on housing prices regulation is not obvious based on the analysis on the monetary policy. Beatrice et al (2015) did the similar study from the angle of land value-added tax.

The third is the analysis based on a certain social scientific theory or model. Ricardo Fontes & Carlos Melo Brito(2014) ,whose research based on the construction of housing price regulation model from the expectations theory angle, insist that policy expectations of market can lead to short-term failure but effectual in medium and long term. Karine Brisset et al(2015) reveal the perplexing interests relationship and its change law from the view of game theory,

The above research can explain the effectiveness of regulation and control policy to a certain extent. But due to certain limitation of study interval, influencing factors selection of the regulation policy and the test theory method, they don't reach agreement on the direction and intensity of regulation policy. This paper constructs a

SVAR model of housing price index, area of land acquisition, domestic enterprises loans and housing loan interest rates to carry out the empirical analysis on the Effects of time delay, the direction and the intensity of regulation policy to housing prices. This research can provide the basis for China's next step for the scientific development of regulation and control policy.

III. THEORY AND MODEL

A. Model Selection

Sims (1980) proposed the vector autoregressive model (VAR) which use the multiple equations form. In each equation of model, endogenous variables of the model contained all the endogenous variables lagged regression was used to estimate the endogenous dynamic relationship between variables, but can not reflect the exact form of the current relationship between variables. In addition, the VAR model parameter estimation requires much more variables, and estimates of VAR that only contains fewer variables can get through the OLS and maximum likelihood test. Meanwhile, with little consideration of economic theory, the impulse response generated by it cannot be identified as the intrinsic structure error. As a result, it is unable to give the structural interpretation.

Therefore, Blanchard and Quah (1989) modified the VAR model and put forward the structural vector autoregression model (SVAR). It's the structural formula of the VAR model in essence. That's to say, we add the current relationship between variables in the general VAR model so that we can extract the current relationship between current relationships hidden in the error term and make the model more clear in economic significance. Therefore, applying the SVAR model to the housing price control policy effectiveness evaluation has three advantages: firstly, any regulation and control policy variable in the model is assumed to be endogenous, not in strict accordance with the priori theory, is not set in advance of internal and external variables, also can be directly used least squares (OLS) estimation; secondly, the current relationship between the policy variables is given to avoid the Cholesky VAR method in the decomposition of initiator endogenous variable ordering sensitive effect on the results; thirdly, the model has less restriction conditions and can avoid the negative effects imposed constraints on the possible long term error model results.

If the P order structural vector autoregression model SVAR (P) containsk (k≥3) variables, the general matrix form can be expressed as below:

$$B_0 y_t = \Gamma_1 y_{t-1} + \Gamma_2 y_{t-2} + \cdots + \Gamma_p y_{t-p} + u_t \qquad (1)$$

Where,

$$t = 1, 2, \cdots, T \text{ , } B_0 = \begin{bmatrix} 1 & -b_{12} & \cdots & -b_{1k} \\ -b_{21} & 1 & \cdots & -b_{2k} \\ \vdots & \vdots & \ddots & \vdots \\ -b_{k1} & -b_{k2} & \cdots & 1 \end{bmatrix},$$

$$\Gamma_i = \begin{bmatrix} \gamma_{11}^{(i)} & \gamma_{12}^{(i)} & \cdots & \gamma_{1k}^{(i)} \\ \gamma_{21}^{(i)} & \gamma_{22}^{(i)} & \cdots & \gamma_{2k}^{(i)} \\ \vdots & \vdots & \ddots & \vdots \\ \gamma_{k1}^{(i)} & \gamma_{k2}^{(i)} & \cdots & \gamma_{kk}^{(i)} \end{bmatrix}, i = 1, 2, \cdots, p \text{ , } u_t = \begin{bmatrix} u_{1t} \\ u_{2t} \\ \vdots \\ u_{kt} \end{bmatrix},$$

$$y_{t-j} = \begin{bmatrix} y_{1t-j} \\ y_{2t-j} \\ \vdots \\ y_{kt-j} \end{bmatrix}, j = 0, 1, 2, \cdots, p \text{ ,}$$

p is the lag order, T represents the number of samples. If B satisfy the reversible conditions, formula (1) can be transformed into:

$$y_t = B^{-1}\Gamma_1 y_{t-1} + B^{-1}\Gamma_2 y_{t-2} + \cdots + B^{-1}\Gamma_p y_{t-p} + B^{-1}u_t = A_1 y_{t-1} + A_2 y_{t-2} + \cdots + A_p y_{t-p} + e_t \qquad (2)$$

Thus, we can estimate structure matrix B according to the simplified formula estimated from $e_t = B^{-1}u_t$. But if we want to get the unique estimation parameter of structural model, it should meet the requirements that the number of unknown parameters of the simplified formula is no more than that of the structural model. That is to say, we need to impose $k(k-1)/2$ constraints to estimate the parameters of the structure model.

B. Variables Determine

Because of the housing price regulation is to proceed from the supply and demand, the core policy will be the supply of land, housing supply structure, credit etc. This paper chooses four variables considering the availability of data as below to construct the model:

Sales index of housing prices (SI). This index which is integrated by a variety of factors can reflect the fluctuation of housing prices.

Domestic loans in the housing development funds (DL). In the process of housing development，domestic loans is the most important source of funds except for the self financing. It can reflect the effect of policies in housing supply by means of credit control.

Land purchase (LB). It's the most sensitive index in reflecting the policy intent and its effects.

Interest rates of housing mortgage loan (MR). The government often takes measures by regulation of interest rates to affect housing demand.

So we construct a can SVAR model consist of four elements as formula (2):

$$By_t = \Gamma_1 y_{t-1} + \Gamma_2 y_{t-2} + \cdots + \Gamma_p y_{t-p} + u_t \qquad (2)$$

where,

$$y_t = \begin{bmatrix} \mathrm{SI}_t \\ \mathrm{DL}_t \\ \mathrm{LB}_t \\ MR_t \end{bmatrix}, B = \begin{bmatrix} 1 & -b_{12} & -b_{13} & -b_{14} \\ -b_{21} & 1 & -b_{23} & -b_{24} \\ -b_{31} & -b_{32} & 1 & -b_{34} \\ -b_{41} & -b_{42} & -b_{43} & 1 \end{bmatrix}, u_t = \begin{bmatrix} u_{1t} \\ u_{2t} \\ u_{3t} \\ u_{4t} \end{bmatrix}, \Gamma_i = \begin{bmatrix} \gamma_{11}^{(i)} & \gamma_{12}^{(i)} & \gamma_{13}^{(i)} & \gamma_{14}^{(i)} \\ \gamma_{21}^{(i)} & \gamma_{22}^{(i)} & \gamma_{23}^{(i)} & \gamma_{24}^{(i)} \\ \gamma_{31}^{(i)} & \gamma_{32}^{(i)} & \gamma_{33}^{(i)} & \gamma_{34}^{(i)} \\ \gamma_{41}^{(i)} & \gamma_{42}^{(i)} & \gamma_{43}^{(i)} & \gamma_{44}^{(i)} \end{bmatrix}$$

C. Constraints of Equation

The SVAR model contains 4 variables, so we need to impose 6 constraints to identify the structural shocks. According to economic theory, the 6 constraints can be used as below:

The domestic loans in residential development investment funds are applied to continue the projects in

construction and maintain the normal operation of enterprises. It will affect the housing price in the lag period. So there is little effect of DL on the current SI, namely $b_{12}=0$ in the matrix B.

The aim of purchase of land current is for the later development, but the housing price is determined by the relation of supply and demand of the current residential commodity available for sale. So the current land acquisition affect little to the current residential prices, namely $b_{13}=0$ in the matrix B.

Changes in interest rates of housing mortgage loan will affect the demand for buying houses, but according to the "land administration law", the enterprise who obtains land must begin to construct in two years. This constraint determines that the loan interest rate changes will not affect the housing development enterprises obtain domestic loans (DL), namely $b_{24}=0$ in the matrix B.

Residential development enterprises have reserve a certain amount of land or some funds for land acquisition for continuous operation, as well as according to the relevant laws and regulations, domestic loans is mainly used in the construction of the project and has little effect on the current land acquisition, namely $b_{32}=0$ in the matrix B.

Changes in interest rates of housing mortgage loan has little effect on land purchase of the current because the commodity housing supply is inelastic, namely $b_{34}=0$ in the matrix B.

The current land acquisition area has little effect on the interest rates of housing mortgage loan. Because the current purchase of land is mainly used for the reserves and later development, and will not affect the current housing market, namely $b_{43}=0$ in the matrix B.

D. Data

The data applied in this paper mainly come from the Macro Industry Database, National Research Network Statistics Database, China Infobank and "China Statistical Yearbook 2014". For individual missing data, make up for it with K- distance to the nearest neighbor method, and have obvious seasonal factors variables were seasonally adjusted using the X11 program. At the same time, because of our country's housing loan interest rates are set by the central bank and have non complete marketization. In order to reflect the real cost of the current housing buyers, we adjust the interest rates of housing mortgage loan, based on more than 5 years of interest rates of commercial bank, with monthly consumer price index. So we get 168 groups of monthly data finally. The following modeling and analysis are operated by eviews 7.0.

Ⅳ. EMPIRICAL RESULTS AND ANALYSIS

A. ADF Test

In the SVAR model, if the series is nonstationary, its impact on the degree of convergence will be greatly reduced, thereby affect the stability of the empirical results. Therefore, stationarity test of the variable should carried out before the estimation of the SVAR model and the optimal lag is determined by AIC information criterion. The stationarity test results are shown in table 1.

We can see from table 1 that each series are non-stationary series before difference, but they all have a unit root after first-order differential. So we denote the original time series as I (1).

TABLE Ⅰ STATIONARY TEST OF EACH VARIABLE

Variables	Test form(C, T, P)	ADF-Statistic	5% Critical value	Prob.	Conclusion
SI	(c，t，1)	-2.4722	-2.8861	0.1249	Unstationary
D(SI)	(c，t，1)	-4.3026	-2.8863	0.0007	Stationary
DL	(c，t，12)	2.0723	-2.8887	0.9999	Unstationary
D(DL)	(c，t，11)	-3.8836	-2.8887	0.0030	Stationary
LB	(c，t，11)	-2.6896	-2.8884	0.0791	Unstationary
D(LB)	(c，t，12)	-3.9254	-2.8889	0.0026	Stationary
MR	(c，t，0)	-1.8702	-2.8859	0.3453	Unstationary
D(MR)	(c，t，0)	-9.6212	-2.8861	0.0000	Stationary

B. Residual and Model Stability Test

Because the longer the lag is, the worse of the model stability become. Stability of the SVAR model is crucial to judge the merits of the model. Therefore, the longest lag is one period before when the SVAR model does not satisfy the stability conditions. That is to say we should first ensure that the SVAR model is stable, then exclude unsignificant model by period according to the residual test. Accordingly, the optimal lag model finally determined for 4. Residual test results (Table 2) shows that the joint distribution of model residuals obey normal distribution, LM autocorrelation test shows that there are no autocorrelation for the model residuals in lag phase 1-11.

Table Ⅱ VAR (4) residual test

	Lag Period	LM Statistic	Prob. Value	J-B Normal Test
Autocorrelation test	1	13.5	0.63	$X^2(55)=1275.61$ (Prob.=0.0000)
	2	21.8	0.15	
	3	6.71	0.98	
	4	21.3	0.17	
	5	14.9	0.53	
	6	6.95	0.98	
	7	8.60	0.93	
	8	11.3	0.79	
	9	7.66	0.96	
	10	14.8	0.54	
	11	21.6	0.16	
	12	242.5	0.00	

AR roots method is applied to test the stability of the model. The result is that the absolute value of all roots of the estimated VAR model are less than 1 as shown in Figure 2. Therefore, the model satisfies the stability condition and the SVAR model is the ideal.

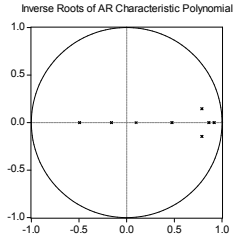

Figure 2. Stability test of the SVAR model

C. Analysis on the Impulse Response Function

1. Observation of the overall contrast

We can see from Figure 3, 4, 5 and Figure 6 that the relaxation of credit, increasing the supply of land and interest rates of housing mortgage loan rising have little effect on the current housing prices. But in the long run, they will produce positive effect on housing prices.

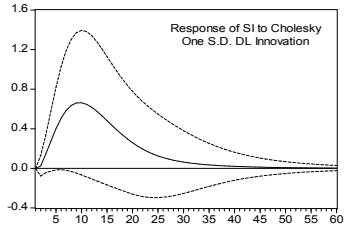

Figure 3 Response of SI to DL

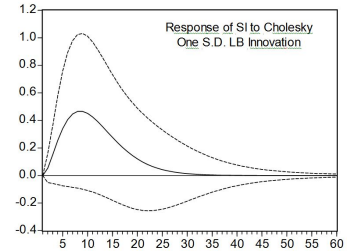

Figure 4 Response of SI to LB

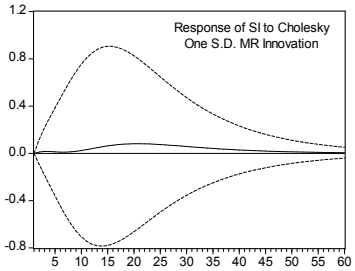

Figure 5 Response of SI to MR

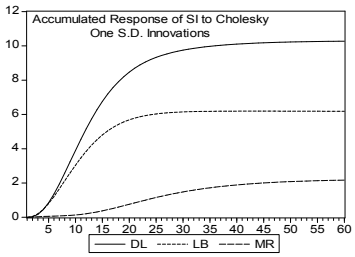

Figure 6 Cumulated response of SI to DL, LB, MR

Note: The horizontal axis represents the lag period (unit: number of months), the vertical axis represents the number of response, the curve represents impulse response function, the dotted line represents plus or minus two times the standard deviation deviation zone.

2. Analysis on the impulse response of housing prices to domestic loans of residential development enterprises

We can see from figure 3 that when a positive impact is given to the current domestic loans, the current housing prices will not change much. But after a quick response, and reach the peak response in the tenth period (0.6632), then the response decline fast until close to zero. We can see the accumulation graph of DL impulse response to SI from figure 6 that the cumulative response rapidly grow from the first period to thirtieth period, but to the 30 period, the cumulative response tends to be stable, but also positive response. Therefore, the current easing in credit of residential development enterprises, housing prices begin to rise rapidly, this effect will gradually disappear in two and a half years. It also reflects that the existence of hoarding behavior in a large number of development enterprises or intermediary property. When they can smoothly access to loans and funds chain will not break, they will not have worries about financial problems, then set high housing prices and boost the housing prices.

3. Analysis on the impulse response of housing prices to land purchase

We can see from figure 4 that when the current land supply is given a positive impact, housing prices response fast to rise starting from scratch, and reach the peak response in the ninth period (0.4659). Then the response decreased rapidly until to zero. We can see the accumulation graph of LB impulse response to SI from figure 6 that the cumulative response and rapidly grow from the first period to the twenty-second period, but the cumulative response tends to be stable at the 22 period, and is also positive response. Look from the surface, which is contrary to the principles of Economics: the supply of land will increase the expansion of housing supply, thereby reducing the housing price, why the reality is that housing prices did not fall but rise? Combination of the analysis on the second part of the paper, we can infer that there are three main reasons: the first is the unreasonable structure of land supply and serious shortage supply of ordinary residential; the second is excessive dependence of local government on land revenue and the high land prices also contributed to rapid rising of housing prices; the third is the massive existence of land enclosure, land hoarding and land speculation behaviors.

4. Analysis on the impulse response of housing prices to interest rates of housing mortgage loan

We can see from figure 5 that when a positive impact is given to the current housing mortgage loan rate, the housing prices for their response is to start to increase from zero very slowly, and reached to the peak response in the twenty-first period (0.0818), from then it begin to decreased slowly, gradually and tends to zero. We can see the accumulation graph of MR impulse response to SI from figure 6 that the cumulative response grow rapidly from the first period to the fortieth period, but by the period of fortieth, the cumulative response tends to be stable, and still is positive response. Look from the surface that this is contrary to the principles of Economics: raise housing loan interest rates mean that the purchase costs will be higher in order to curb the speculative demand. On the contrary, but why the housing prices become higher with the step of curbing? There are two main reasons: one is that China is now at the release stage of housing difficulty relief, improvement and investment demand at the same time and the rigid demand for housing is strong; the other one is that many speculators and hot money access into the housing market under the support of positive feedback trading psychology and excess liquidity.

Ⅴ. CONCLUSIONS AND SUGGESTIONS

A. Conclusions

The conclusions of this paper are as follows:

1. Although the domestic loans in the housing development funding accounts for only about 25%, its effect on the rise of the housing prices is very obvious, as well as long-term lagged effects.

2. The Land supply policy which attempts to increase housing supply and stabilize housing prices doesn't achieve the desired effect. The Land supply policy is counteracted by the rapid rise in housing prices manifested by an additional unit of land supply but will make the 0.466 increase in housing prices. However, the lag effect is short-term that no more than two years.

3. The policy of interest rates of housing mortgage loan which attempts to suppress housing demand doesn't achieve the desired effect. On the contrary, the phenomenon of demand more brisk and house price boost accompany with interest rates of housing mortgage loan higher. Meanwhile, the lag effect is longer up to three and a half years.

4. The psychological expectations, positive feedback trading and the lack of policy coordination etc. may be the mainly reasons for the ineffectual policy of regulation and control.

B. Suggestions

Policy recommendations are as follows:

1. In view of the fact that business loan growth will promote housing prices rising fast, first of all we should stabilize the credit of the development of enterprises to stabilize the housing prices. So we should slow down the growth of domestic loans to the development of enterprises.

2. Only one kind of policy to regulate and control the housing price effects may be not ideal in practice. We should adopt a comprehensive policy according to the market conditions to achieve the desired target. Meanwhile, we should pay attention to maintaining the policy execution and continuity, guarding against the positive feedback trading psychological growth.

ACKNOWLEDGMENT

This material is based upon work funded by Zhejiang Provincial Natural Science Foundation of China under Grant No. LQ14G030019. This is also a stage result for the China Postdoctoral Science Foundation under Grant No. 2013M540312 and Zhejiang Province Federation of Social Sciences project under Grant No. 2013B071. The author is grateful to their support.

REFERENCES

[1] Karsten Lieser and Alexander Peter Groh," The Determinants of International Commercial Real Estate Investment," in *J Real Estate Finan Econ*, vol.48, 2014, pp.611–659.

[2] Heinz Rehkugler, Felix Schindler and Rafael Zajonz," The net asset value and stock prices of European real estate companies," in *Z Betriebswirtsch*, vol.82, 2012, pp. 53–77.

[3] Alireza Bozorgi," Integrating value and uncertainty in the energy retrofit analysis in real estate investment—next generation of energy efficiency assessment tools," in *Energy Efficiency*, vol.2, 2015, pp.9331–9339.

[4] Michael Berlemann and Julia Freese," Monetary policy and real estate prices: a disaggregated analysis for Switzerland," in *International Economics and Economic Policy*, vol.10, 2013, pp. 469–490.

[5] David H. Downs and Lan Shi," The Impact of Reversing Regulatory Arbitrage on Loan Originations: Evidence from Bank Holding Companies," in *J Real Estate Finan Econ*, vol.50, 2015, pp.307–338.

[6] Beatrice D. Simo-Kengne, Stephen M. Miller, Goodness C. Aye," Time-Varying Effects of Housing and Stock Returns on U.S. Consumption," in *J Real Estate Finan Econ*, vol.50, 2014, pp.339–354.

[7] Ricardo Fontes Correia and Carlos Melo Brito," Mutual influence between firms and tourist destination: a case in the Douro Valley," in *Int Rev Public Nonprofit Mark*, vol.11, 2014, pp.209–228.

[8] Karine Brisset, François Cochard and François Maréchal," Is the newcomer more aggressive when the incumbent isgranted a Right-of-First-Refusal in a procurementauction? Experimental Evidence," in *Theory and Decision,* vol.78, 2015, pp.639–665.

[9] Jo´zsef Hegedu¨s," M. Lux: Housing policy and housing finance in the Czech Republic during transition (an example of the schism between the still-living past and the need of reform)," in *J Hous and the Built Environ,* vol.27, 2012, pp.265–266.

[10] Sasha Tsenkova and Dominika V. Polanska," Between state and market: housing policy and housing transformation in post-socialist cities," in *GeoJournal,* vol.79, 2014, pp.401–405.

[11] Berit I. Nordahl," Convergences and discrepancies between the policy of inclusionary housing and Norway's liberal housing and planning policy: an institutional perspective," in *J Hous and the Built Environ,* vol.29, 2014, pp.489–506.

[12] Zhanna Kravchenko," Policy discourse and biography: scripting adulthood into housing policies in comparative perspective," in *GeoJournal,* vol.79, 2014, pp.513–525.

[13] Theresa L. Osypuk," Shifting from policy relevance to policy translation: do housing and neighborhoods affect children's mental health?," in *Soc Psychiatry Psychiatr Epidemiol,* vol.50, 2015, pp.215–217.

[14] Carissa Schively," Sustainable development as a policy guide: an application to affordable housing in island communities," in *Environ Dev Sustain,* vol.10, 2008, pp.769–786.

[15] Mark Stephens and Christine Whitehead," Rental housing policy in England: post crisis adjustment or long term trend?," in *J Hous and the Built Environ,* vol.29, 2014, pp.201–220.

[16] Manuela Madeddu," Housing quality and the rescue of failed private housing schemes in England: a policy review," in *J Hous and the Built Environ,* vol.28, 2013, pp.567–578.

Zhang Xuefeng, born in Luohe City, Henan Province, China. The date of birth is January 8, 1981. The author graduated from Xi'an Jiao Tong University, Xi'an, China, in 2012, Ph.D. in economics.

His working background is as follows: 07/2012 till now, in Business School in Jiaxing University, Jiaxing, China, Lecturer in Finance; 03/2013 till now, part-time postdoctoral research in Financial Resarch Center, Fudan University, Shanghai, China. He has published more than 20 academic papers and 3 books, such as Stability of Housing Affordability: Theoretical Analysis and Empirical Analysis (Beijing, Finance and Trade Economics, 2011); Heterogeneity of Demand, Positive Feedback Trading and Abnormal Fluctuation of Housing Prices (Beijing, Economic Management, 2011); Housing Prices: Dynamic Mechanism, Abnormal Fluctuation and Regulation(Beijing, Chinese Social Science Publishing Press, 2012) etc.

Dr. Xuefeng, now works in Jiaxing University, China, mainly studies the real estate economy and financial markets. He is also the deputy director of Finance Institute, Jiaxing University and expert in performance evaluation, Jiaxing Finance Bureau.

Isolation and screening of halo-tolerant strains and their application in saline soil remediation

Ruimin Fu[1,2] , Wenhui Xing[1], Hong Zhang[1], Xiaowei Wu[2], Tingting Xue[2], Yanan Gu[2], Yaya Wang[2], Feng Yu[2], Maolin Du[2], Wuling Chen[2]

[1]Department of Life Science, Henan Normal of Education, Zhengzhou, China 450046
[2]College of life Science, Northwest University, Xi an, 710069

***Abstract*—Soil salinization is a serious land-degradation problem that affects soil, plants and groundwater within ecosystems. In this work, the saline soil was restored by halo-tolerant microbes.Four strains, with halo-tolerant ability, were isolated from saline soil and selected out by enrichment culture and screening. Through morphological, physiological and biological characterization, the strains were separately identified as Pseudomonas sp., Bacillus subtilis, Bacillus megaterium and Yeast. The four strains were mixed together with the ratio of 1:1:2:2 and fermented to produce bio-organic fertilizer which was used to restore the saline lands. The effect on improvement of soil fertility was investigated with growth assays of *Alopecurus pratensis Swartz*. As was shown in the result, these complex microbial agents could not only reduce the salt content and pH but also increase the organic content of the saline soil. Moreover, the seed germination rate, plant height and grain yield of Alopecurus pratensis Swartz grew in the different treatments had different levels of increasement. Overall, Restoring saline soil by addition of biological organic fertilizer fermented by halo-tolerant complex agents seems to be a promising strategy for saline soil remediation with simultaneous improvements of nutrient/organic matter contents.**

Index Terms*—halo-tolerant, biological organic fertilizer, saline soil, complex agents, *Alopecurus pratensis Swartz

I. Introduction

Saline soils are widely distributed on the earth [1,2]. According to the incomplete statistics of UNESCO and FAO, the saline-alkaline land area is 99.13 million hectares in China, and they are mainly distributed in low terrain, high underwater table, semi-humid, semi-arid and arid inland or coastal areas[3].

When the land was degraded to bare saline-alkaline soil, the plants couldn't grow on it because high toxic ionic content and pH are harmful to the survival of introduced plants ,which inhibit the crop growth and impede the local agricultural sustainable development.[3].

This problem has attracted increasing attention of scientist the entire world. more and more experts have conducted on the study of saline-alkaline soil degradation[4] Tejada et al. [5] tried different strategy for saline soil remediation by using microbiology in saline soil to change the physical, chemical and biological properties of soil.

Saline–alkaline soil exhibits a specific type of extreme habitat for the development of a halo-alkaliphilic prokaryotic community that grows luxuriantly at high electrical conductivity (EC) and alkaline pH. The arid and semi-arid areas are increased by high salinity and alkalinity in local depressions because of their evaporative climate[6].

In this study, the saline soil was restored by halo-tolerant microbes.After isolation and screening, the selected strains were mixed together and fermentated for fertilizer production.At last, the effectiveness of adding biological organic fertilizer to a saline soil in Weinan halogen Saline Park Beach area, near Huanghe river, China was studied during a period of five months.

II. Materials and Methods

A. Test soil sample

Test soil was collected in Weinan halogen Saline Park Beach area, Shaanxi Province, China. It mainly contained tidal soil and saline soil based. Salt content in the soil was more than 1%, in addition, organic matter content in the soil was Low and viscosity was high, with much chloride and a few sulphates et al. By testing, the major physical and chemical properties were shown in table1.

Table1 Main physical and chemical properties of soil

Organic matter (g/kg)	Total nitrogen (g/kg)	Alka-hydr-olyzed nitrogen (mg/kg)	Available phosphorus (mg/kg)	Available Potassium (mg/kg)	Water soluble salt (g/kg)
11.09	0.58	43.36	7.68	113.66	48.24

B. Isolation and screening of the halo-tolerant strains

In this study, the halo-tolerant strain were isolated from saline-alkaine soil (Weinan, Shanxi province ,China) through enrichment [7]and screened in LB plate containing 20mg /mL salinity with pH of 8.5[8]. cultured in mineral plate with salinity of 2% and pH of 8.5

C. Morphological and biochemical characteristics of selected strains

The morphological and microscopic characteristics of the strain were observed under a light microscope. Gram staining was determined according to the standard microbiological procedures. Spore formation was

determined by malachite green staining of cells. After the strain was streak-inoculated onto the plate and incubated at 37 °C for 24 h, the morphology, texture, borderline, color, and optical property of the strain's colonies were observed and recorded.

Catalase and oxidase activity assays, sugar fermentation experiment, Vogues–Proskauer (VP) test, amyl hydrolysis essay, casein hydrolysis assay, citrate utilization test, nitrate deoxidize test, salt endurance test, whether grew on NA plate (pH=5.7) or not, H_2S and indole production tests, and cellulose decomposition test were carried out using standard procedures[9]. The experiments were conducted in triplicate.

D. The mixture of strains and the production of bio-organic fertilizer

After the antagonistic experiment[10], the four strains were mixed in different proportions. Then the maximum temperature and the maximum duration at the maximum temperature were detected to determine the optimum mixed ratio. The four strains were mixed together with the optimum ratio and prepared to be complex microbial agents. Then the complex microbial agents were added into cow manure, with the 3% percent of inoculation, for fermentation and bio-organic fertilizer production.

E. Field experiment design

The field experiment lasted for five months. There were three treatments in the field experiment: Control group (without fertilizer or cow manure); Test group A (with cow manure of 10000kg/hm2); Test group B (with fertilizer of 10000kg/hm2). Each treatment area was 50 m2. 15 days after the treatment, Alopecurus pratensis Swartz were planted on the disposed soil. During the Alopecurus pratensis Swartz planting, the land preparation, the watering, the weeding, the sowing and the planting density were all consistent with each other in the four treatment group. Five months later, the effect on improvement of soil fertility was investigated with seed germination, plant height and yield assays of Alopecurus pratensis Swartz.

F. The effect for improving on saline soil[5]

The soil pH was tested by EA-940 pH meter, soil organic matter content was measured by using proposed modification of the chromic acid titration method[11]. After measuring the height of Alopecurus pratensis Swartz, the Alopecurus pratensis Swartz seed germination rate was calculated according to the following formula:

Alopecurus pratensis Swartz seedling germination rate %= emergence number/ seeding number×100%

All the experiments were conducted in triplicate and the data was analyzed by SPSS19.0 with the n=0.05

III. Result and Discussion

A. Isolation and screening of the halo-tolerant strains

After the enrichment and screening, there were 12 strains which could grow on LB plated containing 2% saline. The result was shown in table2. From the table, we can see four strains with the Data are means of three replicates; Mean within a column followed by different letters are significantly different at p=0.05 according to DMRT. As the result showed in table 2, the four strains (NWW24, NWW36, NWW56 and NWW58), who's colony size were significantly larger than other strains, were selected out for further study.

Table2. Isolation and screening results in the plate

Strain	Diameter of colony(cm)
NWW1	1.60±0.025c
NWW5	1.75±0.035c
NWW13	1.79±0.032bc
NWW16	1.82±0.036b
NWW38	1.88±0.038b
NWW42	1.90±0.032b
NWW48	1.95±0.037b
NWW52	1.98±0.028ab
NWW24	2.02±0.024 a
NWW36	2.06±0.036 a
NWW56	2.10±0.038 a
NWW58	2.15±0.035 a

B. Phenotypic characterization of four strains

The individual and colonial morphologies of the four selected strains were observed and the result was shown in table 3.

Table3 Individual and colonial morphologies results of four strains

strains	Cell shape	Cell size	Gram stain results	Whether form spore
NWW24	rod	1.1μm×0.8μm	+	+
NWW36	rod	1.0μm×0.6μm	+	+
NWW56	rod	2.2μm×0.5μm	-	-
NWW58	oval	3.2μm	+	-

C. Physiological and biochemical characterization

The physiological and biochemical characterization of four strains were also carried out. The results were shown in table 4.

Table4 Physiological and biochemical identification results of four strains

strain	NWW24	NWW36	NWW56	NWW58
Acid produced from glucose	+	+	+	+
Methyl red test	+	+	-	+
Voges-Proskauer test	+	+	-	+
Activity of Catalase	+	+	+	+
Activity of	-	-	+	+

Oxidase				
Growth on sole carbon source of Citrate	+	+	+	+
Hydrolysis of Starch	+	+	-	-
Hydrolysis of Gelatin	-	+	+	-
Nitrate reduction	-	+	+	-
nitrogen source L-tyrosine	+	+	-	-
11% NaCl	+	+	+	+
Growth on 50 degrees Celsius	+	+	+	+

Note: +/- shows the physiological and biochemical identification of

positive / negative reactions.+: positive; -: negative.

Basing on these results, combined with Common bacterial identification system manual[12]and Bergey's bacterial identification manual [13] the strainsNWW24 was identified as Bacillus megaterium .Strain NWW36 was identified as Bacillus subtilis, strain NWW56 was identified as Pseudomonas sp. strain NWW58 was identified as Yeast

D. The mixture of strains and the production of bio-organic fertilizer

The result of antagonistic experiment[10]showed there wasn't any antagonistic activity between every two strains(Data not shown). The four strains were mixed in different proportions. After detecting the maximum temperature and the max duration at the maximum temperature, the optimum mixed ratio was determined. The result was shown in table 5 and figure 1.

Table 5 Compounding agents plan design

Strain / Compound plan	NWW24	NWW36	NWW56	NWW58
Plan1	1	1	1	1
Plan2	2	1	1	1
Plan3	1	2	1	1
Plan4	1	1	2	1
Plan5	1	1	1	2
Plan6	2	2	1	1
Plan7	1	1	2	2
Plan8	1	2	2	1

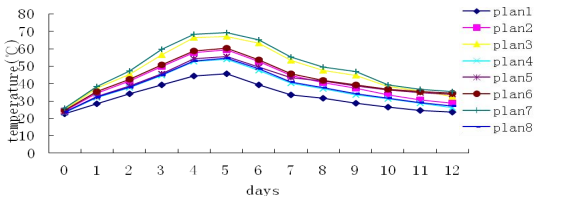

Figure1. The fermentation temperature variation condition by adding into different ratios of strains

Combined the result shown in table5 and figure 1, the best ratio of four strains was 1:1:2:2.Thus the four strains were mixed together with the ratio of 1:1:2:2 to ferment and product bio-organic fertilizer, which was used in saline soil improvement.

E. Result of field experiment

1. Effect of different treatments on pH, saline content and organic content in the saline soil

The saline soil was separately disposed by three different treatments. The processing time lasts for 150 days and PH, total salt content and organic matter of each treatment was measured every 30 days. The result was shown in table 6. Along with the increasement of fertilization time and fertilization amount, the pH value, the saline content and the organic matter content have changed to different degree, which was mainly characterized as follows: for the same test group, the longer treated, the better effect could be obtained; For the different group, with the addition of microbial agents, the test B is more effective than test A and control on improving the saline soil. The results indicated that: bio-organic fertilizer has better effect on reducing pH value, salt content and increasing organic matter of the saline soil.

Table 6 pH, salt content and organic matter content in saline soil of different treatments

		April 15	May15	June 15	July15	August 15
pH	CK	8.81±0.28a	8.80±0.13a	8.79±0.06a	8.80±0.14a	8.81±0.08a
	Test A	8.60±0.22b	8.46±0.09bc	8.18±0.15c	7.99±0.04cd	7.84±0.11d
	Test B	8.34±0.08bc	7.98±0.28cd	7.78±0.06d	7.54±0.13de	7.31±0.07e
Total salt (g/kg)	CK	14.35±0.03A	14.23±0.11A	14.18±0.14A	13.99±0.28A	13.98±0.27A
	Test A	12.58±0.04B	11.44±0.03B	10.41±0.46BC	9.62±0.02C	7.93±0.17D
	Test B	10.91±0.09BC	9.58±0.05C	7.94±0.08D	6.83±0.04E	6.46±0.10DE
Organic matter (g/kg)	CK	11.25±0.12δ	11.23±0.19δ	11.14±0.16δ	11.19±0.20δ	11.12±0.22δ
	Test A	12.48±0.14γ	13.63±0.18γ	15.45±0.27β	15.84±0.23β	15.87±0.24β
	Test β	15.98±0.23β	18.34±0.231α	19.36±0.26α	20.68±0.24α	20.87±0.36α

Note： Different letters mean significant difference between at 0.05 level，the same as the table below.

2. Plants growth to the different soil treatments

.15 days after the treatment, Alopecurus pratensis Swartz was planted on the disposed soil.20days after the planting, the seed germination was tested and Five months later, the plant height and yield assays of *Alopecurus pratensis Swartz* were tested and results were shown in table7. We can see , with the addition of microbial agents, *Alopecurus pratensis Swartz* grew better in group B than group A and control.

Table 7 Effect of different treatment on Alopecurus pratensis Swartz seedling emergence, plant height and maturity of yield

Treatment	Seedlings emergence rate%	Plant height(cm)	Yield(kg/hm^2)
CK	66.4±1.36	55.6±2.36	5577.8±134.8
Test A	78.8±1.68	68.2±1.68	7836.8±116.8
Test B	86.8±1.58	74.6±1.36	9036.5±105.6

Ⅳ. CONCLUSION

Weinan halogen Saline Park Beach area was surrounded by salt marshes in Shaanxi Province[14,15] .The climate there was very dry with a large amount of evaporation and little rainfall. It has brought a series of problems, whose

major effects were soil salinization, water shortages, dust storms, sinking ground, poor water quality and decreased biological resources[16]. They are practically useless for agriculture and animal growth. Therefore, remediation and reclaim of saline soil is the severe problem to be solved.

In this work, the saline soil was restored by halo-tolerant microbes. Four strains, with halo-tolerant ability, were isolated from saline soil and separately identified as *Pseudomonas* sp., *Bacillus subtilis*, *Bacillus megaterium* and *Yeast* by morphological, physiological and biological characterization. After the optimum mixed ratio was determined, they were mixed together with the ratio of 1:1:2:2 and fermented in the cow manure to produce bio-organic fertilizer. The effect on improvement of soil fertility was investigated with growth assays of *Alopecurus pratensis Swartz*. As was shown in the result, these complex microbial agents could not only reduce the salt content and pH but also increase the organic content of the saline soil. Moreover, the seed germination rate, plant height and grain yield of *Alopecurus pratensis Swartz* grew in different treatments had different levels of increasement. The field experiment result indicated that restoring saline soil by addition of biological organic fertilizer fermented by halo-tolerant complex agents seems to be a promising strategy for saline soil remediation[17,18].

ACKNOWLEDGEMENTS

This work was financially supported by Agricultural Science and Technology Achievements Transformation Fund Project (2012GB2G000451).

REFERENCES

[1] Ahmad, S.; Ghafoor, A.; Akhtar, M.E.; Khan, M.Z. "Ionic displacement and reclamation of saline-sodic soils using chemical amendments and crop rotation". Land Degradation & Development 2013, 24, 170-178.

[2 Wang, S.; Li, X.; Liu, W.; Li, P.; Kong, L.; Ren, W.; Wu, H.; Tu, Y. "Degradation of pyrene by immobilized microorganisms in saline-alkaline soil". Journal of Environmental Sciences 2012, 24, 1662-1669.

[3] Zhang, Y.F.; Wang, P.; Yang, Y.F.; Bi, Q.; Tian, S.Y.; Shi, X.W. "Arbuscular mycorrhizal fungi improve reestablishment of leymus chinensis in bare saline-alkaline soil: Implication on vegetation restoration of extremely degraded land". Journal of Arid Environments 2011, 75, 773-778.

[4] Lobell, D.B. "Remote sensing of soil degradation: Introduction all rights reserved. No part of this periodical may be reproduced or transmitted in any form or by any means, electronic or mechanical, including photocopying, recording, or any information storage and retrieval system, without permission in writing from the publisher." J. Environ. Qual. 2010, 39, 1-4.

[5] Tejada, M.; Garcia, C.; Gonzalez, J.L.; Hernandez, M.T. "Use of organic amendment as a strategy for saline soil remediation: Influence on the physical, chemical and biological properties of soil". Soil Biology and Biochemistry 2006, 38, 1413-1421.

[6] Hodge, A.; Fitter, A.H. "Microbial mediation of plant competition and community structure". Functional Ecology 2013, 27, 865-875.

[7] Holliger, C.; Schraa, G.; Stams, A.J.; Zehnder, A.J. "A highly purified enrichment culture couples the reductive dechlorination of tetrachloroethene to growth". Appl Environ Microb 1993, 59, 2991-2997.

[8] Abusham, R.; Rahman, R.; Salleh, A.; Basri, M. "Optimization of physical factors affecting the production of thermo-stable organic solvent-tolerant protease from a newly isolated halo tolerant bacillus subtilis strain rand". Microb Cell Fact 2009, 8, 20.

[9] Gerhardt, P.; Murray, R.G.E.; Wood, W.A.; Krieg, N.R. Methods for general and molecular bacteriology. "American Society for Microbiology": Washington, 1994.

[10] Schwinghamer, E.A. "Antagonism between strains of rhizobium trifolii in culture". Soil Biology and Biochemistry 1971, 3, 355-363.

[11] WALKLEY, A.; BLACK, I.A." An examination of the degtjareff method for determining soil organic

matter, and a proposed modification of the chromic acid titration method". Soil Science 1934, 37, 29-38.

[12] Dong, X.; Cai, M."Identification system manual of common bacteria". Beijing: Science Press: 2001.

[13] Boone, D.R.; Castenholz, R.W.; Garrity, G.M.; Brenner, D.J.; Krieg, N.R.; Staley, J.T. "Bergey's manual® of systematic bacteriology". Springer Science & Business Media: 2005; Vol. 2.

[14] Yang-Ren, W.; Shao-Zhong, K.; Fu-Sheng, L.; Zhang, L.; Zhang, J.-H. "Saline water irrigation scheduling through a crop-water-salinity production function and a soil-water-salinity dynamic model". Pedosphere 2007, 17, 303-317.

[15] Quan, Q.; Shen, B.; Xie, J.; Luo, W.; Wang, W. "Assessing soil salinity in the fields of western china using spatial modeling and remote sensing". Acta Agriculturae Scandinavica, Section B–Soil & Plant Science 2013, 63, 289-296.

[16] Endo, T.; Sadahiro, Y.; Haruta, T.; Kitamura, Y.; Li, Z.; Li, P.; Honna, T. "Soil salinization related to soil morphological and physicochemical characteristics in the luohui irrigation scheme, china". Arid Land Research and Management 2012, 26, 122-136.

[17] Dastgheib, S.M.M.; Amoozegar, M.A.; Khajeh, K.; Ventosa, A. "A halotolerant alcanivorax sp. Strain with potential application in saline soil remediation". Appl Microbiol Biot 2011, 90, 305-312.

[18] Wang, L.; Sun, X.; Li, S.; Zhang, T.; Zhang, W.; Zhai, P. "Application of organic amendments to a coastal saline soil in north china: Effects on soil physical and chemical properties and tree growth". PloS one 2014, 9, e89185.

Research on Affordability of urbanization Cost Agriculture Transfer Population --Based on the empirical analysis of Chongqing

Pan Song Lijiang, Zhang Ying , Pan Shunzhao
School of Economics and Management, Southwest University, Chongqing Beibei 400700

***Abstract*—Chongqing is the only municipality of the Midwest, is the nation's urban-rural comprehensive reform area, in promoting coordinated regional development and promote the overall situation of reform and opening up has an important strategic position. But from an overall point of view, low quality of urbanization, notably for agriculture transfer of population urbanization lagging. Research of Chongqing as an example, quantitative study based on the survey on the basis of public cost, the burden shifted from agriculture population status and affordability analysis the overall sex face and life situation of the group.**

***Index Terms*— urbanization of agriculture transfer of population citizenship cost -sharing mechanism**

I. INTRODUCTION

18 of the decision of the third plenary session of the party: "dual structure in urban and rural areas are the major obstacles to integrated urban and rural development, promoting the transfer of population urbanization of agriculture, gradually moving qualified agricultural population into urban residents, establishing financial transfer payment linked to the agriculture population urbanization mechanism, is the requirement of Socialist construction of towns. "Agro-transfer of population citizenship as" demographic "core of urbanization, it is an important task of modern urbanization in building socialism. Since reform and opening up and rapid development of urbanization in China, but on the whole, China's urbanization quality is not high, highlighting agriculture population urbanization lagging. As of 2014 end, China's urbanization rate of the resident population as 53.7%, but the registered population urbanization is only 36%, a difference of 17%.

Chongqing is the only municipality of the Midwest, is the nation's urban-rural comprehensive reform area, in promoting coordinated regional development and promote the overall situation of reform and opening up has an important strategic position. As of 2013 end of the year, the city's resident population reached 2970 million, urbanization rate reached 58.34%, but urbanization rate of the registered population was only 40.02%. Agriculture population citizenship cost-sharing problems here was the most concentrated and stand out. Chongqing's reform practice provided us samples of agricultural population transfers for us citizenship cost-sharing mechanism provided a window. Through Chongqing agricultural transfer population public of status and the bear capacity of survey, we can more in-depth to understanding current agricultural transfer population public of cost share mechanism of status, and difficult and problem, more clear to awareness current Government building agricultural transfer population public of cost share mechanism of efforts, and difficulties and the development direction, this not only for we further deepening reform, and innovation agricultural transfer population public of cost share mechanism, promoting agricultural transfer population public of provides experience support, For further study of new urbanization road in China during the transition period to provide empirical support.

II. DATA SOURCE

The sample for this article in main urban area of Chongqing City and the surrounding County, the transfer of agricultural workers of the town population. Survey content includes agricultural population of individual characteristics (including gender, age, education, marital status, profession, place of work, the monthly income, duration of work, employment contracts, as well as their children to school), the public cost of the status quo, of the public's willingness to bear the cost, the public cost of capacity. This survey in 2015 year 2 month in Chongqing, Chongqing North railway station, bus station, leading Temple water gathered more populated areas such as high-tech industrial park, extensive surveys, questionnaires were 500 , in which valid questionnaires 451 , survey response rate was 90.2%. Data SPSS19.0 analysis.

III. THE SAMPLE DESCRIPTION

Basic conditions of samples : transfer of agricultural population of 451 people , one male- 303 people , accounted for 67.2%, female- 148 people, accounts for 32.8%. Age in agriculture is concentrated in 20-50 years old, accounted for 85.6%. Agriculture education in junior high school, and the number of people in the population is 178 people, accounted for 39.5%high school and College number is 121 people, accounted for 26.8%; junior college or above the number of 152 people, share 33.7%. Married number of 278 people , accounts for 61.6%unmarried number 153 people , accounts for 34.0%; the number of divorced or widowed at 20 , and accounted for 4.4%. In the field of industry, construction and services number of relatively large proportion accounted for 25.7%, and19.7%; and manufacturing, and

other items were also has 10.0%, and30.2%and, lastly, transportation and a smaller proportion of farming, forestry, animal husbandry and fishery, namely 8.6% and 5.8% 。 In the workplace, formed by the city to neighboring counties to gradually reduce the number of cases in the town alone accounted for nearly half of the city. Monthly income of 1500 Yuan more than the number of 432 people, accounts for 95.8%. In the working age is 3 years for 129 people, accounting for 28.6%;3-5 years of 84 people, accounted for 18.6%;5-10 years of 111 people, accounted for 24.6%;10 The number of years at 127 people, accounted for 28.2%. And employment contracts signed on or not seems relatively balanced, signed by 57.6%; no sign of 42.4%. On the location of children's reading problems are read locally accounted for 41.1%; at home reading accounted for 46.5%.

III.AGRICULTURE STATUS QUO OF POPULATION URBANIZATION COSTS BORNE

A. Living in poverty, it is difficult to fully bear the cost of citizenship

Transfer of population from rural areas to the cities to work in agriculture itself has its own economic difficulties, to urban survival reasons. Unfair treatment by employers to the city, such as unequal pay, etc. During the course of investigation, through the transfer of some agricultural population of interviews we learn about wage arrears also occurred. This all leads to transfer of agricultural economic conditions of the population, lived in poverty, being at the bottom. Although they contributed to urban construction and development is not the same city together to enjoy the city's benefits to the community. Want transferred from agricultural population into immediate citizenship only on the economic cost is huge, unable to commit fully to the agriculture population. 451 -agriculture population survey has nearly 40.0% balance is a pay as you earn or living beyond their means, their life strapped. 55.0% people believe that Chongqing's higher cost of living, there are 13.7% people believe that Chongqing's high cost of living. Low pay and the high cost of living is the direct cause of their financial hardship. More than half are eating class occupy the highest proportion of cost of living due to the cost of living here include food, clothing, transportation, medical, entertainment category, so the proportion of diet accounted for the cost of living here is not the same as the Engel's coefficient, but the higher proportion of will to a certain extent, reflect the life and poverty.

Table 1 transfer of agricultural population living conditions

Basic features	Classification	The number of	Percentage of total
Income and expenses status	Income over expenditure	44	The 9.8%
	Small increases of income over expenditure	227	The 50.3%
	Pay as you earn	136	The 30.1%
	To make ends meet	44	The 9.8%
Cost of living in Chongqing	Very high	62	The 13.7%
	High	248	The 55%
	General	124	The 27.5%
	Lower	17	The 3.8%
	Very low	0	The 0%
Accounted for the highest proportion of cost of living	Diet class	259	The 57.4%
	Clothing	61	The 13.5%
	Traffic class	33	The 7.3%
	Medical class	53	The 11.8%
	Entertainment class	45	The 10%

Data source: questionnaire sorting it.

B. Social insurance and housing Provident Fund scheme coverage shifted to agriculture, lack of corporate functions

Social security is a redistribution function of the social security system. State mandated employers and workers participate in the social insurance and pay social insurance fees. Housing Fund as a long-term housing savings, it also has mandatory. But coverage shifted to agriculture is not high, surveyed 451 agriculture population is 47.2% persons participated in endowment insurance, there are 63.4% persons participated in medical insurance, there are 39.0% people took part in a work-related injury insurance, there are 23.7% people attended the maternity insurance, 26.8% People who participated in the unemployment insurance, there are 20.2% people participated in the Housing Fund. Five of all insurance payments were involved in the shares of only 10.9%, one will not take part in up to 28.4%. When the discussion did not participate in the cause, 40.3% who is the enterprise did not give them to buy, 18.2% say they don't understand the information, 14.4% is not well off myself to participate. On social insurance and housing Provident Fund for employees, enterprises lack serious, did not assume their responsibilities. Social insurance and housing accumulation fund system has been established for many years, but agriculture has still not been a deep understanding of the population. Current payment of proportional part of the low-income people who cannot afford it. Detailed data are shown in table 2.

Table 2 transfer of agricultural population participate in the social security

Basic features	Classification	The number of	Percentage of total	Basic features	Classification	The number of	Percentage of total
Whether participated in endowment insurance	Is	213	The 47.2%	Pension and provident funds to participate in number of items	One will not take part in	128	The 28.4%
	Whether	238	The 52.8%		Only participat	87	The 19.3%

					ed in one		
If they had health insurance	Is	286	The 63.4%		Only participated in two	78	The 17.3%
	Whether	165	The 36.6%		Only participated in three	32	The 7.1%
If they had work injury insurance	Is	176	The 39%		Only participated in four	24	The 5.3%
	Whether	275	The 61%		Only participated in five	53	The 11.7%
Whether to participate in the maternity insurance	Is	107	The 23.7%		Six full participation	49	The 10.9%
	Whether	344	The 76.3%	Why did not participate in the	Not well off	58	The 14.4%
Whether participated in unemployment insurance	Is	121	The 26.8%		No information	73	The 18.2%
	Whether	330	The 73.2%		Businesses have not purchased	162	The 40.3%
Joining the housing accumulation Fund	Is	91	The 20.2%		Did not consider it necessary	51	The 12.7%
	Whether	360	The 79.8%		Precarious work	46	The 11.4%
					Other	12	The 3%

Source: survey data available.

C.Lack of skills training, training methods

Surveyed 451 -agriculture population is 213 who have never participated in vocational training, accounted for almost 50%. We can see agriculture population is lacking in skills training, is to some extent out of rural areas in the city are those who have no skills, but to do some physical work, it is difficult to become skilled workers. Received vocational training, 238 transferred more than half of the population is in agriculture employers training also has a small part to participate in the training at their own expense, rarely part of the through governmental organizations training. Where you can see the comparison of vocational training or a single, largely employer provided training. Can develop in the future a variety of training methods to encourage qualified agricultural population transfers at their own expense to attend training and enhance their skills. To enter populated areas the local Government can also centrally organized training. Combining tables didn't take part in vocational training, professional training and the willingness of these data can be found there is still a lot of people on trains without paying enough attention to subjectively slack. This may be due to insufficient awareness of their own, the future may also need to increase publicity and improve agriculture the population's awareness in this respect to assist them in upgrading their skills and to improve myself.

Table 3 population transfers in agriculture vocational training

Basic features	Classification	The number of	Percentage of total
Whether to participate in the vocational training	Is	238	The 52.8%
	Whether	213	The 47.2%
Participated in any way in vocational training	Free training for governmental organizations	20	The 8.4%
	Attend training	62	The 26.1%
	Employer training	138	The 57.9%
	Other	18	The 7.6%
The reason for not participating in vocational training	No opportunity to participate in	139	The 65.3%
	No time for	43	The 20.1%
	Don't want to join the	31	The 14.6%
The willingness of vocational training	Not willing to	147	The 32.6%
	Willing to	304	The 67.4%

Source: survey data available.

D. Have a fixed home, adrift

Transfer of agricultural population as well as people working in the cities, but of no fixed abode, surveyed 451 agriculture population is 67% people are not living in their own House. Most of them live in their rented houses or flats provide dormitory, no fixed domicile and residence are located in remote areas, poor environment. In surveys and interviews, we learned that the housing problem is a transfer of population reflected most agricultural problems, 64.7% said his pressure or housing is very large. Agriculture population housing is in the process of its realization of the public the urgent need to address the problem. In order to improve their housing in Chongqing, construction of low-rent housing, public rental housing, two limited room, and also made some gains, but the houses still have a serious problem of agricultural population transfers, the future Government may still need to increase investment in this regard. Breaking the agriculture population is nomadic, adrift and arduous task.

Table 4 agriculture housing situation of the population

Basic features	Classification	The number of	Percentage of total
Living conditions	Since the purchase of commercial housing	91	The 20.2%
	Government-provided affordable housing	8	The 1.7%
	Since the purchase of affordable	58	The 12.9%

	housing or two restricted housing		
	Own rent house	153	The 33.9%
	Provides dormitory	97	The 21.5%
	Take friends and family housing	7	The 1.6%
	Other	37	The 8.2%
Housing pressures	Great	99	The 22%
	Large	193	The 42.7%
	General	93	The 20.6%
	The smaller	58	The 12.9%
	Very small	8	The 1.8%

Data source: questionnaire sorting it.

VI. AFFORDABILITY OF FOUR TRANSFER OF POPULATION, AGRICULTURE WILL COST

Data can be seen from the table below whether the willingness or the actual account for a large proportion of the agricultural population transfers were willing to move closer to the main city, around in the main city, County, town of degressive. In various types of cost burden is concerned, most difficult to undertake in recent years rising property prices caused by high housing costs, mean that we cannot assume there are 13.1%, some cannot afford to have 45.2%. Compared to other costs, bear the cost of living is good, but there are still 19.3% who cannot afford or cannot completely affordable. As regards social security and vocational education and training costs are up to 30% the above mean that we cannot cover, or can't afford to . Last agricultural population transferred ability to take comprehensive evaluation, as bearing the majority of middle 56.1%, and consider the affordability of weak and strong respectively 21.7% and 22.2%. Overall affordability set at a medium level.

Table 5 transfer of agricultural population location and its will to work

	Willing to work in				Total
	Main city	Around the main city	County seat	The town of	
Location city	116	43	23	15	197
Around the main city	37	56	14	10	117
County seat	18	23	25	9	75
Town	15	13	18	16	62
Total	186	135	80	50	451

Data source: questionnaire sorting it.

IV. AGRICULTURE POPULATION ANALYSIS OF INFLUENCE FACTORS OF COST AND AFFORDABILITY OF THE PUBLIC

Considered to gender, and age, and education, and marriage status, and by at industry, and work locations, and months income, and workers years, and has no signed employment contract, and children reading locations, and social security and housing Provident Fund participate in items number and whether participate in had career training, factors are may is effects agricultural transfer population public of bear capacity of factors, so we put agricultural transfer population public of cost bear capacity as due to variable, gender, and education, and marriage status, and by at industry, and work locations, and has no signed employment contract, and Children reading location, social insurance and housing Provident Fund to participate in as a factor, age, income, length of working as a covariate, order multiple logistic regression. Use SPSS19.0 software for stepwise regression we found only monthly income, place of work, social security and Housing Fund to participate in vocational training, whether these four variables in 5% with the significant level of passing through inspection.

A. The parallel testing

Table 6 parallel testing

Model	-2 Log likelihood values	Chi-square	df	Significant
The null hypothesis	The 717.094			
Generalized	The 699.849	17.245	11	0.101

Parallel test are multiple ordered logistic regression applied whether or not preliminary examination. Parallel test results can be seen from the above table P=0.101>0.05, so the models through parallel testing, which uses this model is correct.

B. Outputs of regression results and analysis

As can be seen from the model fitting information,-2 log likelihood values less 106.078, but the model adds 11 variables. Chi-square test p- value in the case of three decimal places 0.000. Model 5% significant significance level as a whole.

Table 7 model fitting information

Model	-2 Log likelihood values	Chi-square	df	Significant
Only the intercept	The 823.173			
Final	The 717.094	The 106.078	11	0.000

Stepwise regression, our ultimate regression results shown in the following table. The regression results can be seen from the table below in the 5% level of significance, only monthly income (YSR), workplaces (gzdd), whether to participate in vocational training (train), social insurance and housing Provident Fund to participate in number of items (items) passing through inspection.

Table 8 parameter estimates

		Estimate	Standard errors	Wald	df	Significant
Threshold	[smhcbcdnlzhpj=1]	-0.627	0.492	1.522	1	0.217
	[smhcbcdnlzhpj=2]	2.426	0.505	The 23.117	1	0.000
Location	ysr	0.000	6.763 E-5	30.94	1	0.000

[gzdd=1]	0.692	0.300	5.302	1	0.021
[gzdd=2]	0.149	0.317	0.222	1	0.638
[gzdd=3]	0.726	0.349	4.316	1	0.038
[gzdd=4]	0[a]			0	
[train=0]	-0.567	0.207	7.529	1	0.006
[train=1]	0[a]			0	
[items=0]	-0.979	0.366	7.149	1	0.007
[items=1]	-0.764	0.385	3.944	1	0.047
[items=2]	-1.017	0.391	6.769	1	0.009
[items=3]	-0.903	0.471	3.673	1	0.055
[items=4]	0.117	0.506	0.054	1	0.817
[items=5]	-0.245	0.410	0.357	1	0.550
[items=6]	0[a]			0	

Estimates of monthly income are greater than 0 , which means monthly income is stronger the higher the cost and affordability of the public. Because their numbers were too small, so in the case of three decimal places is shown as 0.000. Work locations around the city, the main city, the county seat of estimated values is 0.692, and0.149, and0.726,, which means working in the main city, the main city, County area surrounding the transfer of agricultural population than to work in the town's agricultural transfer cost of the urbanization of the population can afford more. Whether to participate in the vocational training's estimated value is -0.567, which means people who did not take part in vocational training for those who have participated in vocational training for members of the public can afford even less cost, namely people who took part in vocational training people cost more to bear. Social insurance and housing provident funds participate in the estimate of the number of items in the report are -0.979, and-0.764, and-1.017, and-0.903, and0.117, and-0.245, Its meaning is to take part in fewer than six for six the number of people participating in citizen cost affordability, weaker compared to the, and participate in the cost of fewer people can afford less.

In agriculture the population urbanization process, monthly income is higher, located in large cities, took part in vocational training of technical personnel, social security and housing people on the public bear the cost of more powerful, can be well assumed its citizens should take part in the process, they can walk in the forefront of citizenry. Whereas in agriculture by a large team of people cost ability to bear, after all, is a small, more affordability affordability is moderate or weak. For these people to help satisfy its citizenry, there are two ways: one is to enhance its cost and affordability of the public ; Second is to reduce the cost burden on its citizens, namely implement different mechanisms for cost-sharing ratio of public or shared. The first way, because monthly income fast broader promotion could lead to cost-push inflation and therefore could gradually raise minimum wage standards, raise the income of the lowest income groups. As for workplaces, it is determined by the market, personal preferences and other factors, so it is not a controllable factors. Want to improve the cost and affordability of the public agriculture population focus primarily vocational training and social insurance and Housing Fund. For the second way, needed between Central Government, local governments, enterprises and individuals interest readjustment, reducing personal commitment.

KNOT LANGUAGE

Agriculture population urbanization is a gradual process, it is impossible to complete. Because of urban and rural dual social structure in China's historical background, the citizen must face a series of obstacles the agriculture population, Chongqing is no exception. Solving problems facing agriculture transfer of population urbanization, Chongqing is the key to future development. For, paper proposed to established political transfer paid with agricultural transfer population phase hook of mechanism; strengthened County, and town of industry cluster, active undertake big city of transfer industry, encourages agricultural transfer population settled in County, and town, achieved local near public of; perfect agricultural transfer population social security system, strengthened agricultural transfer population housing guarantees, active introduced market mechanism solution City based facilities construction of funds gap problem; guide enterprise real bear up in agricultural transfer population public of process in the should bear of responsibility ; Stimulating rural assets to realize the "capital city" initiative to enhance their own capabilities, considerable effort and resources to achieve citizenship.

REFERENCES:

[1] Pan jiahua, Wei . China urban development report: agriculture population urbanization [m]. Beijing: social sciences documentation publishing house,2013.

[2] Peter Senge. The Necessary Revolution: How Individuals and Organizations are Working Together to Create a Sustain [M]. New York: Doubleday, 2008.

[3] Zhang Guosheng . Chinese peasant workers ' citizenization: study on the social cost of [m]. Beijing: people's publishing house,2008.

[4] research group of development research center of the State Council . Peasant workers ' citizenization: institutional innovation and the top-level policy design [m]. Beijing: China Development press,2011.

[5] Shen Bing ." Twelve-Five "construction cost estimation of peasant workers ' citizenization and its sharing mechanism – in order to concentration of interprovincial migrant inflows area Ningbo city as case [j]. Study on urban development,2012,(1).

Zero-divisor Semigroups Determined by some Simple Graphs

Mingyang Zhao,Dongwei Wang, Fubang Liu,Saisai Shi ,Jingli Ying and Hailong Hou
School of Mathematics and Statistics, Henan University of Science and Technology,
Luoyang, Henan, 471023, P.R. China

***Abstract*—In this paper, we characterize the structures of the commutative zero-divisor semigroups determined by a class of simple graphs. We also give a formula to calculate the number of mutually non-isomorphic commutative zero-divisor semigroups of these graphs.**

***Index Terms*—Zero-divisor graph, Commutative zero-divisor semigroup, Complete graph**

I. Introduction

For any commutative semigroup S with zero element 0, we can define an undirected simple graph $\Gamma(s)$ associating with S. The vertex set of $\Gamma(s)$ is the set of all zero divisors of S, and two vertices x and y are adjacent if and only if $xy=0$. We call $\Gamma(s)$ the zero-divisor graph corresponding to S. DeMeyer gives some fundamental properties and proper structures of these graphs. For example, it is proved that for any commutative semigroup S, $\Gamma(s)$ is a connected graph with diameter less than or equal to 3, and that for each pair of nonadjacent vertices of $\Gamma(s)$, there is a vertex z with $N(x)\cup N(y)\cup\overline{N(z)}$, where $\overline{N(z)}=N(z)\cup\{z\}$. They also gave many examples of graphs to give positive or negative answers to the following general problems: Give a simple graph G with some conditions, does there exist a semigroup S with $\Gamma(s)=G$?

For any commutative semigroup S, we denote by $T=Z(s)$ the set of all zero-divisors of S. Then T forms an ideal in S and in particular T is a subsemigroup of S. Furthermore, we have $\Gamma(s)=\Gamma(T)$. We call a semigroup S a zero-divisor semigroup if all its elements are zero divisors of itself. For a given connected simple graph G, if there exists a zero-divisor semigroup S such that $\Gamma(s)\tilde{=}G$, then we say G has corresponding semigroups, and we call S a semigroup determined by the graph G

In this paper, we study commutative zero-divisor semigroups determined by a class of graphs. Most of these graphs have multiple corresponding semigroups. According to our results we can list all of these semigroups up to isomorphism. We also give a formula to calculate the number of mutually non-isomorphic commutative zero-divisor semigroups of any of these graphs.

All graphs considered in this paper are connected finite undirected graph without loops and multiplies. For $x,y\in V(G)$, if x and y are adjacent in G, we denote it as $x-y$. All semigroups in this paper are multiplicatively commutative zero-divisor semigroups with zero element 0. The reader is referred to [1-9] for all the notation and terminology not defined here.

II. Main Results

A. The elemental relationship of zero-divisor semigroup determined by K_{n+1}^*

In this section, we characterize the structures of zero-divisor semigroups determined by a class of graphs, denoted by K_{n+1}^*

Theorem 2.1 Semigroup M_{n+1}^* is the zero-divisor semigroup of K_{n+1}^* if and only if M_{n+1}^* satisfies the following conditions:

(1) (I) $a_1a_i=0$, $a_2a_{n+1}=0$, $a_2a_i=0$, $a_ia_{n+1}=0$ and $a_ia_j=0(\forall 3\le i\ne j\le n)$.

(II) $a_i^2\in\{a_3,\cdots,a_n\}$. If $a_i^2=a_j(i\ne j)$,then $a_j^2=0$.

(2) $a_1^2\in\{0,a_1,\cdots,a_{n+1}\}$.

(I) If $a_1^2=0$, then

(A) $a_1a_2=a_l(\forall 3\le l\le n)$, $a_l^2=0$, $a_2^2\in\{0,a_3,\cdots,a_n\}$. If $a_2^2=a_s(\forall 3\le s\le n)$, then $a_s^2=0$.

(B) $a_1a_{n+1}=a_m(\forall 3\le m\le n)$, $a_{n+1}^2\in\{0,a_3,\cdots,a_n\}$. If $a_{n+1}^2=a_t(\forall 3\le t\le n)$, then $a_t^2=0$.

(II) If $a_1^2=a_1$,then

(A) $a_1a_2\in\{a_2,a_{n+1}\}$.

If $a_1a_2=a_2$, then $a_2^2\in\{0,a_2,a_{n+1}\}$. If $a_2^2=a_{n+1}$, then $a_1a_{n+1}=a_{n+1},a_{n+1}^2=0$.

If $a_1a_2=a_{n+1}$, then $a_2^2=a_s(\forall 3\le s\le n)$.

$a_1a_{n+1}=a_{n+1}$, $a_{n+1}^2=0$ and $a_s^2=0$.

(B) $a_1a_{n+1}\in\{a_2,a_{n+1}\}$.

If $a_1a_{n+1}=a_{n+1}$,then $a_{n+1}^2\in\{0,a_2,a_{n+1}\}$. If $a_{n+1}^2=a_2$,then $a_1a_2=a_2$, $a_2^2=0$.

If $a_1a_{n+1}=a_2$, then $a_{n+1}^2=a_t(\forall 3\le t\le n)$. $a_1a_2=a_2$, $a_2^2=0$ and $a_t^2=0$.

(III) If $a_1^2=a_2$, then

(A) $a_1a_2\in\{a_2,\cdots,a_{n+1}\}$

If $a_1a_2=a_2$, then $a_2^2=a_2$.

If $a_1a_2=a_l(\forall 3\le l\le n)$, then $a_2^2=0$, $a_l^2=0$.

If $a_1a_2=a_{n+1}$, then $a_2^2=a_s(\forall 3\le s\le n)$. $a_1a_{n+1}=a_s$, $a_{n+1}^2=0$ and $a_s^2=0$.

(B) $a_1a_{n+1}=a_m(\forall 3\le m\le n)$, $a_m^2=0$, $a_{n+1}^2\in\{0,a_3,\cdots,a_n\}$. If $a_{n+1}^2=a_t(\forall 3\le t\le n)$, then $a_t^2=0$.

Symmetrically, if $a_1^2=a_{n+1}$, then

(A) $a_1a_{n+1}\in\{a_2,\cdots,a_{n+1}\}$

If $a_1a_{n+1}=a_{n+1}$,then $a_{n+1}^2=a_{n+1}$.

If $a_1a_{n+1}=a_m(\forall 3\le m\le n)$,then $a_{n+1}^2=0$, $a_m^2=0$.

If $a_1a_{n+1}=a_2$,then $a_n^2=a_t(\forall 3\le t\le n)$. $a_1a_2=a_t$, $a_2^2=0$ and $a_t^2=0$.

(B) $a_1a_2=a_l(\forall 3\le l\le n)$, $a_l^2=0$, $a_2^2\in\{0,a_3,\cdots,a_n\}$. If $a_2^2=a_s(\forall 3\le s\le n)$,then $a_s^2=0$.

(IV) If $a_1^2=a_r(\forall 3\le r\le n)$,then

(A) $a_1a_2=a_l(\forall 3\le l\le n)$, $a_2^2=a_s(\forall 3\le s\le n)$. $a_l^2=0$ and $a_s^2=0$.

(B) $a_1a_{n+1}=a_m(\forall 3\le m\le n)$, $a_{n+1}^2=a_t(\forall 3\le t\le n)$. $a_m^2=0$ and $a_t^2=0$.

Proof : "$\Rightarrow$"

(A) Obviously, $a_2a_{n+1}=0$, $a_1a_i=0$, $a_2a_i=0$, $a_{n+1}a_i=0$ and $a_ia_j=0(\forall 3\le i\ne j\le n)$.

(B) Because $a_1a_i^2=(a_1a_i)a_i=0$ and $a_2a_i^2=0(\forall 3\le i\le n)$, $a_i^2=\{0,a_3,\cdots,a_n\}$.

When $a_i^2=a_j$,we get $a_j^2=a_i^2a_j=a_i(a_ia_j)=0$.

(2) $a_1^2\in\{0,a_1,\cdots,a_{n+1}\}$.

(I) when $a_1^2=0$,

(A) Because $a_1(a_1a_2)=a_1^2a_2=0$ and $(a_1a_2)a_{n+1}=a_1(a_2a_{n+1})=0$.

(B) $a_1a_2=a_l$ $(\forall 3\le l\le n)$. For $a_l^2=(a_1a_2)a_l=a_1(a_2a_l)=0$,so $a_l^2=0$.

And $a_2^2a_{n+1}=a_2(a_2a_{n+1})=0$,hence $a_2^2\in\{0,a_3,\cdots,a_n\}$.

When $a_2^2=a_s(\forall 3\le s\le n)$, $a_s^2=a_2^2a_s=a_2(a_2a_s)=0$.

In a similar way, (B) is true.

(II) When $a_1^2=a_1$,

(A) Since $a_1(a_1a_2)=a_1^2a_2=a_1a_2$ we obtain $a_1a_2\in\{a_2,a_{n+1}\}$.

When $a_1a_2=a_2$,for $a_1a_2^2=(a_1a_2)a_2=a_2^2$,so $a_2^2\in\{0,a_2,a_{n+1}\}$. When $a_2^2=a_{n+1}$,we have $a_1a_{n+1}=a_1a_2^2=(a_1a_2)a_2=a_2^2=a_{n+1}$ and $a_{n+1}^2=a_2^2a_{n+1}=a_2(a_2a_{n+1})=0$.

When $a_1a_2=a_{n+1}$, because $a_1a_2^2=(a_1a_2)a_2=a_{n+1}a_2=0$ and $a_2^2a_{n+1}=a_2(a_2a_{n+1})=0$, $a_2^2=a_s(\forall 3\le s\le n)$, $a_1a_{n+1}=a_1(a_1a_2)=a_1^2a_2=a_1a_2=a_{n+1}$, $a_{n+1}^2=(a_1a_2)a_{n+1}=a_1(a_2a_{n+1})=0$ and $a_s^2=a_2^2a_s=a_2(a_2a_s)=0$.

In a similar way , (B) is true.

(III) When $a_1^2=a_2$,

(A) Since $(a_1a_2)a_{n+1}=a_1(a_2a_{n+1})=0$,so $a_1a_2\in\{a_2,\cdots,a_{n+1}\}$.

When $a_1a_2=a_2$,we get $a_2^2=a_1^2a_2=a_1(a_1a_2)=a_1a_2=a_2$.

When $a_1a_2=a_l(\forall 3\le l\le n)$,we have $a_2^2=a_1^2a_2=a_1(a_1a_2)=a_2a_l=0$ and $a_l^2=(a_1a_2)a_l=a_1(a_2a_l)=0$.

When $a_1a_2=a_{n+1}$,for $a_1a_2^2=(a_1a_2)a_2=a_{n+1}a_2=0$ and $a_2^2a_{n+1}=a_2(a_2a_{n+1})=0$, so $a_2^2=a_s(\forall 3\le s\le n)$.

$a_1a_{n+1}=a_1(a_1a_2)=a_1^2a_2=a_2^2=a_s$,
$a_{n+1}^2=(a_1a_2)a_{n+1}=a_1(a_2a_{n+1})=0$ and
$a_s^2=a_2^2a_s=a_2(a_2a_s)=0$.

(B) For that $a_1(a_1a_{n+1})=a_1^2a_{n+1}=a_2a_{n+1}=0$ and $(a_1a_{n+1})a_2=a_1(a_{n+1}a_2)=0$,
so $a_1a_{n+1}=a_m(\forall 3\le m\le n)$.
$a_m^2=(a_1a_{n+1})a_m=a_1(a_{n+1}a_m)=0$.
Since $a_1a_{n+1}^2=(a_1a_{n+1})a_{n+1}=0$ and $a_2a_{n+1}^2=a_2(a_2a_{n+1})=0$,we can get $a_{n+1}^2\in\{0,a_3,\cdots,a_n\}$.
When $a_{n+1}^2=a_t(\forall 3\le t\le n)$,we have $a_t^2=a_{n+1}^2a_t=a_{n+1}(a_{n+1}a_t)=0$.

In the similar way, When $a_1^2=a_{n+1}$,(A) and (B) hold.

(IV) When $a_1^2=a_r(\forall 3\le r\le n)$

(A) Because $a_1(a_1a_2)=a_1^2a_2=a_ra_2=0$ and $(a_1a_2)a_2=a_1^2a_2=a_ra_2=0$,
we get $a_1a_2=a_l(\forall 3\le l\le n)$. Since $a_1a_2^2=(a_1a_2)a_2=a_la_2=0$ and $a_2^2a_{n+1}=a_2(a_2a_{n+1})=0$,
so $a_2^2=a_s(\forall 3\le s\le n)$.
$a_l^2=(a_1a_2)a_l=a_1(a_2a_l)=0$ and $a_s^2=a_2^2a_s=a_2(a_2a_s)=0$.

In a similar way, (B) is true.

"$\Leftarrow$"

We consider associative law,that is:
$(uv)w=u(vw)\quad(\forall u,v,w\in M_{n+1}^*\setminus\{0\})$.

(1) When $u=v=w$,we have $(uv)w=u^2u=u^3=uu^2=u(vw),(*)$ holds.

(2) When $u,v,w\in\{a_3,\cdots,a_n\}$,according to theorem 3.1 $(*)$ is true.

(3) When u,v,w are not all identical,only two belong to $\{a_3,\cdots,a_n\}$.

When u or v dose not belong to $\{a_3,\cdots,a_n\}$, $uv=0$ holds,so $(uv)w=0$.

When $u,v\in\{a_3,\cdots,a_n\}$. If $u=v$,then $(uv)=u^2\in\{0,a_3,\cdots,a_n\}$,so $(uv)w=u^2w=0$.

If $u\ne v$,then $uv=0$,hence $(uv)w=0$.

Similarly $u(vw)=0$, so $(*)$ holds.

(4) When u,v,w are not all identical,only one belongs to $\{a_3,\cdots,a_n\}$.

If u or v belongs to $\{a_3,\cdots,a_n\}$,we have $uv=0$, so $(uv)w=0$.

When $w\in\{a_3,\cdots,a_n\}$. If $uv=w$, then $w^2=0$, so $(uv)w=w^2=0$.

If $uv\ne w$, then $(uv)w=0$.

Similarly $u(vw)=0$, so $(*)$ is true.

(5) If $u=w$, then $(uv)w=(uv)u=u(uv)=u(vu)=u(vw)$, $(*)$ holds.

(6) When $u=v\ne w$ (or $u\ne v=w$), and they all belong to $\{a_1,a_2,a_n\}$.

(I) If $a_1^2=0$.

When $u=v=a_1,w=a_2$. $(uv)w=a_1^2a_2=0$.

Because $a_1a_2=a_l(\forall 3\le l\le n)$, we get $u(vw)=a_1(a_1a_2)=a_1a_l=0\ (\forall 3\le l\le n)$. $(*)$ is true.

By the same method, if $u=v=a_1,w=a_{n+1}$, then $(*)$ holds.

When $u=v=a_2,\ w=a_1$.
Since $a_2^2\in\{0,a_3,\cdots,a_n\}$, so $(uv)w=a_2^2a_1=0$.

Because $a_1a_2=a_l(\forall 3\le l\le n)$,we get $u(vw)=a_1(a_2a_1)=a_1a_l=0$. Then $(*)$ is true . Similarly, $(*)$ is true for other cases.

(II) When $a_1^2=a_1$.

As $u=v=a_1,w=a_2$. $a_1a_2\in\{a_2,a_{n+1}\}$.

When $a_1a_2=a_2$, $(uv)w=a_1^2a_2=a_1a_2=a_2$ and $u(vw)=a_1(a_1a_2)=a_1a_2=a_2$. $(*)$ is true.

If $a_1a_2=a_{n+1}$, $a_1a_2=a_{n+1}$.
$(uv)w=a_1^2a_2=a_1a_2=a_{n+1}$ and $u(vw)=a_1(a_1a_2)=a_1a_{n+1}=a_{n+1}$. we have $(*)$.

At the same way, if $u=v=a_1,w=a_{n+1}$, $(*)$ is valid.

A similar argument will show that $(*)$ is true for other cases.

B. The number of zero-divisor semigroups determined by graph K_{n+1}^*

Theorem 2.2 Under isomorphism, the number of zero-divisor semigroups of graph K_{n+1}^* is

$$T(n-2)=\begin{cases} 14S_1(1)+4 & n=3 \\ 14S_1(2)+22S_2(2)+4 & n=4 \\ 14S_1(3)+22S_2(3)+27S_3(3)+4 & n=5 \\ 14S_1(4)+22S_2(4)+27S_3(4)+7S_4(4)+4 & n=6 \\ 14S_1(n-2)+22S_2(n-2)+27S_3(n-2)+7S_4(n-2)+S_5(n-2)+4 & n\geq 7 \end{cases}$$

where $S_i(n)=\sum_{k=i}^{n}\sum_{t=0}^{n-k}p(n-t,k)(n\geq i)$

Proof : Since $a_1a_i=0$, $a_2a_{n+1}=0$, $a_2a_i=0$, $a_i a_{n+1}=0$ and $a_ia_j=0(\forall 3\leq i\neq j\leq n)$,so we only need to discuss the value of $\{a_1^2,a_1a_2,a_1a_{n+1},a_2^2,a_{n+1}^2\}$ and $\{a_3^2,\cdots,a_n^2\}$.

(I) When $a_1^2=0$, $\{a_1a_2,a_1a_{n+1},a_2^2,a_{n+1}^2\}$ can take $\{a_l,a_m,0,0\}$ or $\{a_l,a_m,a_s,a_s\}(\forall 3\leq l,m,s,t\leq n)$ according to symmetry.

① When $\{a_1a_2,a_1a_{n+1},a_2^2,a_{n+1}^2\}$ takes $\{a_l,a_m,0,0\}$,and $a_l=a_m$.

We divide $\{a_i\mid a_i^2=0\}$ as three subsets who are different from each other and they constitute the set $\{a_i\mid a_i^2=0\}$:

1) $A=\{a_i\mid a_i^2=0\}$;

2) $B=\{a_i\mid a_i^2=a_i\}$;

3) $C=\{a_i\mid a_i^2=a_j,a_j\in A\}$.

Let $a_l=a_m=a$,since $a^2=0$,so $a\in A$ and $|A|\geq 1$. Set the base number of A is $|A|=k$ $(0\leq k\leq n-2)$,similarly, $|B|=t$ $(0\leq t\leq n-2-k)$. Do not break general,set the element of A is $a_3,a_4,\cdots,a_{k+2}$,and there are λ_i $r\in C$ making $r^2=a_i(3\leq i\leq k+2)$,then we get the following equation:

$$\lambda_3+\lambda_4+\cdots+\lambda_{k+2}=n-2-k-t \qquad (1)$$

The number of equation (1) is equivalent to the number of the zero-divisor semigroup of the graph K_{n+1}^* under isomorphism. . Let $\mu_3,\mu_4,\cdots,\mu_{k+2}$ is a replacement of $\lambda_3,\lambda_4,\cdots,\lambda_k$ and satisfies $\mu_3\leq\mu_4\leq\cdots\leq\mu_{k+2}$. Let $d_i=\mu_{i+2}-1(\forall 1\leq i\leq k)$,then (1) is equivalent to

$$d_1+d_2+\cdots+d_k=n-2-t \qquad (2)$$

Where $1\leq d_1\leq d_2\leq\cdots\leq d_i$, $0\leq k\leq n-2$, $0\leq t\leq n-2-k$.

The number of solutions of equation (2) is that the number of the zero-divisor semigroup of graph K_{n+1}^* under isomorphism, that is

$$S_1(n-2)=\sum_{k=1}^{n-2}\sum_{t=0}^{n-2-k}p(n-2-t,k).$$

② If $\{a_1a_2,a_1a_{n+1},a_2^2,a_{n+1}^2\}$ takes $\{a_l,a_m,0,0\}$, and $a_l\neq a_m$. the number of zero-divisor semigroups of graph K_{n+1}^* under isomorphism is

$$S_2(n-2)=\sum_{k=2}^{n-2}\sum_{t=0}^{n-2-k}p(n-2-t,k).$$

③ If $\{a_1a_2,a_1a_{n+1},a_2^2,a_{n+1}^2\}$ takes $\{a_l,a_m,a_s,0\}(\forall 3\leq l,m,s\leq n)$,and $a_l=a_m=a_s$, the number of the zero-divisor semigroups of graph K_{n+1}^* under isomorphism is

$$S_1(n-2)=\sum_{k=1}^{n-2}\sum_{t=0}^{n-2-k}p(n-2-t,k).$$

④ If $\{a_1a_2,a_1a_{n+1},a_2^2,a_{n+1}^2\}$ takes $\{a_l,a_m,a_s,0\}(\forall 3\leq l,m,s\leq n)$,and a_l,a_m,a_s take two different values, we assume $a_l=a_m\neq a_s$ or $a_l\neq a_m=a_s$, the number of the zero-divisor semigroups of graph K_{n+1}^* under isomorphism is

$$2S_2(n-2)=2\sum_{k=2}^{n-2}\sum_{t=0}^{n-2-k}p(n-2-t,k).$$

⑤ If $\{a_1a_2,a_1a_{n+1},a_2^2,a_{n+1}^2\}$ takes $\{a_l,a_m,a_s,0\}(\forall 3\leq l,m,s\leq n)$,and a_l,a_m,a_s take values different from each other , the number of the zero-divisor semigroups of graph K_{n+1}^* under isomorphism is

$$S_3(n-2)=\sum_{k=3}^{n-2}\sum_{t=0}^{n-2-k}p(n-2-t,k).$$

⑥ If $\{a_1a_2,a_1a_{n+1},a_2^2,a_{n+1}^2\}$ takes $\{a_l,a_m,a_s,a_s\}(\forall 3\leq l,m,s,t\leq n)$,and $a_l=a_m=a_s=a_t$, the number of the zero-divisor semigroups of graph K_{n+1}^* under isomorphism is

$$S_1(n-2)=\sum_{k=1}^{n-2}\sum_{t=0}^{n-2-k}p(n-2-t,k).$$

⑦ If $\{a_1a_2,a_1a_{n+1},a_2^2,a_{n+1}^2\}$ takes $\{a_l,a_m,a_s,a_s\}(\forall 3\leq l,m,s,t\leq n)$,and a_l,a_m,a_s,a_t take two different values,we let $a_l=a_m,a_s=a_t$; $a_l=a_s,a_m=a_t$; $a_l=a_t,a_m=a_s$; $a_l=a_m=a_s\neq a_t$ or $a_l\neq a_m=a_s=a_t$. the number

of the zero-divisor semigroups of graph K_{n+1}^* under isomorphism is

$$5S_2(n-2)=\sum_{k=2}^{n-2}\sum_{t=0}^{n-2-k}p(n-2-t,k).$$

⑧ If $\{a_1a_2, a_1a_{n+1}, a_2^2, a_{n+1}^2\}$ takes $\{a_l, a_m, a_s, a_s\}(\forall 3\le l,m,s,t\le n)$,and a_l, a_m, a_s, a_t take three different values (let a,b,c),we set $a_l=a_m=a, a_s=b, a_t=c$; $a_l=a, a_m=b, a_s=a_t=c$; $a_l=a_s=a, a_m=b, a_t=0$; or $a_l=a_t=a, a_m=b, a_s=c$,the number of the zero-divisor semigroups of graph K_{n+1}^* under isomorphism is

$$4S_3(n-2)=\sum_{k=3}^{n-2}\sum_{t=0}^{n-2-k}p(n-2-t,k).$$

⑨ If $\{a_1a_2, a_1a_{n+1}, a_2^2, a_{n+1}^2\}$ takes $\{a_l, a_m, a_s, a_s\}(\forall 3\le l,m,s,t\le n)$,and a_l, a_m, a_s, a_t take values different from each other , the number of the zero-divisor semigroups of graph K_{n+1}^* under isomorphism is

$$S_4(n-2)=\sum_{k=4}^{n-2}\sum_{t=0}^{n-2-k}p(n-2-t,k).$$

Consequently ,if $a_1^2=0$, the number of the zero-divisor semigroups of graph K_{n+1}^* under isomorphism is

$$\begin{aligned}A(n-2)&=S_1(n-2)+S_2(n-2)+S_1(n-2)+2S_2(n-2)+S_3(n-2)+\\&\quad S_1(n-2)+5S_2(n-2)+4S_3(n-2)+S_4(n-2)\\&=3S_1(n-2)+8S_2(n-2)+5S_3(n-2)+S_4(n-2)\end{aligned}.$$

In the similar way , we can proof that (II) (III) (IV) is respectively true.

In conclusion ,the number of the zero-divisor semigroups of graph K_{n+1}^* under isomorphism is

$$T(n-2)=\begin{cases}14S_1(1)+4 & n=3\\ 14S_1(2)+22S_2(2)+4 & n=4\\ 14S_1(3)+22S_2(3)+27S_3(3)+4 & n=5\\ 14S_1(4)+22S_2(4)+27S_3(4)+7S_4(4)+4 & n=6\\ 14S_1(n-2)+22S_2(n-2)+27S_3(n-2)+7S_4(n-2)+S_5(n-2)+4 & n\ge 7\end{cases}$$

ACKNOWLEDGMENT

The authors want to express their gratitude to the referees for their helpful suggestions and comments.

This work was supported in part by the National Natural Science Foundation of China(No.11301151), the Key Project of the Education Department of Henan Province(No.13A110249) and student research training program of Henan University of Science and Technology.

References

[1] C. Godsil,G. Royle, *Algebraic Graph Theory,* Springer-verlag,New York,(2000).

[2] I. beck, "Cloring of a commutative ring",*Journal of Algebra,vol.*116,pp. 208-226, 1988.

[3] M. Zuo,T. Wu, "A new tructure of commutative semigroup",*Semigroup Forum*,vol. 70,pp. 71-80, 2005.

[4] P. Redmond Shane, "On Zero-ffivisor graphs of small finite commutative rings",*Discrete Mathematics,vol.* 307, pp. 1155-1166, 2007.

[5] S. Akbari,A. Mohammmadian, "On zero-divisor graphs of finite rings",*Journal of Algebra*,vol. 314,pp.168-184, 2008.

[6] S. B. Mulay, "Cycles and symmetries of Zero-divisors",*Comm. Algebra,vol.* 30,pp. 3533-3558, 2002.

[7] T. Wu, "On directed zero-divisor graphs offinite rings",*Discrete Mathematics*,vol. 296,pp. 73-86, 2005.

[8] T. Wu,D. Lu, "Zero-divisor semigroups and some simple graphs",*Comm . Algebra,*Volume 34,pp. 3043-3052, August 2006.

[9] T. Wu,L. Che, "Simple graph and commutative Zero-divisor semigroups",eprint arXiv： math/ 0512567,Dee 2005.

Research on Face with Glasses Recognition Technology Based on Pixel Scanning

Qingkun QI[1]; YI Cao[1]; aodong Cai[2]; Chunli Wang[1] ; Xingdong Wang[3]

[1]Institute of Information Technology of Guilin University of Electronic Technology, Guilin Guangxi, China
Email: nihaotony@sohu.com
[2]Guilin University of Electronic Technology, Guilin Guangxi, China
[3]Yanbian University, Yanji Jilin , China

***Abstract*—This paper proposes an easy algorithm, named horizontal column pixel scanning (HPS) based on human face pictures, to detect glasses. Firstly, nosepiece is located quickly. Then contour is extracted and filtered, and contour enhancement algorithm is used after judging by HPS algorithm for the first time. Finally use HPS algorithm to achieve result for the second time. This algorithm uses simple pixel operation to manage complicate intelligent detection problem, not only achieving a good result, but also using an easy method to handle a complicate issue. Through examination in Georgia Tech and BioID face database, results show that this method can effectively identify a face wearing glasses.**

***Index Terms*—Nosepiece positioning; Contour extraction; Horizontal column pixel scanning**

I. INTRODUCTION

Nowadays, there is a growing number of groups with a pair of glasses.Whether to wear glasses is one of the most important factors of effective appearance characteristics judgment.In the video image processing, there is an unavoidable problem how to separate human face with glasses from image database.X.jiang and other members[1] proposed to detect the critical regions of the glasses, Black Region and Grey Region, in 1998. Z.Jing and other members[2] used boundary information extraction technology to detect and extract glasses' information, which is single. C.Y.Wu and other members[3]used training templates to detect the glasses, so as to realize the glasses remove from face.There are no detection algorithms about the glasses specifically in the literature, but some processing methods are worthy of learning.Wu H and other members[4] extracted glasses well by using 3D Hof transform.Song and others[5] proposed the 2DUGDP method which can identify human face with glasses commendably.Bo Wu and others[6]used the wavelet features to train the Boost classifier to detect glasses.Literatures[4][5][6] can detect the glasses commendably, but algorithms are relatively complex, and depended on the training samples. Much time need to spend in creating sample library.

By synthesizing literatures [1][2][3], this paper proposes a simple method for detection, which does not need to set up a training sample database.Through a number of image segmentation and pixel processing method, whether the face with glasses or not can be quickly judged.

II. ARITHMETIC STATEMENT

The detection method is mainly divided into four steps: area location of the bridge of the nose, contour extraction, filtering and contour enhancement, pixel scanning detection, where the pixel scanning detection is used two times, as shown in Fig.1.

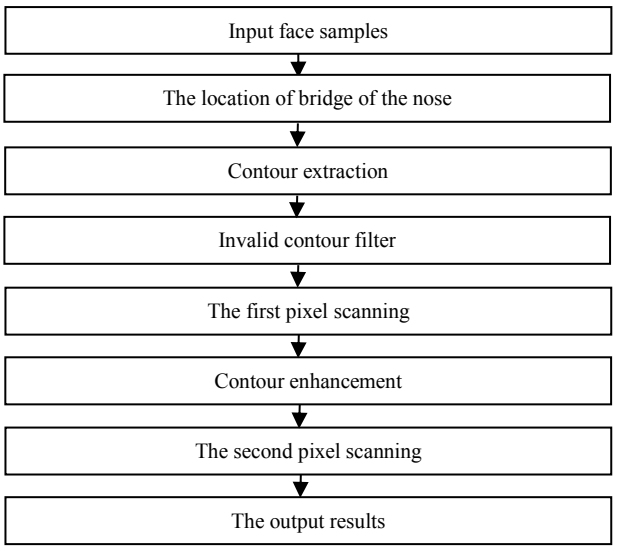

Figure 1. main steps of glasses detection in this paper

A. The location of bridge of the nose

Firstly the bridge of the nose is located in face images, and the apparent color mutation determines whether the person wearing glasses on the bridge of the nose or not. Therefore, the bridge of the nose is needed to quickly locate.Through measurement, a simple method, which can segment out the approximate location of the bridge of the nose, is used. As shown in Fig.2, there are some frontal and common face which can be divided into four parts from top to bottom and three parts from left to right. The coordinates of the bridge of the nose in general is around the area of (1, 1) (facial structure excess does not affect detection).The following processing will be conducted in this area. This area is much smaller

Fund Project:Guangxi University of science and technology research projects(2013YB092)
The corresponding:author:Chunli Wang.

compared to the original image, which greatly improves the speed of algorithm. In the aspect of positioning, the HAAR feature is also a good choice. HAAR features are trained on the bridge of the nose. Then ADABOOST algorithm is used to detect the bridge of the nose, which can obtain better location performance.

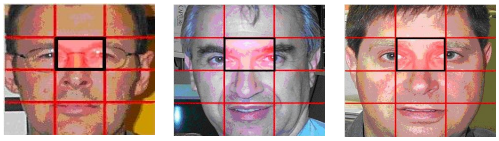

Figure 2. The segmentation results of the bridge of the nose of different human face

B. Contour extraction and filtration

After the bridge of the nose area is got, the next step is to extract the contour.First of all, convert the three channel image into a grayscale of single channel, according to formula (1):

$$Gray = 0.299R + 0.587G + 0.114B \tag{1}$$

Then the canny[7]edge operator is used to get the edge image of this area. The specific algorithm consists of four steps.

1.Noise cancellation.Gaussian Smoothing Filter is used, whose essence is to get the derivative of the original image and match Kernel template and pixel points.The pixel values in the image are multiplied by the value of the corresponding template convolution kernel, and we may get the pixel convolution values. Then we move the template, all the pixels values are calculated out as convolution values, and get the convolution image, which is also called Gaussian Smoothing Image. The kernel of this filter is shown as follows:

$$K = \frac{1}{K_{width}.K_{height}} \begin{bmatrix} 1 & 1 & \dots & 1 \\ 1 & 1 & \dots & 1 \\ . & . & \dots & 1 \\ 1 & 1 & \dots & 1 \end{bmatrix} \tag{2}$$

A Gaussian smoothing kernel whose size is 5:

$$K = \frac{1}{159} \begin{bmatrix} 2 & 4 & 5 & 4 & 2 \\ 4 & 9 & 12 & 9 & 4 \\ 5 & 12 & 15 & 12 & 5 \\ 4 & 9 & 12 & 9 & 4 \\ 2 & 4 & 5 & 4 & 2 \end{bmatrix} \tag{3}$$

2.The calculation of the image gradient values and gradient direction. Two convolution kernels of x and y directions are respectively defined as follows:

$$G_x = \begin{bmatrix} -1 & 0 & 1 \\ -2 & 0 & 2 \\ -1 & 0 & 1 \end{bmatrix} \tag{4}$$

$$G_y = \begin{bmatrix} -1 & -2 & -1 \\ 0 & 0 & 0 \\ 1 & 2 & 1 \end{bmatrix} \tag{5}$$

Convolution operation is done respectively for the image. Finally, according to formula (6) and formula (7) , the gradient magnitude and gradient direction are calculated.

$$G = \sqrt{G_x^2 + G_y^2} \tag{6}$$

$$\theta = \arctan(\frac{G_y}{G_x}) \tag{7}$$

3.Exclusion of some pixels values which are not maximum.After convolution derivative of X and Y directions, only the edge information are remained.Some unimportant edge information is excluded.

4.Threshold hysteresis excluding invalid pixels. If the pixel value is larger than the high threshold value, this pixel point will be retained. If the pixel value is less than the low threshold value, it will be excluded.If the pixel value is between the high and low threshold value, it will be retained if it is near to any pixel which is larger than high threshold value. Otherwise, it will be excluded.

After scanning the edge image, the edge image is denoised to reduce errors, because some wrinkles on the face can be mistaken as a spectacle frame edge. Assuming all the edge information are $x_1, x_2, \dots x_n$, α, a threshold value of edge pixel length is set through calculation of the size of the image. (Half of the region width is set as the threshold value in this paper, which also can be the average value of all the edges.) Edges whose pixel values are larger than the threshold value are regarded as effective edges; otherwise they will be regarded as noise.

$$f(x) = \begin{cases} 1 & x \geq \alpha \\ 0 & x < \alpha \end{cases} \tag{8}$$

"1"represents the edge is effective, and "0" represents the edge is not effective, which are calculated by formula (8).Only the edges of 1 are kepted. Effective edge exclusion, compared with pure Canny algorithm, is more practical in application.

C. Pixel scanning detection

So far, the first judgment can be conducted for the edge image after denoised. If the person doesn't wear glasses, then continuous edge information will not be shown on the bridge of the nose. A scanning algorithm of lateral column pixel is proposed in this paper, which can detect the edge pixel changes. (This method is only applicable to the pictures of noses in the vertical state.) It can quickly detect the chromatic mutation on the bridge of the nose. The pseudo-code of this algorithm are shown in Fig.3.

```
define j = 0
for x = 0 to width of interesting area
        for y = 0 to height of interesting area
                if (pixel value = 255)
                        break
                else if (y = height - 1)
                        j = j + 1
if (j > threshold)
        not has glasses
else
        has glasses
```

Figure 3. pseudocode of horizontal column pixel scanning algorithm

First of all, successively judge columns of image pixels. If it has certain numbers of column pixels which don't contain any edge pixels, i.e. the image is full of black pixels, it can be asserted that this person doesn't wear glasses. For example, a 5*5 pixel matrix is used to represent the original image, in which 0 represents white pixel and 1 represents black pixel, shown in Fig.4. Assuming the threshold value is 1, Fig.4 (left) will be judged as one wearing glasses, and Fig.4 (right) will be directly eliminated as not wearing glasses.

Here, it is the first pixel scanning to clearly exclude those faces without glasses. It can be quickly and directly eliminate through the color variation of the bridge of the nose without following steps. Pay attention to set the threshold value of the first pixel scanning, to avoid misjudgment due to the small threshold value.

1	1	1	1	1
0	1	1	1	1
1	0	1	0	0
0	1	1	1	0
1	1	1	1	1

1	1	1	1	1
0	1	1	1	1
1	0	1	1	0
0	1	1	1	0
1	1	1	1	1

Figure 4. a 5*5 pixel matrix represented by 0 and 1

D. Edge enhancement

If the person has the possibility to wear glasses, we need more precise information to determine its existence. According to the image analysis, an extremely sensitive edge detection method is needed to extract the information of glasses. After tests, the effects of Canny operator and Sobel operator are not applicable. Finally, Laplacian operator is adopted in this paper[2], i.e. Laplasse transform for the original image. Laplacian operator is sensitive to the edge, which does not care for the gray difference of pixels around. Laplacian operator is an edge detection operator based on the second order partial derivative of image $f(x,y)$ in x and y direction. The specific method of contour enhancement is shown as follows.

1.To process the relevant area of bridge of the nose by Gaussian Blur, getting a blurred image, Guess Image.

2.To calculate the first derivative of the Guess Image with respect to Y. Calculate convolution with the convolution kernel, to get derivative image of single Y direction, Sobel Image.

3.To operate Laplace transform of Guess Image, whose operator is showed as follows:

$$Laplace(f)=\frac{\partial^2 f}{\partial x^2}+\frac{\partial^2 f}{\partial y^2} \tag{9}$$

Through formula (9), Laplace transform is actually the second derivative for image with X-axis and Y-axis, getting Laplace Image.

4.To binarize Sobel Image. Transform the original image into a black and white pixel image, then do the open operation. The open operation is shown as follows:

$$\text{open}(src)=dilate(erode(src)) \tag{10}$$

Here, $erode(src)$ is a image corrosion operations, $dilate(src)$ is a image expansion operation. The finally image is called sImage.

5.To do d operation for Laplace Image, and the resulting image is called lImage.

6.To do OR operation for sImage and 1Image, and the finally Image is got.

Then HPS algorithm is used for Image once again. At this time, the Laplace algorithm has higher accuracy, so the threshold value is set as zero. (Every column pixels contain white point.) If it meets the conditions, the face is thought as with glasses.Otherwise, it is not.A part of outputs of this detection process are shown in Fig.5.

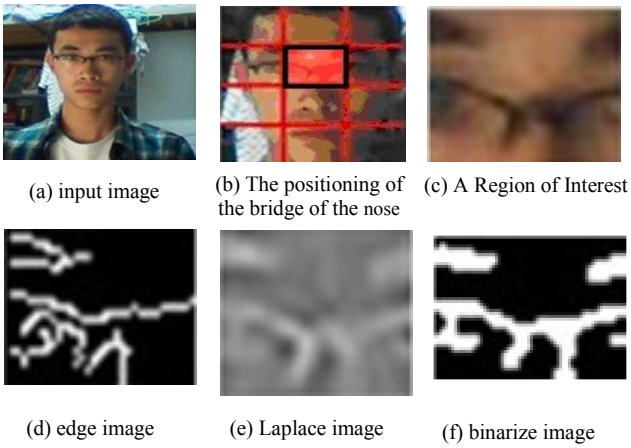

(a) input image (b) The positioning of the bridge of the nose (c) A Region of Interest

(d) edge image (e) Laplace image (f) binarize image

Figure 5. output of different stages

III. EXPERIMENTTAL RESULTS AND ANALYSIS

Georgia Tech and BioID face database are selected in this experiment. In Georgia Tech face database, there are 122 persons with glasses and 470 persons without glasses. It contains colorized face images of different sex and ages, and the head tilt angles are not identical. In BioID face database, there are 480 persons with glasses and 1041 persons without glasses. It is full of gray images. Although the facial poses are not richer than Georgia Tech database, the backgrounds are relatively more complex than those of Georgia Tech database, which is better to detect the robustness of algorithm.

A. The experiment of Georgia Tech human face database

TABLE I. The detection results of Georgia Tech database

	face with glasses	face without glasses
the number of pictures	122	470
The number of correct detection	114	384
accuracy rate	93%	81%

The outcome of the experiment： As shown in Table I, there are more false detection in face without glasses, and the accuracy rate is relatively higher in face with glasses.

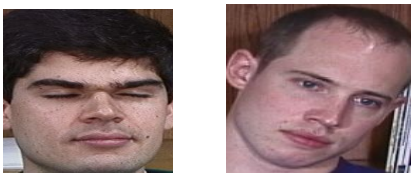

Figure 6. False detection of human face images

The result analysis: The main problem is the obvious wrinkles and the head gradient, shown in Fig.6. There is a false detection in the left picture because of an obvious facial wrinkle. There is also a false detection in the right picture because of an excessive gradient. Absolute positioning is adopted in this algorithm, in which the bridge of the nose is taken as the Interest region. It does not adopt other detectors to locate the nose. It also doesn't adjust the gradient of the face. So misjudgment will not exist because of the positioning.If limit the corresponding conditions in collecting samples, the detection effect will be further improved.

B. The experiment of BioID face database

TABLE II. The detection results of BioID database

	face with glasses	face without glasses
the number of pictures	480	1041
The number of correct detection	351	964
accuracy rate	73%	92%

The outcome of the experiment： As shown in Table II, the accuracy rate of face with glasses obviously decreased. However, the accuracy rate of face without glasses is improved.

The result analysis： The main problem is the edge extraction, as shown in Fig.7.BioID database is composed of gray images. The edges are not particularly clear, which leads to directly remove in the first time HPS operation. High-low threshold values setting of Canny operator is one of the main causes of misjudgment. Too lower α in formula (8) also causes to delete the effective edge when edge denoised.

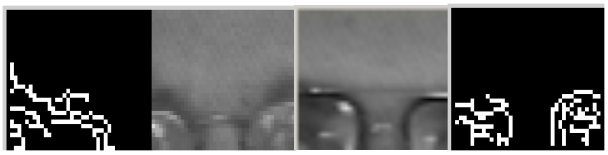

Figure 7. the effective edge of the bridge of the nose which is deleted

Two experimental results show that, the proposed algorithm can effectively detect the face image with glasses. But due to the impact of different environments, the results differ. The positioning errors of the bridge of the nose take a big proportion. Secondly, it is matter to adjust the hysteresis threshold of Canny operator to adapt to different background texture.The binaryzation calculation is as the same as the edge detection algorithm. The accuracy depends on any effective pixel points. It will become the next research focus that how to improve the robustness of algorithm,keep the effective information, and correctly detect bespectacled face in a complex environment.

Ⅳ. CONCLUSION

In this paper, a series of image transformation is completed to detect bespectacled faces. Eliminate parts of faces without glasses using effective information edge, and then do Laplace transform and binarization, combined with horizontal column pixel scanning algorithm, to judge the face image. It is a simple algorithm with low computational complexity, which is verified by experimental results. It obtains better detection results in the condition of clear image and the frontal face with natural expression. It can play a significant role in safety protection, retrieval and classification of identity cards and other important documents.

ACKNOWLEDGMENT

This work was supported in part by a grant from Guangxi University of science and technology research projects(2013YB092).

REFERENCES

[1]X.Jiang,M.Binkert,B.Achermann,H.Buke.“Towards detection of glasses in facial images,” *In Proceedings of Internationa Conference on Pattern Recognition(ICPR)*,1998,pp.1071-1073.

[2] Z.Jing and R.“Marani.Glasses Detection and Extraction by Deformable Contour,” *Proc.Int’l Conf.pattern Recognition*,2000.8,pp.933-936.

[3] C. Y. Wu, C. Liu, H. Y. Shum, Y. Q. Xu and Z. Y. Zhang. “Automatic eyeglasses removal from face images,”*Asian Conference on Computer Vision (ACCV)*,2002,pp.193-198.

[4] Wu H,Yoshikawa G,Shioyama T,Lao S,Kawade M. “Glasses frame detection with 3D Hough transform,” *In Proceedings of International Conference on Pattern Recognition (ICPR)*, 2002,pp.346–349.

[5] SONG Cai-fang,YIN Bao-cai,SUN Yan-feng, CHEN shang-you.“Glasses Recognition Base On 2D Unsupervised Geodesic Discriminant Projection, ”*Beijing University of Technology*,2011,37(3),pp.470-476.

[6] Bo WU, Haizhou AI and Ran LIU. “Glasses Detection by Boosting Simple Wavelet Features, ”*In Proceedings of International Conference on Pattern Recognition(ICPR)*, 2004,pp.292–295.

[7] John F.Canny.“A computational approach to edge detection, ”*IEEE Transactions on Pattern Analysis and Machine Intelligence*, 1986.8,pp.679-698.

The Simulation of Sampling Distribution in the Teaching of Business Statistics to English Majors

Shili Ge
Guangdong Univ. of Foreign Studies/Guangdong Collaborative Innovation Center for Language Research and Services, Guangzhou, China
Email: geshili@gdufs.edu.cn

Fei Fang and Xiaoxiao Chen
Guangdong Univ. of Foreign Studies/School of English for International Business, Guangzhou, China
Email: {819469615, 1227633303}@qq.com

Abstract—**The understanding of sampling distribution is vital for students to move from descriptive statistics to inferential statistics and the Central Limit Theorem (CLT) is one of the most important theorems in statistics. In order to help undergraduate English major students with weak mathematic background understand the process of sampling distribution and the theory of CLT, a teaching simulation of sampling distribution was designed with self-coded Python programs. This simulation is simple and intuitionistic, which improves the teaching effects and lays a solid foundation for undergraduate English major students in their further statistics study.**

Index Terms—**sampling distribution, Central Limit Theorem, statistical simulation, English major undergraduate students, business statistics**

I. Introduction

As a bridge from descriptive statistics to inferential statistics, a thorough understanding of sampling distribution is vital for students, especially the business English major undergraduate students without adequate mathematical background. In practice, we select a single random sample of a predetermined size from the population and use the sample statistic to estimate the population parameter. Yet, a difference, large or small, always exists between the statistic and the parameter, which is called sampling error [1]. If we take sample mean,$\overline{x}$, and population mean,μ,as an example

$$Sampling\ error = \overline{x} - \mu \quad (1)$$

We could examine every possible sample of a given size that could occur. Thus, we have a sampling distribution, which is the distribution of the results if we actually select all possible samples. The single result we obtain in practice is just one of the results in the sampling distribution. The sample mean is often used to estimate the population mean. The sampling distribution of the mean is the distribution of all possible sample means if we select all possible samples of a given size [2].

Sampling distribution of sample means has a relationship with the population that the samples are taken from, no matter what distribution the population follows, which is described by the Central Limit Theorem (CLT). This Theorem is one of the most important and useful theorems in statistics [1] because it relates one sample statistic with the population parameter via the distribution of all sample statistics. The understanding of this relationship lays a solid foundation for the study of parameter estimate and hypothesis testing in inferential statistics.

The definition of CLT for any probability distribution: If x possesses *any* distribution with mean μ and standard deviation σ, then the sample mean $\overline{x}$ based on a random sample of size n will have a distribution that approaches the distribution of a normal random variable with mean μ and standard deviation $\sigma/\sqrt{n}$ as n increases without limit [3].

This is a remarkable statistical fact [4]. That means, as we take more and more observations at random from any population, the distribution of the mean of these observations eventually gets close to a normal distribution. The CLT lies behind the use of normal sampling distributions for sample means. Therefore, the vivid presentation of this fact to English major learners of business statistics is essential for them to understand inferential statistics.

In the teaching of CLT, Ref. [5] proposes that we should select practical examples in students' major fields, so as to help students understand CLT and apply it in real problem solving. Ref. [6], starting from students' confusion and teaching perspective, seeks for problem driven teaching method to teach undergraduate mathematics students effectively. In business statistics, the teaching of CLT is usually brief with a few simple examples or MS Excel simulations, which is far from enough for English major students to understand this important theorem. Therefore, we design a complete calculation of sampling distribution of sample means from small populations and a simulation of sampling distribution of sample means from large populations for students to help them better understand sampling distribution and the Central Limit Theorem.

Corresponding author: Xiaoxiao Chen

II. Simulation Design

In fact, many statistics course books have a section about simulation for the explanation of CLT, but they are either difficult to implement or not clear enough as complained by students.

Random number generators can be used to generate the values of random variables from arbitrary distributions. With this ability to generate arbitrary random variables we will be able to simulate a probability system, all the random quantities of this system as it evolves over time [7].

It is obvious that computerized statistical simulation has an advantage in business statistics teaching. The repetition of calculation becomes very simple with the adjustment of certain variables in computer programs so as to present the simulation of sampling distribution with large quantity of samplings. Therefore, we design some Python programs to calculate sampling distribution of sample means from small populations and simulate sampling distribution of sample means from large populations.

A. The Aims of Statistical Simulation

The teaching of business statistics to English major undergraduate students may have two extremes. One is the pure theoretical explanation, including derivation and proof of statistical principles and formulae. The other is total software operation, mainly SPSS hypothesis testing. Due to the weak mathematical background of English major students, the former is usually too difficult for them, and the latter shows them the final result without any deep understanding. The simulation of sampling distribution can achieve the following aims:

First, by designing the simulation of sampling distribution, we can educate students with experimental method and technique in business study, improve students' ability in problem identification, analysis and solution, and deepen their understanding of statistical concepts, ideas and rules.

Then, we can teach students fundamental experimental methods in business statistics and get familiar with Python script language for statistical computation, so as to lay a foundation for them to further their work and research.

At last, we can encourage students read and refer to relative materials, design experimental plans, write simple Python programs to analyze business phenomenon.

B. The Design of Sampling Simulation

The statistical simulation contains mainly three parts: the generation of random numbers, the simulation of discrete events and the statistical analysis of the simulation data [7]. For the simulation of sampling distribution, the 3 steps are:

First, to generate random numbers following a certain population distribution. In this simulation, we generate a small population of uniform distribution and a large population of Poisson distribution, calculate the means and variances of the populations, and plot histograms.

Then, to simulate the process of sampling distribution. That is, we set sample size *n*. Certainly, for different population, we have different number n. And draw all possible samples from the small population and M samples from the large population; change sample size n and draw samples again; repeat the procedure 3 times.

At last, to analyze the sampling data and plot histograms. That is, for a certain sample size *n*, calculate the mean of all or M means and the variance (or standard deviation), draw histograms, and analyze the relationship between mean and variance of sample means and population mean and variance.

C. Sampling Simulation of a Small Population

To develop a sampling distribution from a small population, firstly, we need a population. Assume there is a population of size N = 5. Random variable, x, is age of individuals. Values of x are 18, 20, 22, 24 and 26 (years).

The summary measures for the population distribution are as following:

$$\mu = \frac{\sum x_i}{N} = \frac{18+20+22+24+26}{5} = 22 \quad (2)$$

$$\sigma^2 = \frac{\sum (x_i-\mu)^2}{N} = 8 \quad (3)$$

$$\sigma = \sqrt{\sigma^2} \approx 2.83 \quad (4)$$

The population distribution is obviously a uniform distribution as plotted below:

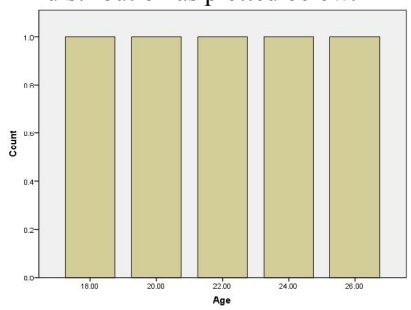

Figure 1. Uniform distribution of a small population

The second step of developing a sampling distribution is to set the sample size n and draw samples from the population. For this small population of 5 individual, we set the sample size n as 2, 3, and 4 respectively to develop 5 sampling distributions.

With a certain sample size, we draw all possible samples with replacement from the population. That means, we can draw $5^2 = 25$ samples for sample size n = 2, $5^3 = 125$ samples for n = 3 and $5^4 = 625$ samples for n = 4, respectively.

It is rather simple to calculate 25 samples from the population manually, but it becomes difficult very soon along with the increase of population and sample size. Therefore, we write a Python program to perform the task. The algorithm of the program is simple with 3 loops:

1) set up a population of N individuals
2) set sample size n
3) draw all possible samples of size n with replacement
4) calculate and output the means of all these samples

The last step is the analysis of the sample means of different sample sizes.

TABLE I.
SAMPLING DISTRIBUTIONS OF THE SMALL POPULATION

sample size (n)	2	3	4
mean of means ($\mu_{\bar{x}}$)	22	22	22
variance of means ($\sigma_{\bar{x}}$)	4	2.67	2

Comparing with formulae 2 and 3, we can see that:

Mean of means is equal to population mean and variance of means is the population variance divided by sample size. That is,

$$\mu_{\bar{x}} = \mu \tag{5}$$

$$\sigma_{\bar{x}}{}^2 = \frac{\sigma^2}{n} \tag{6}$$

Namely,

$$\sigma_{\bar{x}} = \frac{\sigma}{\sqrt{n}} \tag{7}$$

The three sampling distributions are plotted in Figure 2 as below.

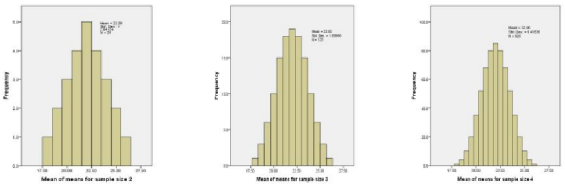

Figure 2. Sampling distributions of the small population (sample size 2, 3 and 4)

Comparing with Figure 1, we can see that the population distribution is uniform and the sampling distributions are all normal with sample size 2, 3, and 4. With the increase of sample size, the sampling distribution becomes smoother.

This is a theoretical simulation with a very small population. In business statistics teaching, we can enlarge the population and the sample size moderately, but the number of samples will grow so fast that we cannot wait to see the result in class. In fact, we usually simulate sampling distribution with a large population and draw a small part of all possible samples.

D. Sampling Simulation of a Large Population

For the simulation of sampling distribution from a large population, we need a population following an arbitrary distribution. For the effect of teaching, we create a typical non-normal population of 100,000 numbers following Poisson distribution, which is created by Python NumPy module. The summary of the simulated population is presented in table II.

TABLE II.
SUMMARY OF RANDOM NUMBERS AS THE LARGE POPULATION

Population size (N)	Min (x_{min})	Max (x_{max})	Mean (μ)	SD (σ)	Variance (σ^2)
100,000	0	16	5.01	2.23	4.98

The distribution of these random numbers are plotted in figure 3. From this figure we can see clearly that this population is right skewed with a long tail on the right side.

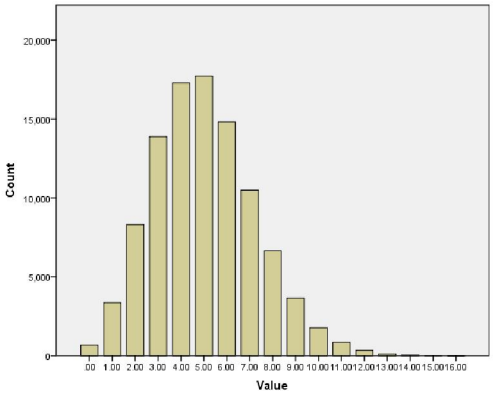

Figure 3. The distribution of random numbers as the large population

To draw samples from the population, calculate sample means, and observe the distribution of these means are the key steps of sampling distribution simulation. Students can learn from course books that for normal population, sample means have a normal distribution even with a small sample size n, but for non-normal population, the sample size n should be large enough to form an approximately normal sampling distribution. Therefore, we set the sample size n as 2, 5 and 30 and sampling times M as 10,000 to observe the sampling results. That is, for each sample size n, we draw 10,000 samples from the population and observe the relationship between the distribution of the means and the distribution of the population.

The sampling algorithm of Python program is as following:

1) Input the population;
2) Set M;
3) Set n;
4) Draw a sample of n elements from the population;
5) Calculate the mean of the sample and store in a list;
6) Repeat step 4) and 5) for M times;
7) Change n and run 4) to 6) until complete all sampling procedures with different n;
8) Output the results, namely, the lists of all sample means.

After executing this program, the sampling results are listed in table III.

TABLE III.
SUMMARY OF SAMPLING RESULTS FROM THE LARGE POPULATION

Sample size (n)	Min ($\bar{x}_{min}$)	Max ($\bar{x}_{max}$)	Mean ($\bar{\bar{x}}$)	SD ($s_{\bar{x}}$)	Variance ($s_{\bar{x}}{}^2$)
2	0.5	12	5.02	1.57	2.46
5	1.4	9.4	5.01	0.99	0.98
30	3.47	6.57	5.01	0.41	0.17

Comparing with the data in table II, we can see that the means of sample means, $\bar{\bar{x}}$, of all sample sizes are same or almost same to population mean, μ, and the variances of these means of samples are very close to the population variance, σ^2, divided by sample size n. That means formulae (5), (6) and (7) are approximately correct for partial sampling distribution from a large population.

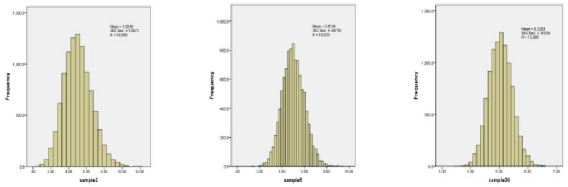

Figure 4. The distribution of random sample means from the large population

The sample means are plotted in Figure 4. When sample size n is 2, the distribution of sample means is obviously positive skewed. When sample size increases to 5, the distribution becomes closer to normal distribution. And along with the increase of sample size, the distribution of means is closer and closer to normal distribution. When sample size n increases to 30, sample means have an almost perfect normal distribution.

With 3 different sample sizes, we draw large quantity of samples from the positive skewed population, the mean of means and the distribution of means completely follow the description of the CLT. That is, with a certain sample size n, if we draw a large amount of samples from the population, the means of the samples approximate the normal distribution, the mean of means approximates the population mean, and the variance of the sample means approximates the population variance divided by the sample size n. Moreover, from the simulation, we can see that for non-normal distribution, sample size should be big enough, the distribution of sample means can approximate the normal distribution.

III. Conclusion

This simulation is designed for undergraduate business English majors. In one hour of teaching, we train students not only statistical theory and histogram plotting, but Python programming, especially the using of random modules as well. With the operation of this simulation, students can gain a direct perceptual awareness of sampling distribution and the Central Limit Theorem, which lays a solid foundation for the further study of inferential statistics.

This statistical simulation of sampling distribution has a relatively low requirement for teaching conditions. We need only a computer installed the software of Python and SPSS. With a few years of teaching practice, this simulation has a vital catalytic role in teaching business statistics to those undergraduate English majors with relatively weak mathematic background.

Acknowledgment

This work was supported in part by the grants from 2014 Guangdong Province Higher Education Teaching Reform Program (GDJG20141094), 2013 Department of Education of Guangdong Province Program (2013KJCX0070), and 2013 Guangdong University of Foreign Studies Key Program of Teaching Reform "Research Driven Teaching Practice and Exploration of Business Statistics".

References

[1] R. Larson and B. Farber, *Elementary Statistics: Picturing the Wrold*, Beijing: Qinghua University Press, 2004.

[2] Mark L. Berenson, David M. Levine and Timothy C. Krehbiel, *Basic Business Statistics: Concepts and Applications* (12th edition), Boston: Prentice Hall, 2012.

[3] Charles H. Brase and Corrinne P. Brase, *Understandable Statistics: Concepts and Methods* (10ed), US: Cengage Learning, 2012.

[4] David S. Moore and William I. Notz, *Statistics: Concepts and Controversies*, New York: W. H. Freeman and Company, 2009.

[5] Y. Huang, "The Teaching of Central Limit Theorem in Classroom," *The Field of Entrepreneur*, vol. 8, 2008, p. 196.

[6] Y. Li, "Central Limit Theorem of Teaching Methods," *China Science and Technology Information*, vol. 24, 2010, pp. 220-221.

[7] Sheldon M. Ross, *Simulation*, San Diego: Elsevier, 2013.

Shili Ge, born in Yantai City, Shandong Province, China in Oct. 1969; gaining Ph. D in the field of language engineering from the Research Center of Language Information Processing of Beijing Language and Culture University, Beijing, China in 2008.

He is presently a professor in the School of English for International Business, a graduate students supervisor in the School of Interpreting and Translation Studies of Guangdong University of Foreign Studies in Guangzhou City, and at the same time, he also works as the deputy director of Guangdong Collaborative Innovation Center for Language Research and Services.

Fei Fang, born in Loudi City, Hunan Province, China in May 1991; gaining Bachelor of Arts in the field of English Language from the Institute of Foreign Language of Xiangtan University, Xiangtan, China in 2014.

She is currently a graduate student in the School of English for International Business in Guangdong University of Foreign Studies in Guangzhou City.

Xiaoxiao Chen, born in Anshan City, Liaoning Province, China in Nov. 1975; gaining Ph. D in the field of mass communication from the School of Journalism and Communication, Wuhan University, Wuhan, China in 2010.

She is presently a professor in the School of English for International Business, Guangdong University of Foreign Studies in Guangzhou City.

The Project Risk Analysis And Measures Of The Main Exhibition Stage

Xiaohong Chen
Department of Management Shandong Jiaotong University
Jinan , China

Abstract—**In recent years, the exhibition many of the city economy has become the new economic growth point. However, as the exhibition process, the exhibition itself has a lot of the urgent problem of the inevitable risks. Based on the exhibition project risk identification, risk assessment, risk monitoring are analyzed, focusing on the MICE events that start, implementation, closeout phase of the various risks and proposed strategies to address these risks, hoping for MICE business Project risk management has a guiding role.**

Index Terms-**exhibition project; risk analysis; risk strategy**

In the current context of the global economy, all countries must be integrated into almost the world economic system, its goods, services, movement of production factors such as increasing the size and form. This set of product display, trade and economic cooperation, conferences, exhibitions will be developed rapidly. large-scale group exhibition project, a high level of consumption, guests stay longer, involving more related industries, and its huge market potential and high returns, so many government departments and exhibition business to join the competitive ranks of the exhibition.

Exhibition huge profits generated by the project, potential risks will come with it all. Risk is uncertain. The current exhibition is full of many activities held in the uncertainty factor, which is the exhibition can't avoid the fact that the project organization as a convention planner, can only take the initiative to adopt the relevant preventive management measures to deal with these uncertainties, to help the project proceed smoothly.

I.EXHIBITION OVERVIEW OF A PROJECT RISK MANAGEMENT

Exhibition project risk management is the objectives management activities that exhibition project manager development strategies, and then remove and reduce the risk of harm through the early identification, development strategies. Exhibition project risk has the following features:

A Uncertainty

Exhibition project risks with strong uncertainty, it happened is not inevitable, but the likelihood is great anytime, anywhere. The degree of risk on the impact of the project is uncertain. In different circumstances, the risk of the project can also change. Changes in the nature of project risks, the project will change the results or even lead to new risks.

B phased

Exhibition project risk is a phased development, each stage has clear boundaries. Exhibition stage of project risks consist of risks of potential stage and occurring stage and consequences of risk occurring 。 We must identify the various stages of the risk as soon as possible, and take measure to reduce its losses.

C relative

Exhibition project risk is relatively different in terms of risk management body, a variety of factors consisting of project risk management capacity of the main risk the project's expected return the size of the risk factors will impact Exhibition consequences. Therefore, the project risk is relative. The exhibition project risk and benefits are reciprocal for the exhibition. Person in charge of project-related exhibition must bear the associated risks in order to obtain certain amount of revenue.

II.THE PROJECT RISK ANALYSIS OF THE MAIN EXHIBITION STAGE

Risk identification should first understand the composition of the project, the nature of the various project components and relationships between the project and the environment. Only a comprehensive and correctly indentify the risks exhibition projects, estimates of risk, evaluation and selection of risk management techniques have practical significance. Therefore, a major exhibition project analysis phases are more important.

A start-up phase

For exhibition project, project feasibility analysis is a necessary pre-decision-making process, so the proposed project implementation framework needs to conduct a feasibility analysis before we can determine the need for project. Feasibility analysis is to avoid losses from blindly make a decision.

The risk of lacking feasibility analysis lies in: lacking of market demand, feasibility studies lack good understanding of the current market demand, not to determine whether the project is necessary according to business situation; lack of resources feasibility study. Exhibition project requires a lot of resources, such as human resources and government support, and other senior managers, Lack of economic viability: These phenomena may cause losses such as lack of adequate financial support, and lack the economic feasibility of the project costs and expected benefits.

B Implementation phase

Financial risk: Exhibition project in the financial management in potential risks mainly displays in: Exhibition project cash flow problems themselves, budget overruns. Main sponsors temporary exit caused economic pressure.

Schedule risk: Progress risk mainly displays: Exhibition project work in implementing project started no feasible plan; Leading personnel and implementing personnel work deviation Project lacks visibility, Its negative effects could lead to various aspects of discontent， Project the more likely fail.

Operational risk: Operational risk in exhibition projects mainly in: market momentum is relatively small. Exhibition project itself isn't attractive, the strength of the exhibitors or industry celebrities to participate less, the result of inadequate advertising aspects of the market is smaller than expected; the absence of the major exhibitors: For the exhibition project, the industry's leading exhibition companies participated in very important. Main key exhibitors absence will make project effect the discount and will make other exhibitors mistrust of project products.

Human resources risk: Exhibition project in human resources exist mainly manifested in the potential risks : Staff turnover will give projects have a big impact, The new personnel training and gradually to communicate with existing members, thus making the existing members work productivity , members can't adapt to the work don't transfer project team and influence other members' enthusiasm.

C Closure phases

If you did not pay much attention to the project ending work, it will make the project cannot normal ended

No attention staggered results ending: Although exhibition project ending, collect is full of previous work, Job itself skills project ending is very important also, Ending is complex and characteristics of a multitude, if you can't attach importance to finish off achievements, it will not promptly of the project documentation, acceptance and archiving.

No ending work system: Project ending is a trivial work, we must formulate standard ending system. Formulation standardized system to guarantee the project document submitted smoothly, ending up in the continuity of the conference &exhibition projects is very important significance.

III. THE COUNTERMEASURES OF THE RISK IN EXHIBITION PROJECT PHASE

A Financial risk strategies

Establishing perfect risk prevention system: Grasping the enterprise internal control system. Constructing to ensure financial risk pre-warning and monitoring system; establishing and standardizing enterprise statement analysis system in financial risks to improve liquidity analysis and perfect the risk early-warning system.

Establish financial warning system: Project must be established, Comprehensive and dynamic financial warning system in the implementation of the project is necessary, the activities of real-time monitoring potential risk will penetrate throughout the whole process of exhibition project implementation.

B Progress risk strategies

Implement efficient team, founded in scientific management: It is a necessary choice at the start of a project to build an effective project team. To ensure progress goal realization, It is necessary to enhance the cooperation between each other and spirit in members of the team and to construct team training team knowledge and cultural.

Establish a practical project plan: It is a required step to establish a practical project plan to project schedule examinations and assessment, Project according to various plans to make reasonable project about plan worked, and timely feedback parties opinion suggestion, to adjust the parties project.

Develop plans to schedule the main content: Schedule plan is the key work schedule management, other plan is more scientific within the schedule, and plans can be adjusted according to schedule in the implementation process.

C Operational risk strategies

Set up a risk management organization: Formulate risk management system applying early warning management methods to prevent various processes link appeared in risk. Through standard risk prevention operation is flow and system, Formulate risk management system may reduce the risk and losses.

Perfect risk management information system: Using of the existing system, we can increase risk management related modules and collect of information for risk events, statistics, trend analysis in order to propose more specific risk response options. According to the changes in the internal and external environment we can track and supervise exhibition project.

Encourage participation in insurance of exhibition project ： Modern risk insurance of convention and exhibition activities have been gradually pushed, but the insurance category is also relatively simple. It is another important content and the new task to encourage participation in the risk management of insurance.

D Human resources risk strategies

Human resources in the exhibition project mainly include the following aspects of risk management strategies: we should establish the correct concept of human resources、 risk management concepts and ideas to ensure the proper and advanced concepts. Establishing human resources management system is to improve the construction of the system and to protect the integrity of the system, systematic and continuous. In the specific human resources management activities with actual project, the implementation of adaptive and practical technical approach is to ensure systematic and coordinated the project. Establish a scientific

performance appraisal system, and encourage more effective and adequate is based on the scientific evaluation of job performance. Establish a scientific system of performance appraisal to enhance Human resource level.

IV. CONCLUSION

Exhibition project risk management is an important issue for the exhibition industry. Because it exists in every stage of exhibition, the risk may be constantly changed at the implementation process, the exhibition on the main task of project risk:

With the progress of the project, we can monitor residual risk and identify new risks following the known risks, we must analyze the degree of realization of project objectives exhibition and changes in risk factors. We must look for opportunities to refine the risk response measures to achieve the goal.

REFERENCE

[1] Wang qi-ji *Exhibition Project Management* [M]. Bei jing：China Business Press，2004.

[2] Bai si-jun *Modern Project Management*[M] . Beijing：Machinery Industry Press，2004．32

[3] Liu da-ke,Wang qi-jing *Introduction to exhibition activities* [M] . Beijing ： Tsinghua University Press.2004.

[4]Luyou-jie,Lujia-yi *Project Ri sk Management*[M] . Beijing：Tsinghua University Press.2000

[5] Gu meng-di, Lei peng . *Risk Management*[M] . Beijing：Tsinghua University Press.2005.

[6] 2010 Shanghai World Expo (Volume I, Volume II, Volume III). Shanghai World Expo 2010 Bid Committees.2002.1

[7] Wu zhong， Xu bo. “Risk in the Shanghai World Expo” [J]. International Business Studies，2007

[8] Robert K Wysocki. Little Robert. *Baker. Effective project management*[M]. 2002

[9] Kathy. *Project risk management. Market Management*.2002

Robust Double-level Watermarking of Facial Images Based on Spread Spectrum and Dirty Paper

Fei WANG
School of Computer Science, Sichuan University of Science and Engineering, Zigong China

Abstract— **In the paper, we have presented a robust double-level watermarking scheme for facial images. Based on the face rectangle window size of facial image, the proposed method takes consideration to image authentication and copyright protection simultaneously, which uses a spread spectrum encoding the rectangle face region and dirty-paper trellis codes for whole image area. This technique can meet special requirements. We have shown experimentally that using of this robust watermarking scheme can significantly improve embedding effectiveness.**

Index Terms— **double-level watermarking, facial image, spread spectrum, dirty paper first term**

I. INTRODUCTION

The proliferation of digitized media (audio, image, and video) across networks is creating a pressing need for copyright enforcement schemes that protect copyright ownership. There are two parts to building a strong watermark: the watermark structure and the insertion strategy. In order for a watermark to be robust and secure, these two components must be designed correctly. The watermark should not be placed in perceptually insignificant regions of the image, since many common signal and geometric processes affect these components. Watermarking as communications with side information [1-2], the frequency domain of the image is viewed as a communication channel, and correspondingly, the watermark is viewed as a signal that is transmitted through it. Attacks and unintentional signal distortions are thus treated as noise that the immersed signal must be immune to. Based on this methodology to hide watermarks in data, secure spread spectrum (SS) watermarking [3-6] and dirty-paper trellis codes (DPTC) watermarking [7-10] are the most well-known scheme.

This work was supported by the Scientific Research Foundation of Sichuan University of Science and Engineering (Grant No. 2012RC22) and Sichuan Provincial Department of Education Fund (Grant No.13ZB0139)

Most of the existing watermarking methods for image authentication embed watermarks into the whole image without taking into account the underlying semantic content [11-13]. However, for many applications, some portions contain more important information than the rest of the image. For facial image, these portions are usually referred to face region. Faces are particular objects, which need a higher level of protection as the multimedia content, involving more and more well-known person faces, is always subject to falsification and illegal copy redistributions and being attacked to synthesize a new image such as copied, cropped or grafted.

In the present paper, we present a robust double-level watermarking scheme, which ensures integrity verification of slightly modified digital images. The double-level scheme is that encoding face region using spread spectrum watermarking and encoding whole image area with dirty-paper trellis codes. The face region is a window size of facial image witch has most semantic significance. The parts strengthened protection can prevent attacked to synthesis and graft a new image. In order to improve the robust, we use dirty-paper trellis codes to encode the whole image area. The proposed authentication scheme combines digital watermarking techniques with automatic detection of faces window size as salient regions. The paper is organized as following: section 2 briefly discusses related work spread spectrum and dirty-paper trellis codes watermarking. We illustrate in section 3 our approach based on the face window size detection and embedding scheme. A discussion on advantages and limitations of the proposed method is followed in section 4 and we conclude in section 5.

II. RELATED WORK

A. Spread Spectrum Watermarking

In spread spectrum communications, one transmits a narrowband signal over a much larger bandwidth such that the signal energy present in any single frequency is undetectable. Similarly, a watermark is placed in the frequency domain of the facial region so as to make the watermark spread over the whole region ensure a large measure of security against unintentional or intentional attack.

A general embedding system for spread-spectrum-based watermarking is shown in Figure 1. In the figure, the box “good transform” is intended to represent a transform from the original signal domain to a domain where the data is more equally sensitive to tampering. Ideally, a “good transform” also removes any part of the data that is not perceptually significant. In the case of images, for example, the transform should be insensitive to translation, small contrast manipulations, low-pass filtering, and other common signal processing techniques.

The idea is that after the transform, any significant change in the signal would significantly impair the image. Note that we include a box with the inverse transform, but the transform does not need to be strictly invertible since we can pass some side in-formation from the original signal to the inverse transform.

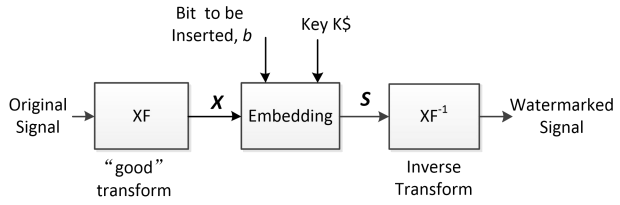

Figure1. Spread spectrum watermarking(embedding)

Spread Spectrum Watermarking

Figure 2 depicts a typical dirty paper trellis codes watermarking system. For a given source message *m* to be hidden, the message encoder proposes a set of watermark patterns and one of them ($\boldsymbol{w_m}$) is chosen for embedding based on the original cover work $\boldsymbol{c_o}$. Next, this watermark pattern undergoes some modifications with the influence of $\boldsymbol{c_o}$ to produce an added mark $\boldsymbol{w_a}$. Finally, this mark is added to the cover work to produce the watermarked work $\boldsymbol{c_w}$. The difference between blind coding and informed coding is that, for a given message $\boldsymbol{m}$, the blind encoder will always output the same watermark pattern, and it's a one-to-one mapping, while informed encoder will output several alternative code words, and it's a one-to-many mapping.

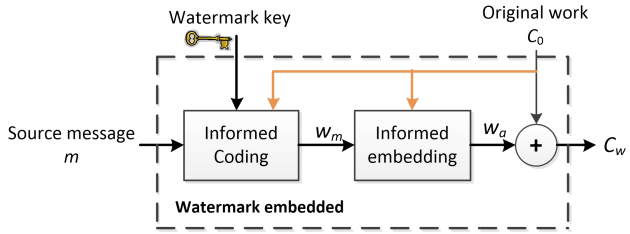

Figure2. Dirty Paper Trellis Codes

- Trellis structure

In DPTC, a special trellis is used. In this trellis, each state owns multiple possible transitions given an input bit. Each transition generates outputs coefficients. Figure 3 gives an example of a trellis with 8 states and 4 arcs per state. With this trellis, an input sequence owns multiple possible output codewords (a codeword is the results of the concatenation of outputs coefficients) since for each state there is multiple possible transitions for the same input bit. This signifies that an input sequence may be coded with different codewords. This property is essential in informed watermarking. In the original DPTC algorithm, the trellis own 64 states, 64 arcs per state and there is N_{arc} = 12 real coefficients pseudo-randomly generated as output arcs values.

- Informed Coding

The set of all the trellis paths i.e. all the possible outputs sequences, is the codebook C of the coder. A codeword $c^i \in C$ is the resultant coding of a message m. The informed coding is a way to choose the codeword c^i (encoding a given message m) the closet (for a given distance) to the host signal $\mathbf{x}$. Thus, informed coding allows to encode a message m by taking into account the host signal $\boldsymbol{x}$.

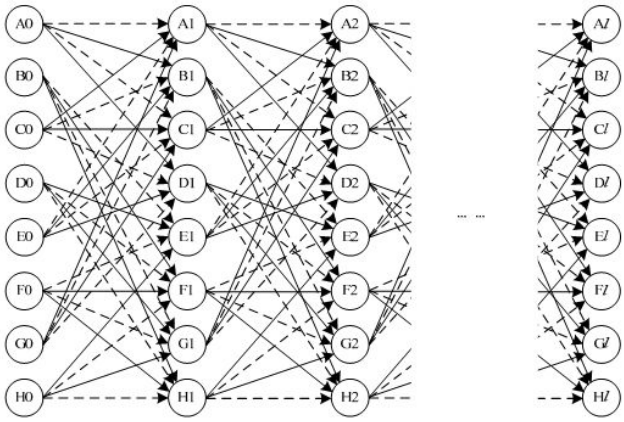

Figure3. Dirty-paper trellis with 8 states / 4 arcs per state

- Informed Embedding

In the original DPTC algorithm, a Monte Carlo approach is used in order to displace the host signal x into the Voronoi region of the codeword c^*. This embedding is achieved in order to meet a given robustness. Moreover the modification of x is achieved by taking into account the psycho-visual degradation by using the Watson perceptual measure. The Monte Carlo principle is iterative and consists to attack a counter-attack a watermarked signal y.

The resulting watermark w_m is subsequently embedding into the cover Work using a simple blind additive approach:

$$c_w = c_o + \alpha w_m \quad \backslash^* \text{ MERGEFORMAT (1)}$$

Where α is the embedding strength.

III. PROPOSED WATERMARKING SCHEME

The proposed scheme is based on three steps: face window size detection, embedding watermarks into each detected face using spread-spectrum technology, and embedding watermarks into the whole area with dirty paper trellis coding. These steps are discussed in the following subsections.

A. Face Window Size Detection

First we use face detection and eyes detection to find eye-center locations in a digital image. According to eyes location, the window size of original image can be generated to embed the watermark. Face plays an important role in many security and integrity protection applications. Thus, this step is very significant, since the facial features that will be localized (eyes, mouth) via geometric templates are unique for the facial region.

Aiming to detect the face region, we exploit color in-formation to discriminate the skin-colored image region, which corresponds to the facial region. The original RGB image is converted to the HSV domain, because it is easier to perform skin-tone color segmentation in this color space. More specifically, the parameter ranges for

hue (H), saturation (S), and value (V) that fulfill our requirements have experimentally been found to be:

$$0 \le H \le 25 or 335 \le H \le 360$$
$$0.2 \le S \le 0.6 \qquad \backslash* \text{ MERGEFORM}$$
$$0.4 \le V$$

We follow a connected component algorithm after binary thresholding, in order to isolate all the compact skin-colored regions. A similar pattern matching technique is used for the localization of the mouth, except that the model now consists of two concentric ellipses having major semi axes of the same magnitude and minor semi axes of considerably different magnitude. This pattern is again unique for the mouth, and the search is performed in the lower half of the elliptical region. A rectangle window size of facial region is obtained by enlarge the eyes and mouth location.

B. Face Region Encoding

From above step, a rectangle window size of facial region is obtained. In order to place a length watermark into an image, we computed the DCT of the rectangle window image area and placed the watermark into the highest magnitude coefficients of the transform matrix, excluding the DC component. We extract a sequence of values $V = v_1, ..., v_n$ in Fourier domain method based on the DCT. A watermark consists of a sequence of real numbers $X = x_1, \ldots, x_n$. The each value x_i is chosen independently according to $N(0,1)$ (where $N(\mu,\sigma^2)$ denotes a normal distribution with mean μ and variance σ^2). Then we insert X into V to obtain V' with a scaling parameter α, which determines the extent to which X alters V'. In this paper, the formulate for computing is

$$v_i' = v_i + \alpha x_i \backslash* \text{ MERGEFORMAT (3}$$

where α is scaling parameter, in practice, α = 0.1. The choice of n dicates the degree to which the watermark is spread out among the relevant components of the image. Accoding to the form of watermarks, one can recover the watermark when α is proportional to $\sigma/n^{1/2}$.

It is highly unlikely that the extracted mark X^* will be identical to the original watermark X. Even the act of requantizing the watermarked image for delivery will cause X^* to deviate from X. We measure the similarity of X and X^* by

$$sim(X, X^*) = \frac{X^* \cdot X}{\sqrt{X^* \cdot X^*}} \qquad \backslash* \text{ MERGEFORM}$$

To decide whether X and X^* match, one determines whether $sim(X, X^*) > T$, where T is some threshold. Setting the detection threshold is a classical decision estimation problem in which we wish to minimize both the rate of false negatives and false positives.

C. Whole Image Encoding

The encoding for whole image performed the following steps:

Step 1: Convert the image into the 8×8 block-DCT domain.

Step 2: Place low-frequency AC terms of the blocks into a single, length $L \times N$ vector v, in random order. We refer to this as the extracted vector.

Step 3: Use a dirty-paper trellis code to encode the desired message, into a watermark vector w. This was done by running Viterbi's algorithm on v using a trellis modified for message m.

Step 4: Embed w into with blind embedding: $v_w = v + \alpha w$, where α is the embedding strength.

Step 5: Place the values of v_w into the low-frequency AC terms of the block-DCT of the cover image, in the same order as used in step 2.

Step 6: Convert the image back into the spatial domain. This resulted in an image that, when input to the extraction process of steps 1 and 2, would yield the vector v_w.

The detector performed the following steps:

Step 1: Extract a vector $\hat{v}$ from the image in the same manner as in steps 1 and 2 of the embedding algorithm.

Step 2: Apply the Viterbi algorithm to $\hat{v}$ using the whole trellis, to identify the path whose code vector yields the highest correlation.

Step 3: Report that the message associated with the path found in step 2 $\hat{m}$ is embedded in the image

IV. Experiment Result

In our experiment, the cover-work is the 512×512 pixels color image. The spreading watermark is 64 bits independently for window size of face region, and the watermark for dirty- paper trellis codes is 98 bits pseudo-random binary sequence for whole image area. The result illustrates as figure 4. The rectangle window size is 128×160 pixels and the peak signal to noise ratio (PSNR) is 42.34.

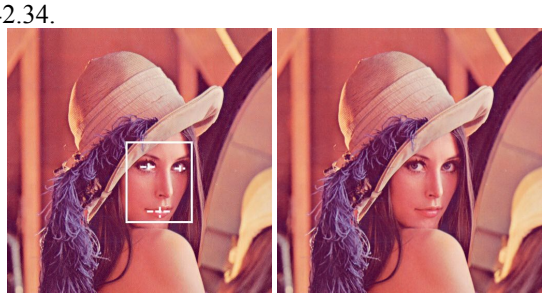

(a) (b)

Fig.4 Original image with rectangle window size and watermarked image

In practice, the watermarked image is taken under common attacks in order to illustrate effectively of our proposed watermarking scheme. The attacks are image copied, image scaling, Gaussian noise, cropping and so on. We use bit error rate (BER) to measure the robust of our proposed scheme, and the results show as figure 4.

From table 1, it shows that the watermarking scheme can effectively withstand the scaling attack; and has a robust to other common attacks.

TABLE 1. BER UNDER COMMON ATTACKS

Attacks	*rectangle copied*	*1/2 scaling*	*2 scaling*	*Gaussian noise*	*1/8 cropped*

Attacks	*rectangle copied*	*1/2 scaling*	*2 scaling*	*Gaussian noise*	*1/8 cropped*
BER	0.1324	0	0	0.1875	0.1581

V. CONLUSION

In the paper, we have presented a robust double-level watermarking scheme for facial images. The proposed method takes consideration to image authentication and copyright protection simultaneously which uses a spread spectrum encoding the rectangle face region and dirty-paper trellis codes for whole image area. This technique can meet special requirements. Experiments show our watermarking scheme can significantly improve embedding effectiveness and there are many feature is our scheme:

1) Combination of double-level watermarks can detect any modifications in the face rectangle window of target image as well as copying protection.

2) Double-level watermarking pay attention to the integrity of rectangle face window, which may be more attacked in many special applications.

3) The robust watermarking is greatly improved with associate-sequences technique. In conclusion, this dual-watermark can be used for facial image security in many respects.

ACKNOWLEDGMENT

This work was supported by the Scientific Research Foundation of Sichuan University of Science and Engineering (Grant No. 2012RC22), Sichuan Provincial Department of Education Fund (Grant No.13ZB0139 and No. 14ZB0217) and Key Laboratory for Enterprise Information and IOT Measurement and Control Technology of the education department of Sichuan province Open Fund (Grant No.2013WYY04).

REFERENCES

[1] M. Costa, “Writing on dirty paper (corresp.)”, IEEE Trans. Inf. Theory, vol. 29, pp.439, 1983.

[2] Cox I.J, Miller M.L, Mckellips A.L, “Watermarking as commu- nications with side information”, Proceedings of the IEEE, 1999, 87(7): 1127-1141.

[3] I.J. Cox, et al. “Secure Spread Spectrum Watermarking for Multemedia”, IEEE Trans. Image Processing, Vol. 6, No. 12, Dec. 1997.

[4] M. Kutter, “Performance improvement of spread spectrum based image watermarking schemes through M-ary modulation”. In A. Pfitzmann, editor, Third Int. Workshop on Information Hiding, volume 1768 of Lecture Notes in Computer Science,pages 237–252, 1999.

[5] F. Hartung, J. K. Su, and B. Girod, “Spread spectrum watermarking: Malicious attacks and counterattacks,” Proc. SPIE, vol. 3657, pp. 147–158, Jan. 1999.

[6] D. Kirovski and H. Malvar, “Robust spread-spectrum audio watermarking,” in Proc. Int. Conf. Acoust., Speech, Signal Process., Salt Lake City, UT, May 2001.

[7] M. L. Miller , G. J. Doërr and I. J. Cox "Dirty-paper trellis codes for watermarking", Proc. IEEE Int. Conf. Image Processing, vol. 2, p.129 , 2002.

[8] B. Chen and G Wornell, “Quantization index modulation: A class of provably good methods for digital watermarking and information embedding,” IEEE Trans. Inform. Theory, vol. 47, pp. 1423–1443, May 2003

[9] Miller, M. L., Doerr, G. J., and Cox, I. J., “Applying Informed Coding and Informed Embedding to Design a Robust, High Capacity Watermark”, IEEE Transactions on Image Processing, 2004, 13(6), pp.792-807

[10] Chaumont, M., “Fast Embedding Technique For Dirty Paper Trellis Watermarking,” in 8th International Workshop on Digital Watermarking, IWDW’ 2009, pp.110-120.

[11] Anil K. Jain, Umut Uludag, Rein-Lien Hsu, "Hiding a Face in a Fingerprint Image," icpr, vol. 3, pp.30756, 16th International Conference on Pattern Recognition (ICPR'02) - Volume 3, 2002

[12] Yaghmaee, F. Jamzad, M. "Achieving higher perceptual quality and robustness in watermarking using Julian set patterns", IEE Proceedings - Information Security, Vol.153, Iss.4, pp.167, 2006.

[13] Cintra, Renato J. Cooklev, Todor V. "Robust image watermarking using non-regular wavelets", Signal Image and Video Processing, Vol.3, Iss.3, pp.241, 2009

Fei Wang received the M.S. degree in computer science from Southwest University of Science and Technology, Mianyang, China, in 2006.

He is currently a lecture with the School of Computer Science, Sichuan University of Science and Engineering, Zigong, China. His areas of research include computer vision, information fusion, and pattern recognition. His latest research focuses on face detection and recognition, facial expression analysis, image segmentation, object tracking, and active information fusion for monitoring human fatigue.

Learning Capability Study On Improved RBF Neural Network

Quan-bing HE
Computer school, Sichuan University of Science and Engineering, Zigong, Sichuan, China
Email: ajax081022@gmail.com

***Abstract*—In order to improve RBF neural network's learning capability, this paper uses genetic clonal selection algorithm to optimize the centers and widths of the hidden units of RBF network and dynamic self-adapted concept is used to set the node number of the hidden layer. Also, recurrent least square method is used to train the weights between hidden layer and output layer. Meanwhile, a new method of mutation is put forward to improve the algorithm's accuracy. Compared with BP algorithms, the simulation results of GIS aided location show that it can speed the learning capability of improved RBF network with those methods and thus it has a more wider applicability in many fields.**

***Index Terms*—RBF neural network, GIS aided location, genetic clonal selection algorithm, learning capability**

I. INTRODUCTION

Radial-Basis Function(RBF) neural network is a new kind of effective and feed forward network. It has many features,such as local approximation, best approximation, global optimum and its network is simple and learning speed is fast. Therefore, it has been widely applied on pattern recognition, function approximation, system modeling, signal processing and so on. Now, it has been proved that RBF can approach any continuous functions of multi-variable in any precision if there are enough hidden node radial-basis functions. At present, many training methods have been put out and they mainly concentrated in two areas:1)the centers and widths and node number of hidden layers; 2)the weights between hidden layer and output layer. Hidden layer nodes is usually determined by past experience. However, a better network is constructed usually by repeated experiments. So, it is not a good network if the node number of hidden layer is defined at first. The center value of hidden layer has a great effect on function approximation and result accuracy. However, the best approximation result of K-means clustering algorithm usually used is not good because its sample is not enough or it can not correctly show the relationship of input and output. For these problems, this paper introduces genetic clonal selection algorithm to improve the centers and widths of hidden layer of RBF neural network and dynamic self-adapted concept to set the node number of hidden layer.

Genetic clonal selection algorithm is a genetic algorithm based on clonal selection concept. The main search way is high-frequency mutation clone and it can approach fast to the optimum solution if we can introduce related operator to the traditional evolutionary algorithms. Meanwhile, it can guarantee of global optimization and has been proved in combinational optimization and pattern recognition and so on. So this paper use genetic clonal selection algorithm to train the centers and widths of hidden layer and a new method of mutation is put forward. Dynamic self-adaptive method can solve the problem that too many hidden layer node can reduce the algorithm's efficiency and too few can reduce the accuracy. At last, recurrent least square method is used to train the weights between hidden layer and output layer. The simulation results show that genetic clonal selection algorithm can improve the learning capability of RBF network when it used in GIS aided location.

II. IMPROVED RBF NEURAL NETWORK ALGORITHM

A. the concept of genetic clonal selection algorithm

The aim of clonal selection algorithm is to achieve success of adaptive change of individual development by focusing on accumulated mutation and selection within the organism. Antigen is varied and so antibodies have to maintain diversity to recognize antigen to invade. Therefore, diversity is the most important feature of antibody. Living organisms can form a type of antibody diversity only through various mechanisms. The generation of antibody diversity can be attributed to the following aspects of the mechanism: random gene recombination; presence of multiple V-gene in germ-line; random combination of H chain and L chain; somatic mutation; diversity of connection and insertion and so on. There are some basic operations such as mutation, cloning, but isn't crossover (recombination) operation in algorithm models of early stage. For these reasons, Liang Qin-ou (2004)[4] think that clonal selection algorithm in the design of gene rearrangement should be taken into account and thus genetic clonal selection algorithm is proposed. The flowchart is showed as Figure 1.

The basic steps of improving RBF neural network with genetic clonal selection algorithm is as follows. 1.Establishing the initial antibody population and determining the fitness function and affinity function, which determines the degree of affinity between training results and expected results; 2.Determining the genetic

cloning strategy, such as selection, crossover, clone and mutation and so on so as to train the centers and widths of hidden layer of RBF network; 3.Using least square method to train the weights between hidden layer and output layer. The flowchart is showed as Figure 2.

1)RBF antibody coding: antibodies here are the candidate solutions. Randomly generates initial antibody population Ak which is real-coded (setting K=0). In this algorithm, the value of centers and widths of RBF network are obtained by self-correction with genetic clonal selection algorithm.

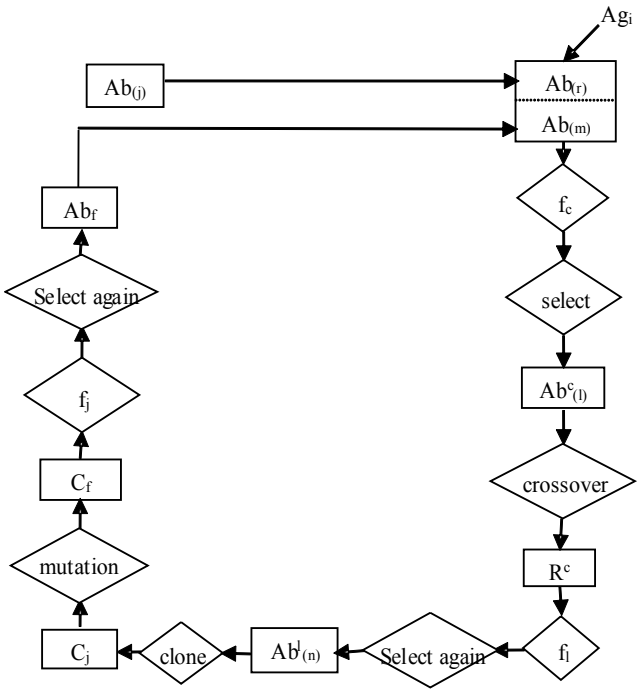

Figure 1. Genetic clonal selection algorithm flowchart

B. the improved RBF neural network algorithm

Supposing there are *n* input nodes and *p* hidden layer nodes and m output nodes in RBF network. Then the output of *i-th* hidden unit is showed as (1).

$$h_i = \varphi(\frac{\|X - r_i\|}{b_i}) \qquad (1 \le i \le p) \qquad (1)$$

In (1), $\phi(\bullet)$ is the transformation function of hidden units(RBF function, usually is Gaussian function); ri is the center of the i-th RBF, X is n-dimensional input vector, that is $X = [x_1, x_2, \cdots, x_n]^T$; bi is the width of the i-th nonlinear transformation unit.

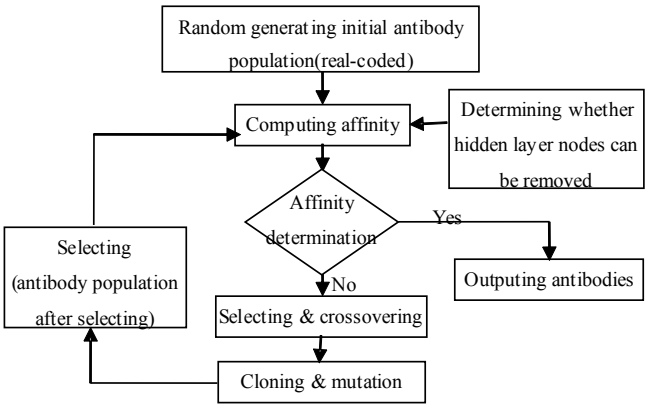

Figure 2. Flowchart of improved RBF neural network algorithm

2) Computing the affinity of antibodies: affinity is used to measure the matching degree between antibodies and antigens. In practical problems, it is used to measure the error between the actual output and expected output of network. Greater affinity, the smaller the error between the two, which is showed as (2).

$$ff(a) = \frac{1}{(\frac{1}{M}\sum_{i=1}^{M}\left[Y_e(i) - Y(i)\right]^2) \times K} \qquad (2)$$

In (2), Y is the network actual output and Ye is the expected output, M is the training sample and $0 < K \le 1$.

At this stage, there should be dynamic adjustment for the hidden nodes according to the presence conditions. In the practical application of RBF network, the nodes of input layer and output layer are usually determined by specific conditions. Too many hidden nodes will cause too much overhead and too few nodes won't achieve the accuracy and cause more training times. So appropriate hidden layer nodes is important for the solution of problems. Dynamic self-adaptive strategy, which means more hidden layer nodes at first and then gradually remove the hidden nodes which is not important for the problem in the processing, can determine the least number of hidden layer nodes meanwhile the network has the best convergence.

3)Crossover and clone operation: crossover or recombination and clone operating for the optimal value. The better affinity the more Cloning. The main purpose is to generate individuals with more better weights and thresholds. The method to calculate clone scale is showed as (3).

$$Q_a = round\ (\beta \times ff(a) / \sum ff(a)) \qquad (3)$$

In (3), β is the clone coefficient, which is used to control the clone scale.

4)antibody mutation: it is an important process to realize population diversity in genetic clonal selection algorithm, which can generate more excellent antibodies. However, degradation may occur after high-frequency

variations, antibody mutation can only be take effects on the temporary antibodies after cloning.

Because of its complex coding of traditional Gaussian mutation and it doesn't reflect the relationship between mutation range and the affinity, this paper use an improved affinity mutation method(showed as (4)), which can improve the algorithm accuracy and reflect the feature of antibody mutation, that is the higher the affinity, the smaller variation.

$$a_i^{'} = a_i + \gamma \times N_i(0,\sigma^2) \tag{4}$$

$$\sigma = \sqrt{\frac{\lambda \times i}{ff(a_i)}} \tag{5}$$

In (4), $N_i(0,\sigma^2)$ is Normal Random Variables and its mean is 0 and standard deviation is σ; γ is a vector randomly generated in the interval [0,1] and its length is 2H. Equation (4) not only represent the features of antibody mutation, but also accelerate the convergence speed and thus avoid getting into local optimum.

5)Antibody selection: it is a process to select N more excellent individuals to replace the original antibody group according to affinity from the original group and the new group after crossover, cloning and mutation.

6)Recurrent least square method: weights between the hidden layer and output layer can be obtained by related network training of each generation. This paper use the most common recurrent least square method. The basic idea is that the exact solution of the weights can be obtained by iterating the covariance matrix formed by training sample, the solution when error gradient is 0.

This algorithm has many good features, such as strong directional iteration, fast convergence. More details can be find in [9].

III. CASE STUDYING

This paper studies a three-tier highway in Chongqing of China with GIS aided location system with the improved RBF algorithm (more details about the case can find in [14]). This paper only gives the results of the improved RBF algorithm and other two BP algorithms. Selecting the first 30 raster objects as the investigated objects and the first 20 as the training input and the last 10 as validation input. Network uses three-layer structure. There are 6 input nodes, which respectively represent land price, deviation, elevation, geological disasters, land use types, across facilities(V1、V2、V3、V4、V5、V6). 1 output node representing the final land price (also the training value of model); 25 hidden layer nodes at first. Then, this paper compares results from the improved RBF algorithm with that from the old BP algorithm and the improved BP algorithm. In order to get a clear comparison, it gives two comparing ways that is when the error is less than or equal to 0.01% or the iteration time is 350. Results from three algorithms are showed in "TABLE I." and the comparison result is showed in "TABLE II.".

TABLE I. Results from three algorithms(¥/m^2)

ID	*V_1*	*V_2*	*V_3*	*V_4*	*V_5*	*V_6*	*Land price 1*	*Land price 2*	*Land price 3*	*Land price 4*	*Land price 5*
21	82	0.78	0.49	1	4100	0	43.12	43.21	43.77	43.15	43.820
22	59	0.55	0.11	4	1180	0	36.46	35.99	35.86	35.48	35.741
23	67	0.1	0.54	3	670	0	9.9	9.99	9.98	9.89	9.983
24	52	0.64	0.31	5	52	0	24.79	24.21	24.32	24.55	24.431
25	54	0.97	0.36	4	54	0	38.65	39.19	39.15	38.76	39.000
26	98	0.409	1.86	1	98	0	20.57	20.57	20.59	20.88	20.605
27	105	0.486	1.94	1	105	1	42.49	42.59	42.72	42.59	42.658
28	95	0.122	0.11	3	950	0	9.87	9.74	9.74	9.77	9.742
29	84	0.208	0.39	2	84	0	13.12	13.17	13.27	13.26	13.250
30	64	0.695	1.35	1	640	1	28.15	28.99	28.88	28.73	28.781

Note: *land price 1 is from the original BP algorithm, which has iterated 350 times and the error is less than or equal to 0.01%; land price 2 is from the improvedl BP algorithm, which has iterated 263 times and the error is less than or equal to 0.01%; land price 3 is from the improved BP algorithm, which has iterated 350 times and the error is less than or equal to 0.001%; land price 4 is from the improved RBF algorithm, which has iterated 45 times and the error is less than or equal to 0.01%; land price 5 is from the improved RBF algorithm, which has iterated 350 times and the error is less than or equal to 0.0001%.*

TABLE II.

Comparing results from three algorithms

ID	*Expected results*	*Training Value 1*	*Error 1(%)*	*Training Value 2*	*Iteration times*	*Training Value 3*	*Error 3(%)*	*Training Value 4*	*Iteration times*	*Training Value 5*	*Error 5(%)*
21	43.83	43.12	1.63	43.21	263	43.77	0.1	43.15	45	43.820	0.02
22	35.75	36.46	-1.99	35.99	263	35.86	-0.3	35.48	45	35.741	0.02
23	9.984	9.9	0.84	9.99	263	9.98	0	9.89	45	9.983	0
24	24.44	24.79	-1.45	24.21	263	24.32	0.4	24.55	45	24.431	0.04
25	39.01	38.65	0.92	39.19	263	39.15	-0.4	38.76	45	39.000	0.02
26	20.62	20.57	0.25	20.57	263	20.59	0.2	20.88	45	20.605	0.07
27	42.67	42.49	0.42	42.59	263	42.72	-0.1	42.59	45	42.658	0.02
28	9.742	9.87	-1.3	9.74	263	9.74	0	9.77	45	9.742	0
29	13.24	13.12	0.92	13.17	263	13.27	-0.2	13.26	45	13.250	-0.07
30	28.79	28.15	2.23	28.99	263	28.88	-0.3	28.73	45	28.781	0.03

Note: *the training value in table 2 is the land price in table 1; error 1 is from training value 1; iteration times of 263 is from training value 2; iteration times of 45 is from training value 4.*

IV. CONCLUSION

Because of so many advantages of RBF neural network, such as consistent approximation for nonlinear continuous functions, learning speed and large-scale data fusion, it has a more wide applicability than BP algorithm. However, RBF has some defects, such as hidden layer nodes is usually determined by past experience, the best approximation result of K-means clustering algorithm usually used is not good because its sample is not enough or it cannot correctly show the relationship of input and output. For these problems, this paper introduces genetic clonal selection algorithm to improve the centers and widths of hidden layer of RBF neural network and dynamic self-adapted concept to set the node number of hidden layer. The simulation results of GIS aided location show that genetic clonal selection algorithm can improve the learning capability of RBF network and it has a wide applicability in many fields.

ACKNOWLEDGMENT

This work was supported in part by a grant from key Laboratory's projects of universities from Sichuan provice about Enterprise Informatization and Measurement & Control technology on the Internet of things(Project No.: 2013wyy02).

REFERENCES

[1] Gholam Ali Montazer, Hessam Khoshniat and Vahid Fathi, "Improvement of RBF neural networks using Fuzzy-OSD algorithm in an online radar pulse classification system," Applied Soft Computing, vol. 13, pp. 3831 – 3838,Sep. 2013.

[2] MENG Xi,QIAO Jun-fei and HAN Hong-gui, "RBF neural network based on ART neural network," Control and Decision, vol. 29,pp. 1876 – 1880,Oct. 2014.

[3] Lukas Falat and Dusan Marcek, "Financial Time Series Modelling with Hybrid Model Based on Customized RBF Neural Network Combined With Genetic Algorithm," Advances in Electrical and Electronic Engineering, vol.12, pp. 307-318,Dec. 2014.

[4] Wang Bing, Li Pan-chi, Yang Dong-li and Yu Xiao-hong, "Research on Cloud Process Neural Network Model and Algorithm,"Journal of Electronics & Information Technology, vol.37, pp. 110 – 115, Jan. 2015.

[5] Suha Afaneh, Raed Abu Zitar and Alaa Al-Hamami, "Virus detection using clonal selection algorithm with Genetic Algorithm (VDC algorithm)," Applied Soft Computing, vol 13, pp. 239 – 246, Jan. 2013.

[6] Ezgi Deniz Ulker and Sadk Ulker, "Comparison Study for Clonal Selection Algorithm and Genetic Algorithm," International Journal of Computer Science & Information Technology, vol.4, pp. 107-118, Apr. 2012.

[7] DAI Hongwei, YANG Yu, WANG Yongquan and LI Cunhua, "Adaptive Quantum Crossover Clonal Selection Algorithm," Journal of Xi'an Jiaotong University, vol.48, pp. 6 – 12, Sep. 2014.

[8] Xue Fu-qiang, Ge Lin-dong and Wang Bin, "RBF neural network classifier based on improved hierarchy genetic algorithm," Journal of system simulation, vol.22, pp. 399-402, Feb. 2010.

[9] Zhong Luo, Rao Wen-bi and Zou Cheng-ming, "Integration and application technology of artificial neural network," Science press, pp. 69-90, Jan. 2007.

[10] Feng Xiao and Xie Yuan-guang, "Theory and method of computer aided location for linear engineering," Southwest jiaotong university press, pp. 125-134, Aug. 2008.

[11] Liu Xia-bi, "Introduction to artificial intelligence------ approaches and systems," National defense industry press, pp. 127-150, Aug. 2008.

[12] Liang Qin-ou and Zhu Guo-rui, "Research on location - allocation problem based on clonal selection principle," Bulletin of surveying and mapping, pp. 17-19, Nov. 2004.

[13] Li Heng-jie, "Research on multi-objective clonal selection algorithm chemical and its applications," Lanzhou university of technology, pp. 38-47, May 2006.

[14] Du Juan, Lu Xiao and Jiao Ning, "An optimum design of RNF neural networks based on immune monoclonal algorithm," Microcomputer information, vol. 15, pp. 207-209, 2009.

[15] Chen Yi and Wan Mei-fang, "The application of RBF neural networks in logistical system," Computer simulation, vol. 27, pp. 159-162, Apr. 2010.

Available reservoir identification of tight sand based on Support Vector Machine classification

Shu YAN[1], Shizhong MA[1], Xiaolei TIAN[2], Yao LI[1], Zhiyi ZHOU[1]
[1]Northeast Petroleum University
[2]The Third Oil Deposit of No.6 Oil Extraction Plant, Daqing Oilfield Company Ltd

***Abstract*—Based on the research that statistical learning theory of the application of Support Vector Machine Regression in Classified Fluid Unit Recognition. Aiming at the question of the tight sand's poreperm characteristics, on the basis of a number of data about the borehole log, using the FZI classification of flow unit types to build a relation of porosity-permeability so that the correlation factor can be greatly improved. But the relationship between the flow unit types and the borehole log is too complex to make a simple linear fitting to classify the flow units, we introduce a method of Support Vector Machine Regression to build a prediction model of flow unit and make comparative analysis. Compared with the traditional linear mapping methods, the results show that the SVM regression model which concentrates multiple borehole log characteristics and makes a effective use in nonlinear mapping of Support Vector Machine Regression, has a good application results not only in the sandstone segment fitting precision that has core data scale but also in the noncore data segment's fluid unit prediction makes a certain improvement.**

***Index Terms*—support vector machine regression; flow unit prediction; tight sand**

I. Regional Geological Background

Qingshui Depression locates at southwest of south of western sag, Liaohe Depression, with higher degree of exploration. The next key development horizon is the deep sha-3 member. The whole sha-3 member, grows sublacustrine fan facies, shallow lake, semi-deep lake and deep lake, is the place that locates at basin subsidence and uplift transition stage. Among them, sublacustrine fan subphase grows three kinds of sedimentary facies, which are braided channel, front-channel and margin-channel, inter-channel and the deposit type is the transition from gravity flow to traction flow. It grows more sand lens reservoir and updip pinchout reservoir. The main reservoir lithologies are glutenite and packsand that mixes with a small amount of gritstone and medium sand. The shale content is about 5% and the main clay mineral is kaolinite that distribute from the middle to the northeast area in the whole research area. Generally speaking, the sha-3 member is characterized by a wide perpendicular span of 2300 to 4300 meters, and a dramatic horizontal anamorphic phase variation whose scale of the braided channel appears to be relatively small. Physical properties of the analyzed section were defined with evident distinctions: porosity ranges from 4% to 25% and permeability from 0.1 to $500\times10^{-3}\mu m^2$. Besides, formations with a medium scale of porosity and permeability mingled with those depicted with a behavior of tightness. Therefore, the calculation method of conventional permeability is inapplicable. So that, this text, on the basis of the application of Support Vector Machine Regression in flow unit classification, greatly improves the prediction accuracy of flow unit classification. And according to the porosity-permeability relation by flow unit classification, the interpretation accuracy of reservoir physical property is also greatly enhanced.

II. Division of Flow Unit

A. Selection of Flow Unit Characteristic Parameter

Through the collecting and assorting of the data analysis about the coring segment's core physical property, the adopted method is FZI partitioning method that based on the minor modified Kozeny-Carman equation.

$$FZI = RQI/\Phi_Z$$

Among them:

$$RQI = 0.0314\sqrt{\frac{K}{\Phi_e}}$$

$$\Phi_Z = \frac{\Phi_e}{1-\Phi_e}$$

The flow unit can be divided into four categories by the clustering analysis method; the division values of FZI are respectively 0.4, 0.8 and 1.5 um. The porosity-permeability fitting relationship of the four flow unit categories are:

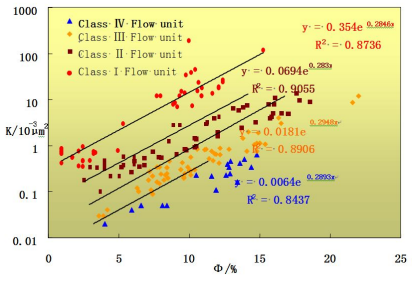

Figure 1 the Φ-K cross-plot under FZI division

Class Ⅰ $K = 0.354e^{0.2846\Phi}$

Class Ⅱ $K = 0.0694e^{0.283\Phi}$

Class Ⅲ $K = 0.0181e^{0.2948\Phi}$

Class Ⅳ $K = 0.0064e^{0.2893\Phi}$

As can be seen from the figure 1, there are improvement about the porosity-permeability correlation under different FZI reservoir classification.

B. Characteristic Analysis of Flow Unit

In the internal of the connected body， the quality of the reservoirs have some differences， most people thinks that these differences reflect the differences of the internal connected bodies ’ penetration ability, and impose the different classification of penetration ability to reflect the type of flow units. But speaking of the tight sandstone， penetration abilities are more reliable on the calculation of the permeability and the development of the flaw. This makes it difficult to determine the seepage ability accurately in the conventional logging. Based on this understanding， coming up with imposing the contribution of porosity to permeability to devise the flow unit. Based on the proper relationship of FZI classification, it can reveal permeability of different types of the flow unit and improve the calculations more precisely.

For a data x to classify, working out the result, and then classify it based on the data is plus or minus.

Using the capillary pressure curves and casting slice to analyze the porosity-permeability structural characteristics of different flow unit in tight oil reservoir.

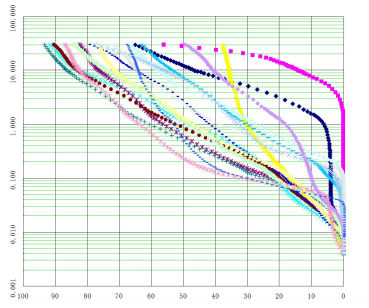

Figure 2 IV class flow unit capillary pressure plot

C. Linear Fitting Division in Flow Unit

In coring hole, we can use the core analysis data to calculate FZI to classify the reservoir. But as for noncoring well, it can only been set up the relation model between reservoir flow unit index and log response through the widespread log data to calculate FZI first, then use it to classify the reservoir.

After the sensitivity analysis of all the log response, a multiple parameter fitting equation for variable can be established by choosing the intercal transit time, the resistivity of the destination formation, the resistivity of the invasion zone and the natural gamma.

Where, Δt is the interval transit time logging value, $\mu s \cdot m^{-1}$; R_t is the resistivity of the destination formation, $\Omega \cdot m$; R_i is the resistivity of the invasion zone, $\Omega \cdot m$

As can be seen from the Φ-K relation plate, it is beneficial to improve the interpretation precision by using the method of FZI classification flow unit, and it will be useful to get permeability accurately especially under the condition that there is two orders of magnitude difference between permeability given the porosity is same. But there are problems in the method: Even in the same flow unit, it is difficult to get an accurate relationship between porosity and permeability due to that FZI is related to porosity; Uniform FZI can be gained if permeability and porosity magnify or minify certain times. So it does not fit with the requirement “minimum reservoir physical difference in internal flow unit, maximum reservoir physical difference in diverse flow unit” by using such method to classify the flow unit.

To solve these problems, this text thinks that there exist contradictions between the FZI classification result and flow unit classification principle. What is more, there will be a limitation in the equation precision by using multiple parameters to fit FZI. But there is certain rationality in the Φ-K relation plate by FZI classification. So that in this text, FZI is defined as pore structure factor, no longer indicates a flow unit parameter delimiting index but a parameter that can reflect the straightest cause of variation in the relationship between porosity and permeability. The combination of deposition and diagenesis affects the value. According to the problem that simple fitting can not meet the FZI accuracy, we introduce the support vector machine method to solve it.

D. Flow unit classification based on SVM.

SVM (support vector machine) is first proposed by Vapnik in 1995.It has many unique advantages in solving the nonlinear and high dimension problem with small sample set. The principle of SVM classification is that to change the linear space into a much higher space when it is infeasible to classify these data points with one-dimensional or two-dimensional space partition. And use a hyper plane to classify under the higher space. SVM, same as the neural net, is a learning mechanism. But what is different from the neural net is that the method used by SVM is the mathematics method and optimization technology. By contrast, there is no longer any problem such as how to confirm the problem of network structure, over learning and lack learning, local minimum point.

To sort a data point x, actually, is to substitute x into a formula, $f(x) = \omega^T x + b$, for calculating it and then classify them according to the positive and negative signs. The interesting thing about form is that as for the prediction about the new point x, what we need is to calculate the inner product of training data points and it. It is the basic premise to use Kernel to extends nonlinearly. The coefficient α correspond to all the non Supporting Vector is equal to zero. Therefore, in fact, the inner product calculation of new points only aim at a

little ‘Supporting Vectors’ rather than all the training datas. Why the α corresponding to non Supporting Vectors is zero. Intuitively speaking, the posterior points have no effect on hyper plane. Due to the classification totally determined by hyper plane, these irrelevant won’t be taken into the classification calculation. So there will be no effect.

Objective function is got though Lagrange multiplier:

$$\max_{\partial_i \geq 0} L(\omega, b, \alpha) = \max_{\partial_i \geq 0} \frac{1}{2}\|\omega\|^2 - \sum_{i=1}^{n} \alpha_i (y_i(\omega^T x_i + b) - 1)$$

If the Xi is support vector, for non-support vector, the functional margin is greater than 1, but ai is non-negative. In order to satisfy the maximization, ai must be equal to 0. This is also the limitations of non-Supporting Vector points.

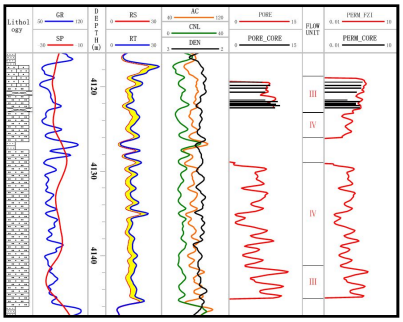

Figure 3 Logging interpretation comprehensive map

Use SVM to study FZI value of every kind flow unit and each borehole log after the classification by FZI. All kinds of borehole log parameters are chosen that can reflect the -K relation and are sensitive enough, including six dimension of Φ,K,AC,GR,(RLLD-RLLS)and FZI. This time, 68 groups are selected as learning samples and 9 groups are selected as cross-validation samples. Its accordance is 89 percent. By use of the method, it will be much easier and more accurate to classify the flow unit, and interpretation of physical property is applied to the real wells. What’s more, the precision is greatly improved.

III. CONCLUSION

Considering the analysis of connected component and single sand body reservoir quality evaluation result,we can build flow unit distribution model according to the classification and comparation about flow unit between single well and cross-well.In the continental reservoir,the facies change frequently in transversal and longitudinal directions and the distribution of flow unit is complex.So,on the research of reservoir flow unit,we not only consider the differences in the reservoir conficients distribution,but consider the geological interface phenomenon.To use the reservoir quality difference in connected component to classify the flow unit.The practice shows that it is an effective thought and method about the research in continental facies reservoir flow unit.

ACKNOWLEDGMENT

This paper is supported by Northeast Petroleum University graduate research innovation funding " SVM-based classification of tight sandstone reservoir parameters study "(YJSCX2014 -003NEPU). And National Science and Technology major projects (2011ZX 05006-005-005).

REFERENCE

[1] Ahr W M. “*Pore characteristics as surrogates for permeability in mapping reservoir flow units: Vaccum San Andres field, Lea County, New Mexico*”, AAPG Bulletin, 1991, 75(3):532

[2] Amaefule ,J O, et al. “*Enhanced reservoir description: using core and log data to identify hydraulic(flow) units and predict permeability in uncured intervals wells. Formation Evaluation and Reservoir Geology Proceedings*”, SPE, Annual technical conference and Exhibition, Omega SPE, Richardson, TX, CSA. 1993. 205～220

[3] Davies D K Vessel R K. “*Flow unit characterization of a shallow shelf carbonate reservoir: North Robertson Unit, West Texas. Proceedings*” SPE, Symposium on Improved Oil Recovery.V2.1996 SPL. Richardson. TX. GSA. 1996 . 295～304

[4] Lybanks W J Jr. “*Flow unit concept- integrated approach to reservoir description for engineering projects*” AAPG annual meeting AAPG Bulletin, 1987, 71(5):551～552

[5] Jackson S R .et al. “*Construction of a reservoir model by integrating geological and engineering information - Bell Creek Field*”. Lake L W. Carroll H B, eds. Reservoir Characterizations [C]. Academic Press Inc, Orlando, FL, 1991.524～555

[6] Cross T A, Raynolds R G. “*Illustration of Correlation Techniques, Facies Prediction and Reservoir Compartment Identification through Genetic Stratigraphy Gallup Sandstone and Mesa Verde Croup (Cretaceous), Four-Corners Region*”. In:USA. Rocky Mountain Association of Geologists 1993 Fall Field Trip, 1993:45-47.

[7] John Holbrook, Robert W S， Francisca E 0. “*Sequence Stratigraphy of Fluvial System Base-Level Buffers and Buttresses: A Model for Upstream Versus Downstream Control on Fluvial Geometry and Architecture Within Sequences*”. Journal of Sedimentary Research, 2006, 76 (1):162-174.

[8] Bart Makaske, Henk J T Weerts. “*Muddy lateral accretion and low stream power in a sub-recentconfined channel belt, Rhine-Meuse delta, central Netherlands*”. Sedimentology, 2005, 52:651-668.

[9] Journel A G. “*Combining knowledge from diverse sources: an alternative to traditional data independence hypotheses*”. Mathematical Geology, 2002, 34(5): 573-596.

[10] David W., Bowen, Paul Weimer. Regional sequence strigraphic setting and reservoir geology of Morrow incised-valley sand stones (lower Pennsylvanian) eastern Colorado and western Kansas. AAPG, 2003, 87(5): 781-815